Экологическая безопасность прибрежной и шельфовой зон моря

Ecological Safety of Coastal and Shelf Zones of Sea
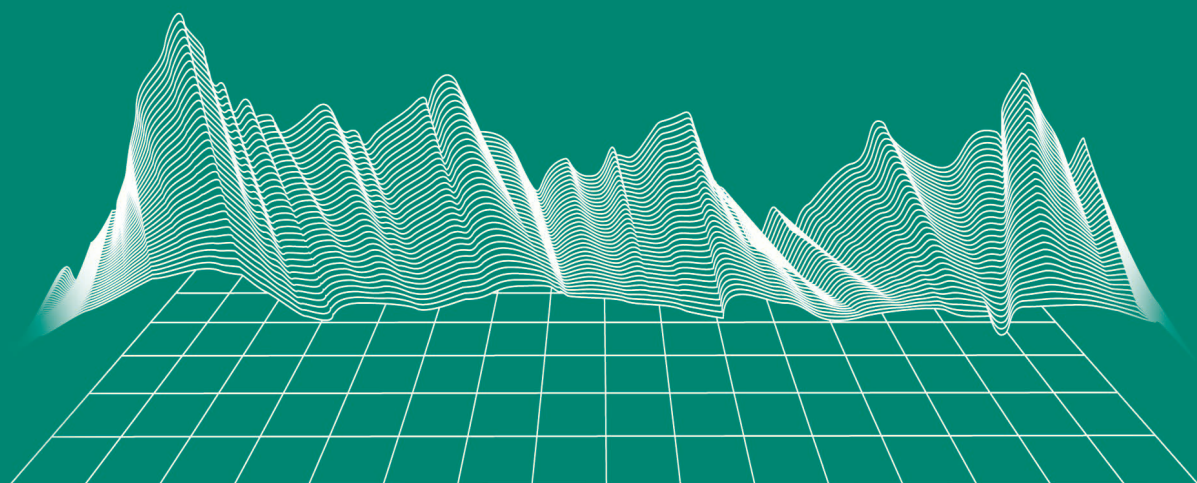
ECOLOGICAL SAFETY
OF COASTAL AND SHELF ZONES OF SEA

Scientific and theoretical peer reviewed journal

The Journal publishes original research results, review articles (at the editorial board's request) and brief reports.

The Journal aims at publication of results of original scientific research concerning the state and interaction of geospheres (atmosphere, lithosphere, hydrosphere, and biosphere) within coastal and shelf areas of seas and oceans, methods and means of study thereof, ecological state of these areas under anthropogenic load as well as environmental protection issues.

The Journal's editorial board sees its mission as scientific, educational and regulatory work to preserve the ecological balance and restore the resource potential of coastal and shelf areas believing that despite the geographical limitations of the areas under study, the processes taking place within them have a significant impact on the waters of the seas and oceans and economic activity.

The Journal publishes original research materials, results of research performed by national and foreign scientific institutions in the coastal and shelf zones of seas and oceans, review articles (at the editorial board's request) and brief reports on the following major topics:
- Scientific basis for complex use of shelf natural resources
- Marine environment state and variability
- Coastal area state and variability; coast protection structures
- Monitoring and estimates of possible effects of anthropogenic activities
- Development and implementation of new marine environment control and monitoring technologies

The outcome of the research is information on the status, variability and possible effects of anthropogenic activities in the coastal and shelf marine areas, as well as the means to perform calculations and to provide information for making decisions on the implementation of activities in the coastal zone.

EDITORIAL BOARD

РЕДАКЦИОННАЯ КОЛЛЕГИЯ

CONTENTS

СОДЕРЖАНИЕ

Original paper

Sea Surface Temperature Variability off the Crimea Coast in 2022–2023 According to *in situ* and Satellite Measurements

Yu. V. Artamonov, E. A. Skripaleva *, A. V. Fedirko

Marine Hydrophysical Institute of RAS, Sevastopol, Russia
*** e-mail: sea-ant@yandex.ru*

Abstract

The paper studies the variability of the temperature field at the sea surface on different time scales using hydrological measurements made off the coast of Crimea during 2022–2023 cruises of R/V *Professor Vodyanitsky* and *Copernicus* satellite data. It is shown that the intra-annual temperature amplitude according to *in situ* measurements in 2022 was 18.2 °C, whereas in 2023, it was 16.6 °C. The maximum ranges of spatial temperature changes at the polygon (up to 4–5 °C) were observed during periods of intense heating and cooling of surface waters in April–May and December 2022 and October 2023. On the synoptic scale, the periods of temperature increases (decreases) corresponded to those of local wind decreases (increases) with a delay in the temperature response to changes in the wind speed by 10–12 hours. Satellite data showed differences in the temperature intra-annual cycle and the level of its synoptic variability in 2022 and 2023 from climate norms. In 2022, the minimum and maximum temperatures in the intra-annual cycle were observed two weeks later than according to climate data. In 2023, the time of occurrence of the minimum corresponded to the climate one, and the maximum was observed two weeks earlier than it had been expected from the climate data. The main maximum in the level of synoptic temperature variability was observed in November 2022 and in December 2023, but not in May as it had been expected from the climate data. It is shown that from 2022 to 2023, predominantly positive average monthly temperature anomalies against the climate norms were observed. This reflects the upward tendency in temperature over the past two years.

Keywords: Black Sea, sea surface temperature, satellite measurements, *in situ* measurements, spatiotemporal variability

For citation: Artamonov, Yu.V., Skripaleva, E.A. and Fedirko, A.V., 2024. Sea Surface Temperature Variability off the Crimea Coast in 2022–2023 According to *in situ* and Satellite Measurements. *Ecological Safety of Coastal and Shelf Zones of Sea*, (4), pp. 6–26.

Изменчивость температуры поверхности моря у берегов Крыма в 2022–2023 годах по данным экспедиционных и спутниковых измерений

Ю. В. Артамонов, Е. А. Скрипалева *, А. В. Федирко

Морской гидрофизический институт РАН, Севастополь, Россия
* e-mail: sea-ant@yandex.ru

Аннотация

По данным гидрологических измерений, выполненных у берегов Крыма в ходе рейсов НИС «Профессор Водяницкий» в 2022–2023 гг., и спутниковым данным *Copernicus* исследована изменчивость поля температуры на поверхности моря на разных временны́х масштабах. По данным контактных измерений показано, что внутригодовая амплитуда температуры в 2022 г. составила 18.2 °C, в 2023 г. – 16.6 °C. Максимальные диапазоны пространственных изменений температуры на полигоне (до 4–5 °C) наблюдались в периоды интенсивного прогрева и охлаждения поверхностных вод в апреле – мае и декабре 2022 г. и в октябре 2023 г. На синоптическом масштабе периоды повышения (понижения) температуры соответствовали периодам ослабления (усиления) локального ветра с запаздыванием реакции температуры на изменения скорости ветра на 10–12 ч. По спутниковым данным показаны отличия внутригодового цикла температуры и уровня ее синоптической изменчивости в 2022 и 2023 гг. от климатических норм. В 2022 г. минимум и максимум температуры наблюдались на две недели позже, чем по климатическим данным, в 2023 г. время наступления минимума соответствовало климатическому, а максимум наблюдался на две недели раньше, чем по климатическим данным. Основной максимум уровня синоптической изменчивости температуры прослеживался в 2022 г. в ноябре, в 2023 г. – в декабре, а не в мае, как по климатическим данным. Показано, что в период с 2022 по 2023 г. наблюдались преимущественно положительные среднемесячные аномалии температуры относительно климатических норм, отражающие тенденцию к повышению температуры в течение последних двух лет.

Ключевые слова: Черное море, температура поверхности моря, спутниковые измерения, контактные измерения, пространственно-временная изменчивость

Introduction

The solution of modern problems related to the rational use of the Black Sea resources and preservation of its ecosystem requires constant monitoring of the waters hydrological structure state. Particular emphasis is placed on the investigation of the temperature field variability, as this parameter represents a pivotal abiotic factor influencing the marine ecosystem. Works [1] [1–7] show that seasonal and interannual variations are the main contributors to the total variability of the sea surface temperature (SST) field. It is shown that the SST seasonal variability is largely determined by the advection of waters by the Rim Current (RC) in addition to heating and cooling processes. Transport of warm waters with the RC from the east and southeast to the Crimean coast results in an increase in the SST in the winter–spring period, weakening of intra-annual temperature contrasts and, as a consequence, minimum level of the SST seasonal variability near the Crimean coast [6]. It is established that large-scale atmospheric processes and changes in the RC intensity influence the SST interannual variability [6, 8–10]. Works [3, 11–17] demonstrate that in recent years, a notable increase in the Black Sea temperature can be observed even in the cold intermediate layer.

Works [5, 7, 18–26] show that in addition to seasonal and interannual processes, the variability of the Black Sea temperature field is also influenced by a number of other factors including synoptic eddies, local meteorological conditions and upwelling. The intensive formation of synoptic meanders and circulations leading to the formation of temperature anomalies [24–26], as well as the export of the Azov Sea waters through the Kerch Strait [27], determined a high level of the SST synoptic variability within the coastal zone of Crimea from the Kerch Strait to the Heracleian Peninsula [7]. It is important to note that over the past decade, the hydrological water structure monitoring and assessment of the spatio-temporal evolution of the temperature field directly off the Crimean coast, where the anthropogenic impact is most pronounced, have been conducted primarily on the basis of *in situ* measurements on R/V *Professor Vodyanitsky* with a relatively large distance between stations (20–30 km). In this regard, the results of measurements made in 2022–2023 are of particular interest, given that hydrological surveys off the Crimean coast were conducted on a more frequent grid of stations and in a number of cruises the surveys were repeated twice. The repeat survey data obtained during the 122nd and 123rd cruises of R/V *Professor Vodyanitsky* in conjunction with satellite temperature measurements permitted a comprehensive analysis of the SST field spatial structure and characteristics of its synoptic variability off the Crimean coast during the summer of 2022 [30].

The objective of the present study is to examine the SST field variability in the northern Black Sea off the Crimean coast on different time scales. To this end, data collected during eight cruises of R/V *Professor Vodyanitsky* in 2022–2023 is integrated with *Copernicus* satellite data.

---

[1] Nelepo, B.A., ed., 1984. [*Variability of Hydrophysical Fields of the Black Sea*]. Leningrad: Gidrometeoizdat, 240 p. (in Russian).

Materials and methods

In 2022 and 2023, hydrological measurements were carried out during the 121st, 122nd, 123rd, 124th, 125th, 126th, 127th and 129th cruises of R/V *Professor Vodyanitsky* off the Crimean coast within the Russian territorial waters (Fig. 1). Table shows timing of measurements and number of stations carried out during the cruises. In consequence of the diminished extent of the survey area in 2022–2023 in comparison with that of the preceding cruises, the number of hydrological stations within the polygon was augmented, thereby facilitating the acquisition of more comprehensive SST spatial distributions off the Crimean coast. The expedition time reserve made it possible to carry out repeated hydrological surveys in four cruises (122nd, 123rd, 127th and 129th), with the coordinates of the stations remaining almost identical throughout. Hydrological measurements were taken in all seasons in 2022 and in spring, summer and autumn in 2023, providing a comprehensive data set for the assessment of the SST seasonal changes. Seawater temperature was recorded at each station using IDRONAUT OCEAN SEVEN 320PlusM CTD measuring system with an error of 0.001 °C and a resolution of 0.0001 °C (http://www.technopolecom.ru/downloads/doc_212.pdf) predominantly during daylight hours. The temperature field distribution was analysed in the surface layer at a distance of 2 m. During all cruises, five multi-hour hydrological stations were carried out at locations indicated in Fig. 1.

In this study, we also used daily averaged data from the SST satellite measurements from 1 January 2008 to 31 December 2023 with an ultra-high spatial resolution of 0.01° × 0.01° from the Black Sea High Resolution and Ultra High Resolution
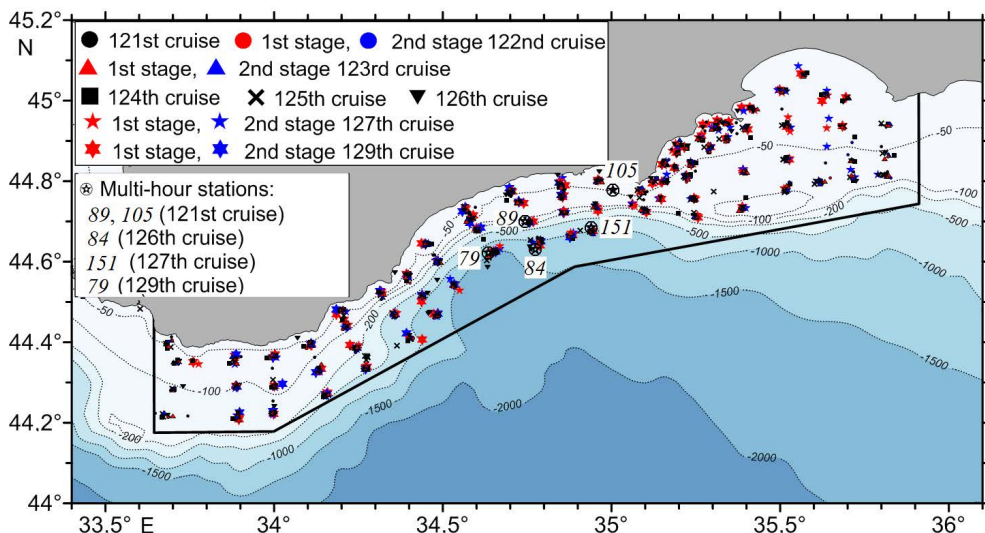
F i g . 1 . Map of hydrological stations carried out off the Crimea coast during the 121st, 122nd, 123rd, 124th, 125th, 126th, 127th and 129th cruises of R/V *Professor Vodyanitsky*

Timing of measurements and number of stations carried out at the polygon during the cruises of R/V *Professor Vodyanitsky* in 2022–2023

Cruise number		Date	Number of stations
121		19.04.2022–14.05.2022	*87*
122	1st stage	07.06.2022–13.06.2022	*75*
	2nd stage	17.06.2022–23.06.2022	*73*
123	1st stage	16.08.2022–23.08.2022	*78*
	2nd stage	26.08.2022–31.08.2022	*78*
124		02.10.2022–22.10.2022	*113*
125		02.12.2022–25.12.2022	*128*
126		16.03.2023–07.04.2023	*90*
127	1st stage	14.06.2023–20.06.2023	*64*
	2nd stage	22.06.2023–05.07.2023	*71*
129	1st stage	05.10.2023–17.10.2023	*66*
	2nd stage	17.10.2023–25.10.2023	*34*

Sea Surface Temperature Analysis array [2] (product SST_BS_SST_L4_NRT_OBSERVATIONS_010_006) of Copernicus Marine Environment Monitoring Service (CMEMS) obtained using advanced processing algorithms [31]. These data made it possible to calculate statistical characteristics of spatiotemporal temperature variability.

Actual wind speed values were selected from continuous records made at each station using the AIRMAR-220WX shipboard weather station and referred to the beginning of the hydrological sounding period.

---

[2] Black Sea High Resolution and Ultra High Resolution Sea Surface Temperature Analysis / E.U. Copernicus Marine Service Information (CMEMS). Marine Data Store (MDS). https://doi.org/10.48670/moi-00159 (date of access: 25.11.2024).

Main results

The analysis of the *in situ* measurement data carried out in 2022–2023 revealed a complex pattern of the actual SST horizontal distributions (Fig. 2), which can be attributed to the combined influence of seasonal, synoptic and diurnal variability. It is important to note that the accurate accounting of the SST diurnal variations based on *in situ* data necessitates continuous measurement of data at each hydrological station for a minimum of one day. However, this is currently unfeasible within the constraints of the allocated time of cruises. Earlier estimates of the SST diurnal variations based on *in situ* and satellite data [32, 33] indicated that it could reach several degrees and was significantly influenced by the measurement area, season and local synoptic conditions (cloudiness and wind speed). The data obtained from the SST measurements at the multi-hour hydrological stations carried out during the 121st, 126th, 127th and 129th cruises also demonstrated that the SST diurnal variations exhibited notable differences on varying days, across different seasons and in multiple areas of the polygon, reaching a maximum of 1.6–2 °C. Conversely, during daylight hours, when the primary measurements were carried out at the polygon, the changes in the SST did not exceed 0.5 °C.
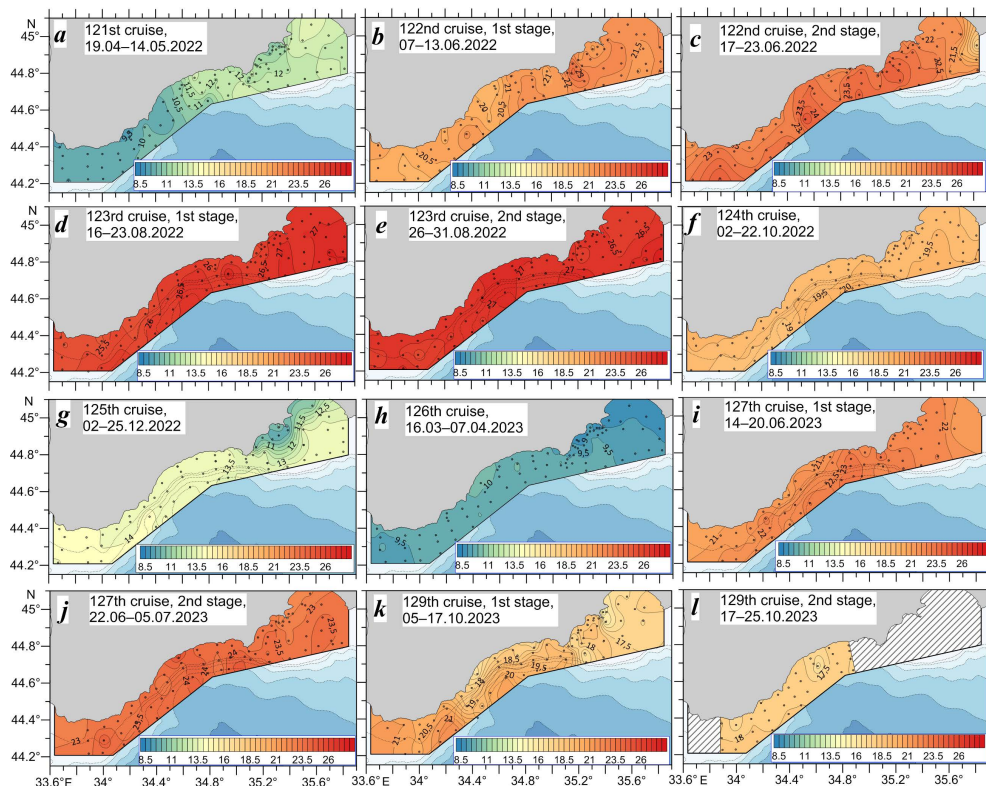
F i g . 2 . SST distribution according to the measurements carried out in the 121st (*a*), 122nd (*b*, *c*), 123rd (*d*, *e*), 124th (*f*), 125th (*g*), 126th (*h*), 127th (*i*, *j*) and 129th (*k*, *l*) cruises of R/V *Professor Vodyanitsky*

The SST spatial distributions from all surveys demonstrated that seasonal variability was most clearly evident in the SST fields. Thus, according to measurements taken in 2022, the SST minimum at the polygon was observed in April – May (121st cruise), with values fluctuating between 9.3 and 13.4 °C (Fig. 2, *a*). The SST values increased to 19.5–23.6 °C in the first half of June (122nd cruise, 1st stage) and to 17.5–24.5 °C at the end of June (122nd cruise, 2nd stage) (Fig. 2, *b*, *c*). During the second half of August, the maximum SST values were observed, reaching 24.9–27.5 and 25.6–27.5 °C, respectively, during both stages of the 123rd cruise (Fig. 2, *d*, *e*). In October (124th cruise), the SST decreased markedly, with values varying within the polygon from 18.7 to 20.3 °C (Fig. 2, *f*). In December (125th cruise), a further decrease in the SST values was observed, with a minimum range of 9.5–14.5 °C. (Fig. 2, *g*).

According to measurements taken in 2023, the lowest SST values (8.7–10.2 °C) were observed in the second half of March and early April (126th cruise) (Fig. 2, *h*). During the summer months, specifically the second half of June, there was a notable rise in the SST values, which reached a range of 20.5–23.5 °C during the 1st stage of the 127th cruise and increased subsequently to a range of 22.2–25.3 °C during the 2nd stage of the cruise (Fig. 2, *i*, *j*). In the autumn, in October, a decrease in the SST was observed, with values ranging from 15.5 to 21.5 °C during the 1st stage of the 129th cruise and from 16.1 to 18.4 °C during its 2nd stage (Fig. 2, *k*, *l*).

Thus, the minimum SST values were observed in spring 2022 (19 April – 14 May) and 2023 (16 March – 7 April), while the maximum ones were observed in late August 2022 and in late June – early July 2023. The intra-annual SST amplitude, as determined by measurements conducted in 2022, was 18.2 °C, while in 2023 it was 16.6 °C.

Against the background of clearly pronounced seasonal changes during each separate survey, the SST distribution in the polygon water area exhibited notable spatial heterogeneity. The minimum ranges of the SST spatial changes at the polygon not exceeding 1.5–2 °C were observed at the end of August 2022 (2nd stage of the 123rd cruise) (Fig. 2, *e*) and in the second half of March and early April 2023 (126th cruise) (Fig. 2, *h*), when the warmest and coldest surface waters, respectively, were observed over the entire water area. The maximum SST spatial changes reaching 4–4.5 °C were observed at the polygon in April – May (121st cruise) and December (125th cruise) 2022 and in the first half of October 2023 (1st stage of the 129th cruise), when intensive heating and cooling of surface waters occurred (Fig. 2, *a*, *g*, *k*).

The changes in the SST revealed at the polygon during each separate survey under conditions of non-synchronous survey execution can be considered a superposition of spatial and temporal variability. In order to accurately assess the correlation between the levels of different types of variability, continuous daily averaged data derived from satellite measurements were employed. Fig. 3, *a* shows the SST distribution from satellite data for the period from 1 January 2022 to 31 December 2023 along a 50 m isobath across the entire polygon. A comparison of the SST values derived from *in situ* and satellite data for the same day in grid nodes situated in close proximity to the coordinates of hydrological stations revealed a strong correlation between the change in the SST from *in situ* data and from satellite data during the measurement period (Fig. 3, *b*). The linear relationship coefficient R
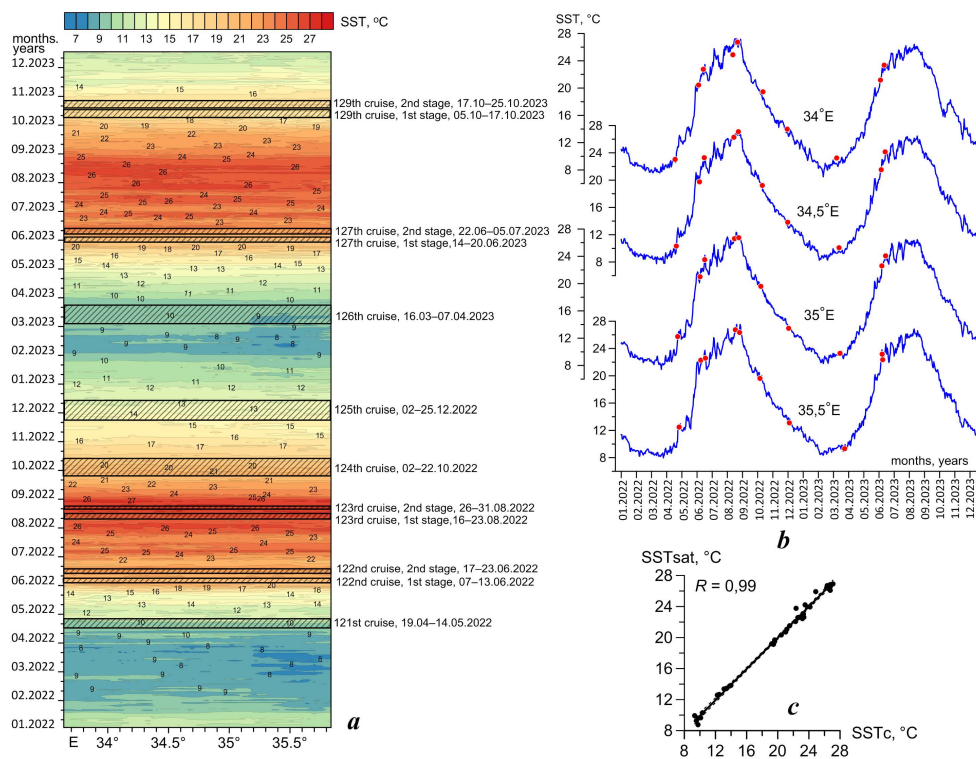
F i g . 3 . Distributions of SST daily averaged values based on satellite data from 1 January 2022 to 31 December 2023 along the 50 m isobath (the periods of surveys are highlighted by black rectangles) (*a*), satellite SST daily averaged values on separate meridians (blue curves) and in situ SST values at these meridians on the same day (red dots) (*b*), a graph of the linear relationship between the satellite (SSTsat) and in situ (SSTis) temperature series (the dashed lines – 99% confidence interval boundaries) (*c*)

between the series of satellite and *in situ* SST values reached 0.99 (Fig. 3, *c*) with statistical significance level α = 0.01 (99% level of statistical confidence).

High spatiotemporal resolution of the satellite SST data and good agreement between the *in situ* and satellite SST values allow the latter to be used to assess the relationship between temporal and spatial temperature variability at the polygon. Fig. 4 demonstrates the distribution of the values of spatial RMS deviation of the SST (SST RMSDs) for each day and temporal RMSD of the SST (SST RMSDt) calculated at each grid node with a step of 0.01° along the 50 m isobath for the period from 1 January 2022 to 31 December 2023. The daily averaged values of spatial SST RMSDs throughout the time period varied from 0.1 to 1.0 °C (Fig. 4, *a*). The increase in the level of the SST spatial variability from satellite data (up to 0.7–0.8 °C) in the second half of April 2022 and the first half of October 2023 (Fig. 5, *a*) is consistent with *in situ* measurements. High spatial heterogeneity of the SST field was also observed in April – May 2022 (121st cruise) and October 2023 (1st stage of the 129th cruise) (Fig. 2, *a, k*).
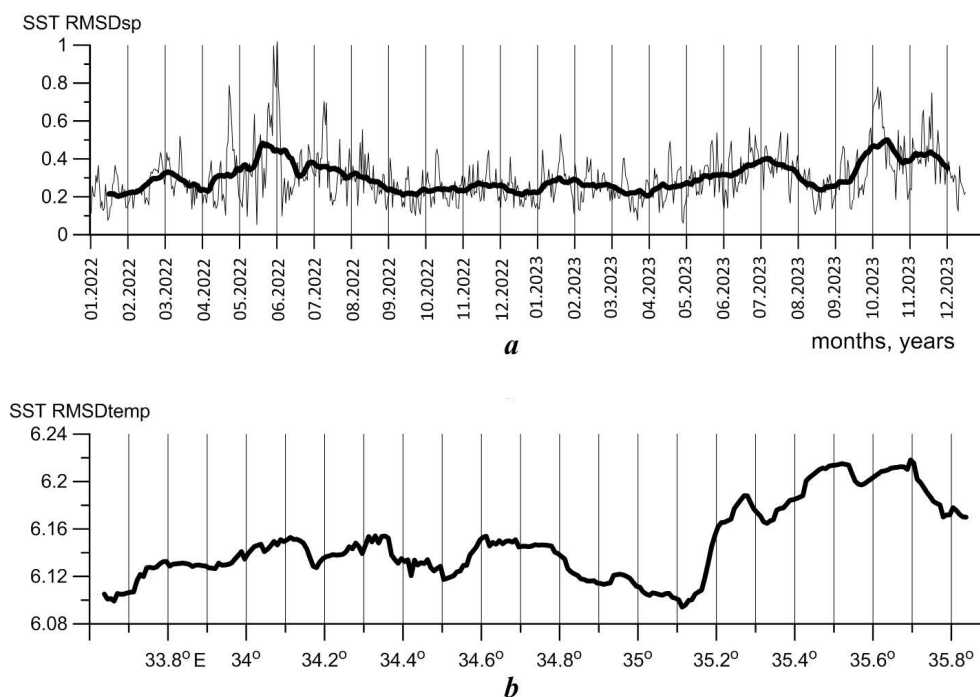
F i g . 4 . Distributions of daily averaged values of spatial SST RMSD (heavy curve – smoothing by a 31-day moving average) (*a*) and values of temporal SST RMSD for the period from 1 January 2022 to 31 December 2023 (*b*) along the 50 m isobath within the measurement polygon based on the satellite data

Distribution of the SST RMSDt values from satellite data indicated that they exhibited minimal spatial variability. For instance, the observed variations within the polygon range from 6.10 to 6.22 °C along the 50 m isobath (Fig. 4, *b*). The highest SST RMSDt values (exceeding 6.16 °C) were observed in the eastern region adjacent to Cape Meganom, within the coastal shelf extension zone.

Thus, the satellite data analysis has revealed that the level of the SST temporal variability is almost an order of magnitude higher than the level of its spatial variability in the water area of the polygon. Spatial homogeneity of the distribution of the SST values at the polygon for each day and high consistency of satellite data with *in situ* measurement data give grounds to believe that the changes in the SST in the water area detected from *in situ* measurement data during each separate survey are mostly related to the SST temporal variability caused by synoptic and seasonal fluctuations.

It is observed that the impact of intra-day variability on the SST distributions was insignificant, as evidenced by data from multi-hour stations. During the daytime, when *in situ* measurements were conducted, changes in the SST did not exceed 0.5 °C while its seasonal fluctuations reached 16.6–18.2 °C. Additionally, the SST variations at the polygon during the intervals of separate surveys ranged from 1.5 to 4.5 °C.

Let us examine the specific characteristics of the SST distribution in greater detail, with a focus on how it varies depending on the time of stations being carried out during the periods of those surveys when the maximum temperature changes at the polygon were observed, namely April – May (121st cruise) and December (125th cruise) 2022 and the first half of October 2023 (1st stage of the 129th cruise) (Fig. 5, *a, e, i*). Based on the data of the 121st cruise in April – May 2022, the SST distribution was characterised by a significant increase of its values at the stations from west to east. This increase was reflected in a positive trend significant at the 95% level of statistical confidence ($\alpha = 0.05$) which shows intensive surface water heating, i.e. the manifestation of the seasonal signal during the survey period (Fig. 5, *a*). Note that measurements in the eastern part of the polygon were made almost two weeks later than in its western part. Distribution of the SST anomalies (AnSST) reflecting shorter-period fluctuations of synoptic scale relative to trend showed an alternation of the SST decreasing and increasing events with a period of 3–4 days in April – May 2022 (121st cruise). At the outset and conclusion of the survey, negative anomalies of the SST in relation to the prevailing trend (up to 1.5 °C) were observed and during the midpoint of the period, high positive anomalies (up to 2.5 °C) were recorded (Fig. 5, *b*). It should be noted that the period of measurements revealed no sharp local decrease of the SST by several degrees accompanied by salinity increase, which is typical for upwelling [34, 35]. Furthermore, an examination of meteorological data revealed the absence of discernible atmospheric irregularities that could have potentially influenced the observed changes in the SST (e.g., prolonged intense precipitation, cold atmospheric intrusion with a pronounced decline in air temperature, passage of cyclones) during the course of this cruise. The aforementioned facts indicate that, under these conditions, the primary influence on the changes in the SST on the synoptic scale was exerted by the local wind which caused the mixing of the surface water layer.
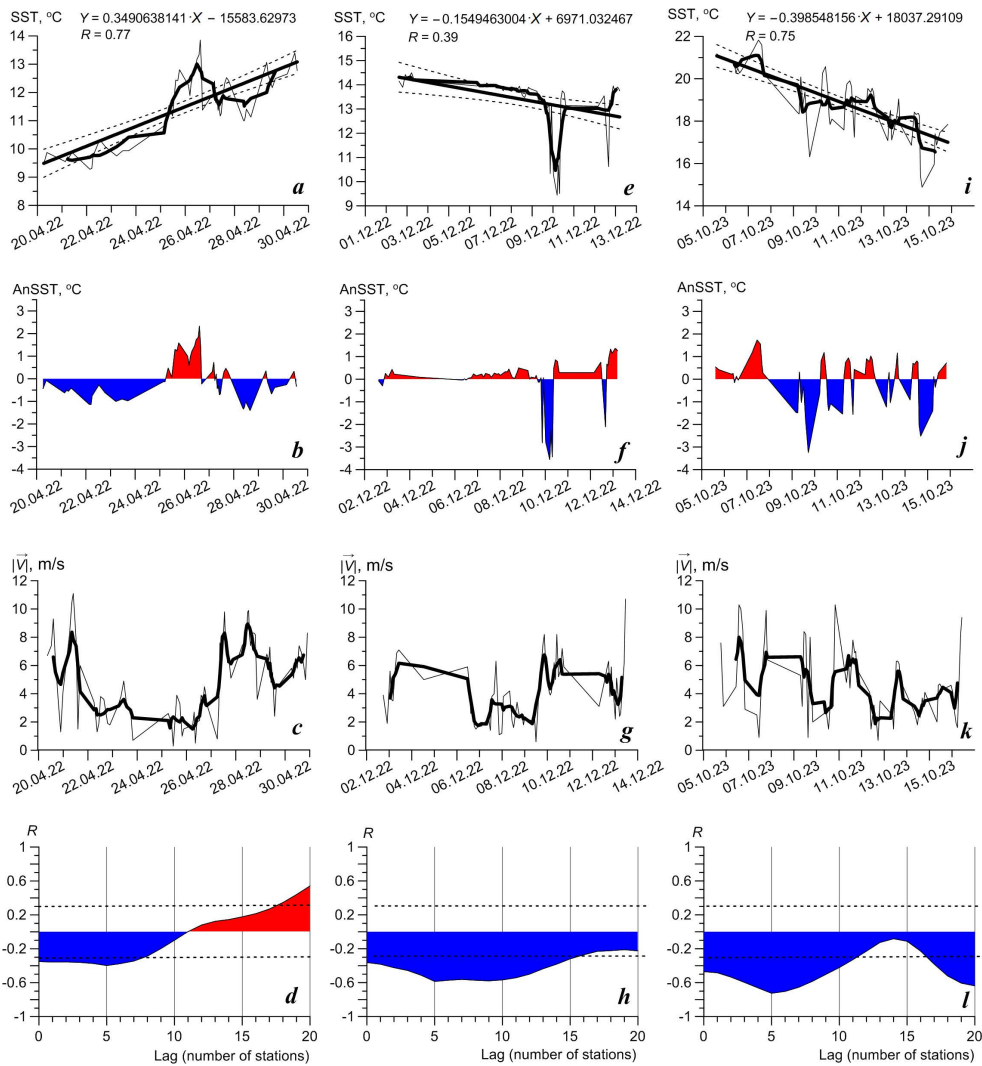
F i g . 5 . Distributions of SST (fine lines) at stations depending on the time of their execution (bold lines – linear trend) (*a*, *e*, *i*); SST anomalies relative to the trend (*b*, *f*, *j*); wind speed modulus (*c*, *g*, *k*); cross-correlation functions between SST values and the wind speed modulus (*d*, *h*, *l*) according to the data from the 121st (*a – d*), 125th (*e –h*), 1st stage of the 129th (*i – l*) cruises. Heavy curves – smoothing by moving average over 7 stations, dashed curves – 99% confidence interval boundaries

According to the distribution of near-water wind speed modulus $|\overline{V}|$ (Fig. 5, *c*), periods with positive SST anomalies corresponded approximately to the periods of wind weakening and, vice versa, wind strengthening led to the appearance of negative SST anomalies. In order to quantify the relationship between changes in the SST and changes in wind speed at the stations, the mutual correlation functions between the SST values and wind speed modulus were calculated with statistical significance level α = 0.01 (99% level of statistical confidence). It should be noted that the series of the SST and wind speed were formed depending on the station number without taking into account the difference in the time intervals between the execution of neighbouring stations, which can have affected the accuracy of the calculated cross-correlation function. This discrepancy can be attributed to the fact that the distance between neighbouring stations at the polygon is, in the majority of cases, approximately the same. However, the time interval between the execution of neighbouring stations can vary considerably, up to several hours. Consequently, the calculation requires the same shift step. Analysis of the cross-correlation function between the SST values and wind speed modulus showed that the highest level of feedback with correlation coefficient *R* up to –0.35 was observed at the phase shift near five stations (Fig. 5, *d*). The average time for five stations to be carried out is 10–12 h, since the average time for neighbouring stations to be carried out, calculated as the ratio of the total number of hours in the measurement period to the number of stations to be carried out, is 2–2.5 h. A similar delay of about 10–12 h in the SST response to wind speed changes was obtained from data from the 122nd and 123rd cruises in the summer of 2022 [30].

In December 2022 (125th cruise), a relatively weak but significant negative trend was observed in the SST distribution, which was attributed to seasonal cooling of the waters (Fig. 5, *e*). In the second half of the survey period, when measurements were made in the shallow part of the polygon east of Cape Meganom (Fig. 2, *g*), high negative SST anomalies (up to 3.5 °C) were observed (Fig. 5, *f*). During this period, south and south-westerly winds prevailed (180–225°), which, given the configuration of the coastline, had the nature of negative surge and could have caused the development of upwelling. At the same time, the analysis of vertical temperature and salinity distributions at the stations in the area of the SST decrease showed that this decrease was not traced deeper than 25 m, with the waters of decreased temperature being characterised by the minimum salinity. If the observed decrease in the SST was caused by upwelling, namely the rise of deeper, colder and saltier waters, the area would be expected to show an increase in salinity throughout the subsurface rather than a decrease. It seems reasonable to conclude that the observed decrease in the SST was caused by the mixing of the upper layer which occurred as a result of a significant increase in wind speed (Fig. 5, *g*). Upon conclusion of the measurement period, a positive SST anomaly (up to 1.3 °C) was identified in the vicinity of the eastern boundary of the polygon, accompanied by a notable decrease in wind speed (Fig. 5, *f*, *g*). Similarly to the findings of the 121st cruise data, a significant relationship was identified between the SST and wind speed modulus with a delay in the response of the SST to wind speed changes of approximately 10–12 hours. The maximum values of coefficient *R* reached –0.6 indicating a strong correlation between two variables (Fig. 5, *h*).

In the first half of October 2023 (1st stage of the 129th cruise) (Fig. 5, *i*), a well-defined negative trend was observed in the SST distribution characterising surface water cooling. Alternation of positive and negative SST anomalies relative to the trend was observed (Fig. 5, *j*). Maximum negative anomalies (−2.5...−3.3 °C) were observed in the coastal zone to the east of Cape Ayu-Dag and in Feodosiya Bay, while maximum positive anomalies (up to 1.5 °C) − at the sea station on the traverse of Cape Ay-Todor (Fig. 5, *j*). Wind speed modulus distribution (Fig. 5, *k*) also demonstrated alternation of periods of wind speed strengthening and weakening on the synoptic scale, corresponding to the periods of the SST decrease and increase, with a maximum *R* value of −0.7 at a shift of about 10−12 h (Fig. 5, *l*).

Therefore, it was established that the SST variability observed at the polygon during each individual survey was attributable to two distinct factors: firstly, the manifestation of seasonal changes on the intra-monthly scale at non-synchronous measurements; and secondly, the SST synoptic variations caused by changes in the local wind speed.

Despite the fact that *in situ* measurements were carried out in all seasons, they are discrete in nature with large time intervals between surveys. The presented data are insufficient to illustrate the continuous evolution of the SST field. Furthermore, they do not indicate the specific phase of the intra-annual SST cycle during which the voyage measurements were conducted. To clarify these features, continuous series of daily averaged data of satellite measurements were analysed.

The spatial homogeneity of the distribution of the SST daily averaged values from satellite data determines the quasi-synchrony of its intra-annual changes in the water area of the entire polygon. This is illustrated by the SST seasonal cycle in different areas of the water area under study obtained from daily averaged values for the period from 1 January 2022 to 31 December 2023 and from daily averaged climate values for the period from 1 January 2008 to 31 December 2023. The SST intra-annual distributions in different water areas demonstrate that the SST intra-annual cycle in 2022 and in 2023 (Fig. 6, *a*) and its climate intra-annual cycle (Fig. 6, *b*) exhibit insignificant variation within the polygon. Some differences were found only for the SST climate values which decrease by almost 1.5 °C during the period of surface water cooling from December to March in the eastern part of the polygon (35.5°E) compared to the rest of the water area (Fig. 6, *b*). Lower surface water temperatures over an extensive shelf in the eastern part of the polygon were also observed from *in situ* data in December 2022 (Fig. 2, *g*) and in late March – early April 2023 (Fig. 2, *h*). The SST minimum climate values (6.5–8 °C) are observed from mid-February to mid-March, the SST maximum ones (25 °C) – in mid-August (Fig. 6, *b*).

Comparison of the SST seasonal cycle in 2022 (Fig. 6, *a*) with its climate seasonal cycle (Fig. 6, *b*) revealed that the SST minimum and maximum in that year were observed in the second half of March and in late August, respectively. This is approximately two weeks later than the climate data would suggest. The SST maximum (27.5 °C) and minimum (8–9 °C) values were higher than the climate ones
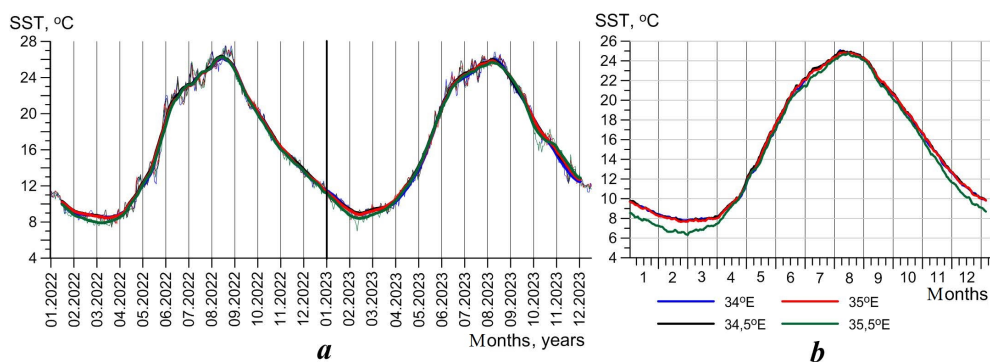
F i g. 6. Distribution of SST daily averaged values for the period from 1 January 2022 to 31 December 2023 (*a*) and its daily averaged climate values from 1 January to 31 December (*b*) at different meridians at grid nodes located above the 50 m isobath according to the satellite data. Heavy curves on fragment *a* are smoothed by a 31-day moving average

by almost 2.5 and 1–1.5 °C, respectively (Fig. 6). It is noteworthy that the data from the *in situ* measurements indicate that the SST maximum values were also observed in the second half of August in 2022, reaching 27.5 °C (Fig. 2, *d, e*).

In 2023, the time of occurrence of the SST minimum according to satellite data corresponded to the climate values. Furthermore, the SST values were found to be 1–1.5 °C higher than the climate ones, with an average of 8–9 °C (Fig. 6). The maximum SST values (26.5 °C) were observed in late July – early August, approximately two weeks earlier than according to climate values, and were almost 1 °C lower than in 2022 and 1.5 °C higher than the climate values (Fig. 6).

Daily averaged satellite data enabled an assessment of the SST synoptic (intra-month) variability in both 2022 and 2023 as well as identification of differences from the climate norms. According to [7, 22], climate annual cycle of the level of the SST synoptic variability, i.e. the SST RMSD values on a synoptic scale (SST RMSDsyn), in the northern Black Sea is characterised by a semi-annual periodicity with maxima in May (main maximum) and October and minima in February – March (main minimum) and August. Our data indicate that the SST RMSDsyn main maximum values occurred in November 2022 (1–1.1 °C) (Fig. 7, *a*), rather than in May, as indicated by the climate data, and in 2023 – in December (1.2–1.25 °C) (Fig. 7, *b*). The second, weaker increase in the level of the SST synoptic variability in 2022 and 2023 was observed not in October, as in the climate data, but in July, with the SST RMSDsyn values reaching 0.95–1.05 °C in 2022 and 1–1.1 °C in 2023 (Fig. 7). It is noteworthy that the SST variability high range at the polygon in the first half of October 2023 revealed by the *in situ* measurements (Fig. 2, *k*) is consistent with the increase in the level of the SST synoptic variability in October 2023 from satellite data (Fig. 7, *b*).
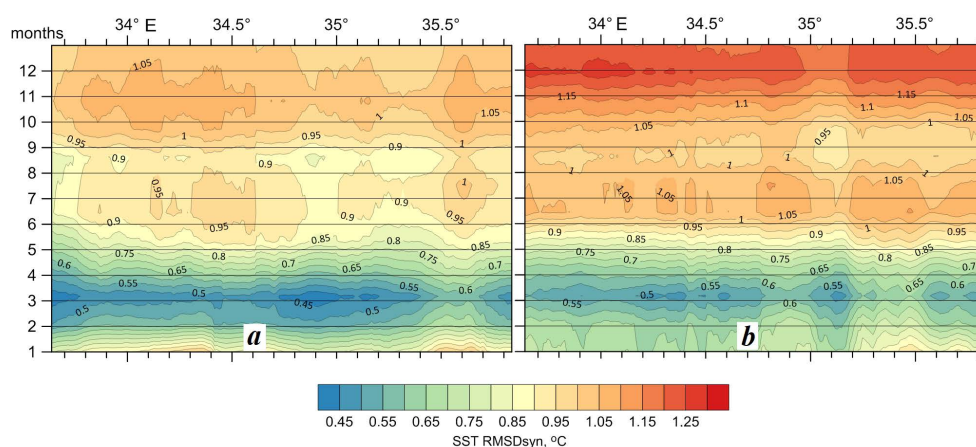
F i g . 7 . Intra-annual variation of the SST RMSDsyn values based on the satellite data in 2022 (*a*) and 2023 (*b*) along the 50 m isobath within the survey area

In 2022 and 2023, the SST RMSDsyn minimum values (0.4–0.5 °C) were observed in March. The second decrease in the level of synoptic variability was observed in August – September (SST RMSDsyn ~ 0.85–0.9 °C in 2022 and 0.9–0.95 °C in 2023) (Fig. 7). In general, the periods of lowering of the level of the SST synoptic variability, as indicated by satellite data, corresponded to the climate intra-annual cycle and periods of maximum cooling and heating of surface waters in 2022 and 2023. According to *in situ* measurements, the minimum ranges of the changes in the SST at the polygon associated with synoptic variations were also observed in late August 2022 and in the second half of March – early April 2023, when the warmest and coldest surface waters, respectively, were observed throughout the water area (Fig. 2, *e*, *h*).

In addition to the peculiarities of seasonal and synoptic variability, continuous series of satellite data enabled the assessment of the interannual changes in the SST over a two-year period. Given that the SST interannual variability level in the area under study is comparable to that of its synoptic variability [7], the daily averaged SST values were taken on a monthly basis for each month of both 2022 and 2023. This allowed for the minimisation of the manifestation of synoptic variability. Subsequently, the SST monthly averaged anomalies (AnSST) for 2022 and 2023 were calculated as the difference between the actual SST value and the SST climate annual averaged value for the specified month. Distribution of these anomalies, excluding the manifestation of seasonal and synoptic variability, made it possible to identify the differences of monthly averaged SST values in 2022 and 2023 from the climate norm and to assess the SST interannual variations. The AnSST distributions in different areas of the polygon showed that interannual changes in the SST as well as its intra-annual cycle are qualitatively similar throughout the water area (Fig. 8, *a*). Estimates of the linear relationship of the AnSST series at different grid nodes showed their high spatial consistency with correlation coefficients R ~ 0.90–0.99 with statistical significance level $\alpha = 0.01$ (Fig. 8, *b*).
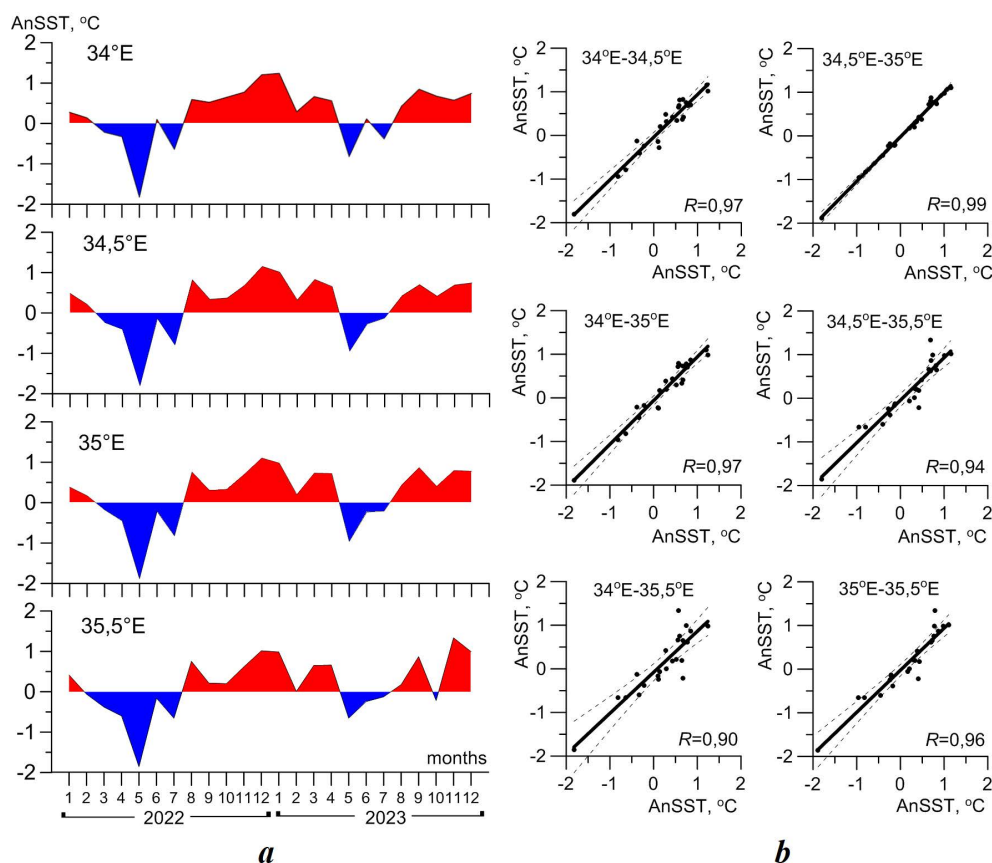
F i g . 8 . Distribution of AnSST from January 2022 to December 2023 at separate grid nodes above the 50 m isobath (*a*), graphs of the linear relationship between AnSST series on different meridians (the dashed lines – 99 % confidence interval boundaries) (*b*)

The AnSST distributions demonstrated that the discrepancies between the SST monthly averaged values derived from satellite data between 2022 and 2023 and the climate norms reached a magnitude of nearly 2 °C. The SST values were observed to exceed the climate values during the period from January to February 2022, from August 2022 to April 2023 and from August to December 2023. The SST maximum positive anomalies (1–1.3 °C) were observed in December 2022 and January 2023 as well as in November – December 2023 (Fig. 8, *a*). The SST values were lower than the climate ones only from March to July 2022 and from May to July 2023. The SST maximum negative anomalies (in their magnitude) observed during the 2022 and 2023 periods were recorded in May, with the values in 2023 (–0.7...–1 °C) exhibiting a decrease of approximately 100% compared to those observed in 2022 (−1.8...−2 °C) (Fig. 8, *a*). In general, the series of the SST monthly averaged anomalies for 2022−2023, with a predominance of their positive values, reflect a trend towards the higher SST during the last two years (Fig. 8, *a*).

Conclusions

The SST variability on different time scales was estimated based on the hydrological measurements made off the Crimean coast of during 2022–2023 cruises of R/V *Professor Vodyanitsky* and *Copernicus* satellite data. The results of the survey demonstrate that the SST minimum values were recorded in April and May 2022 and March and April 2023. Conversely, the SST maximum values were observed in late August 2022 and late June – early July 2023. The SST intra-annual amplitude was 18.2 °C in 2022, while in 2023 it was 16.6 °C.

The data demonstrate that the minimum ranges of changes in the SST at the polygon (1.5–2 °C) were recorded in late August 2022 and in the second half of March – early April 2023, when the warmest and coldest surface waters, respectively, were observed throughout the water area. The maximum changes in the SST (up to 4–4.5 °C) were observed in April – May and December 2022 and in the first half of October 2023, when intensive heating and cooling of surface waters occurred.

It is demonstrated that the SST field spatial heterogeneity was associated with seasonal heating or cooling of water, which manifested on the intra-monthly scale, and with the SST synoptic variations determined by local atmospheric conditions. The SST increase (decrease) periods on the synoptic scale were found to correspond to periods of weakening (strengthening) of the local wind, with the SST response to wind speed changes delayed by 10–12 h.

A high level of agreement between the SST satellite and *in situ* measurements was observed, as indicated by correlation coefficient $R \sim 0.99$. The present study revealed notable differences in the intra-annual cycle of the SST daily averaged values from satellite data in 2022 and 2023 when compared to the climate norms. In 2022, the SST minimum and maximum values were higher than the climate ones by almost 2.5 and 1.5 °C, respectively, and were observed about two weeks later than according to climate data. In 2023, the SST maximum and minimum values were higher than the climate ones by almost 1.5 °C; at that, the time of occurrence of the SST minimum corresponded to the climate data and the SST maximum was observed approximately two weeks earlier than according to the climate data.

The intra-annual cycles of the level of the SST synoptic variability were found to deviate from the climate norm. In 2022, the main maximum was observed not in May, as follows from the climate data, but in November, while in 2023 – in December. The second increase in the level of synoptic variability in 2022 and 2023 occurred in July, not October, as indicated by the climate data. The periods of decreased level of the SST synoptic variability in 2022 and 2023 corresponded to the climatic intra-annual cycle and were observed in March (main minimum) and August – September. In accordance with the data obtained from *in situ* cruise measurements, the SST minimum synoptic variations were also observed in late August 2022 and in the second half of March – early April 2023.

The satellite data indicate that the SST monthly averaged anomalies relative to the climate norms were predominantly positive from 2022 to 2023. The SST maximum positive anomalies (1–1.3 °C) were observed from December 2022 to January 2023 and in November – December 2023.

R E F E R E N C E S

1. Ginzburg, A.I., Kostianoy, A.G. and Sheremet, N.A., 2004. Seasonal and Inter-annual Variability of the Black Sea Surface Temperature as Revealed from Satellite Data (1982–2000). *Journal of Marine Systems*, 52(1–4), pp. 33–50. https://doi.org/10.1016/j.jmarsys.2004.05.002

2. Oguz, T., Dippner, J.W. and Kaymaz, Z., 2006. Climatic Regulation of the Black Sea Hydro-Meteorological and Ecological Properties at Interannual-to-Decadal Time Scales. *Journal of Marine Systems*, 60(3–4), pp. 235–254. https://doi.org/10.1016/j.jmarsys.2005.11.011

3. Ginzburg, A.I., Kostianoy, A.G. and Sheremet, N.A., 2008. Sea Surface Temperature Variability. In: A. G. Kostianoy, A. N. Kosarev, eds. *The Black Sea Environment. The Handbook of Environmental Chemistry.* Berlin, Heidelberg: Springer-Verlag. Vol. 5Q, pp. 255–275. https://doi.org/10.1007/698_5_067

4. Tuzhilkin, V.S., 2008. Thermohaline Structure of the Sea. In: A. G. Kostianoy and A. N. Kosarev, eds. *The Black Sea Environment. The Handbook of Environmental Chemistry.* Berlin, Heidelberg: Springer-Verlag. Vol. 5Q, pp. 217–253. https://doi.org/10.1007/698_5_077

5. Ivanov, V.A. and Belokopytov, V.N., 2013. *Oceanography of the Black Sea*. Sevastopol: ECOSI-Gidrofizika, 210 p.

6. Artamonov, Yu.V., Skripaleva, E.A. and Fedirko, A.V., 2017. Regional Features of Long-term Variability of the Black Sea Surface Temperature. *Russian Meteorology and Hydrology*, 42(2), pp. 105–112. https://doi.org/10.3103/S1068373917020042

7. Artamonov, Yu.V., Skripaleva, E.A. and Fedirko, A.V., 2020. Regional Features of the Temperature Field Synoptic Variability on the Black Sea Surface from Satellite Data. *Physical Oceanography*, 27(2), pp. 186–196, https://doi.org/10.22449/1573-160X-2020-2-186-19

8. Ginzburg, A.I., Kostianoy, A.G. and Sheremet, N.A., 2008. [Long-Term Variability of the Black Sea Surface Temperature and Its Response to Global Atmospheric Effects]. *Sovremennye Problemy Distantsionnogo Zondirovaniya Zemli iz Kosmosa*, 5(2), pp. 76–83 (in Russian).

9. Kazmin, A.S. and Zatsepin, A.G., 2007. Long-Term Variability of Surface Temperature in the Black Sea, and its Connection with the Large-Scale Atmospheric Forcing. *Journal of Marine Systems*, 68(1–2), pp. 293–301. https://doi.org/10.1016/j.jmarsys.2007.01.002

10. Capet, A., Barth, A., Beckers, J.-M. and Marilaure, G., 2012. Interannual Variability of Black Sea's Hydrodynamics and Connection to Atmospheric Patterns. *Deep-Sea Research. Part II: Topical Studies in Oceanography*, 77–80, pp. 128–142. https://doi.org/10.1016/j.dsr2.2012.04.010

11. Shapiro, G.I., Aleynik, D.L. and Mee, L.D., 2010. Long Term Trends in the Sea Surface Temperature of the Black Sea. *Ocean Science*, 6, pp. 491–501. https://doi.org/10.5194/os-6-491-2010

12. Sakalli, A. and Başusta, N., 2018. Sea Surface Temperature Change in the Black Sea under Climate Change: A Simulation of the Sea Surface Temperature up to 2100. *International Journal of Climatology*, 38(13), pp. 4687–4698. https://doi.org/10.1002/joc.5688

13. Lima, L., Ciliberti, S.A., Aydoğdu, A., Masina, S., Escudier, R., Cipollone, A., Azevedo, D., Causio, S., Peneva, E. [et al.], 2021. Climate Signals in the Black Sea from a Multidecadal Eddy-Resolving Reanalysis. *Frontiers in Marine Science*, 8, 710973. https://doi.org/10.3389/fmars.2021.710973

14. Podymov, O.I., Zatsepin, A.G. and Ocherednik, V.V., 2021. Increase of Temperature and Salinity in the Active Layer of the North-Eastern Black Sea from 2010 to 2020. *Physical Oceanography*, 28(3), pp. 257–265. https://doi.org/10.22449/1573-160X-2021-3-257-265

15. Dorofeev, V.L. and Sukhikh, L.I., 2023. Analysis of Long-Term Variability of Hydrodynamic Fields in the Upper 200-Meter Layer of the Black Sea Based on the Reanalysis Results. *Physical Oceanography*, 30(5), pp. 581–593.

16. Stanev, E.V., Peneva, E. and Chtirkova, B., 2019. Climate Change and Regional Ocean Water Mass Disappearance: Case of the Black Sea. *Journal of Geophysical Research: Oceans*, 124(7), pp. 4803–4819. https://doi.org/10.1029/2019JC015076

17. Morozov, A.N. and Mankovskaya, E.V., 2020. Cold Intermediate Layer of the Black Sea according to the Data of the Expedition Field Research in 2016–2019. *Ecological Safety of Coastal and Shelf Zones of Sea*, (2), pp. 5–16. https://doi.org/10.22449/2413-5577-2020-2-5-16 (in Russian).

18. Sokolova, E., Stanev, E.V., Yakubenko, V., Ovchinnikov, I. and Kos'yan, R.D., 2001. Synoptic Variability in the Black Sea. Analysis of Hydrographic Survey and Altimeter Data. *Journal of Marine Systems*, 31(1–3), pp. 45–63. https://doi.org/10.1016/S0924-7963(01)00046-X

19. Zatsepin, A.G., Ginzburg, A.I., Kostianoy, A.G., Kremenetskiy, V.V., Krivosheya, V.G., Stanichny, S.V. and Poulain, P.-M., 2003. Observation of Black Sea Mesoscale Eddies and Associated Horizontal Mixing. *Journal of Geophysical Researches*, 108(C8), 3246. https://doi.org/10.1029/2002JC001390

20. Tuzhilkin, V.S., Arkhipkin, V.S., Myslenkov, S.A. and Samborsky, T.V., 2012. Synoptic Variability of Thermo-Haline Conditions in the Russian Part of the Black Sea Coastal Zone. *Vestnik Moskovskogo Universiteta. Seria 5, Geografia*, (6), pp. 46–53 (in Russian).

21. Lishaev, P.N., Korotaev, G.K., Knysh, V.V., Mizyuk, A.I. and Dymova, O.A., 2014. Recovery of Synoptic Variability of Hydrophysical Fields of the Black Sea Based on Reanalysis for 1980–1993. *Morskoy Gidrofizicheskiy Zhurnal*, (5), pp. 49–68 (in Russian).

22. Novikov, A.A. and Tuzhilkin, V.S., 2015. Seasonal and Regional Variations of Water Temperature Synoptic Anomalies in the Northeastern Coastal Zone of the Black Sea. *Physical Oceanography*, (1), pp. 39–48. https://doi.org/10.22449/1573-160X-2015-1-39-48

23. Kubryakov, A.A. and Stanichny, S.V., 2015. Seasonal and Interannual Variability of the Black Sea Eddies and its Dependence on Characteristics of the Large-Scale Circulation. *Deep Sea Research. Part I: Oceanographic Research Papers*, 97, pp. 80–91. https://doi.org/10.1016/j.dsr.2014.12.002

24. Kubryakov, A.A., Bagaev, A.V., Stanichny, S.V. and Belokopytov, V.N., 2018. Thermohaline Structure, Transport and Evolution of the Black Sea Eddies from Hydrological and Satellite Data. *Progress in Oceanography*, 167, pp. 44–63. https://doi.org/10.1016/j.pocean.2018.07.007

25. Artamonov, Yu.V., Fedirko, A.V., Skripaleva, E.A., Shutov, S.A., Garmashov, A.V., Deryushkin, D.V., Zavyalov, D.D., Kolmak, R.V., Shapovalov, R.O., Shapovalov, Yu.I. and Shcherbachenko, S.V., 2019. Seasonal and Synoptic Changes in the Water Structure to the Southwest of the Crimean Peninsula in the Autumn and Winter 2017 (98th and 101st cruises of R/V *Professor Vodyanitsky*). *Ecological Safety of Coastal and Shelf Zones of Sea*, (3), pp. 4–18. https://doi.org/10.22449/2413-5577-2019-3-4-18 (in Russian).

26. Artamonov, Yu.V., Skripaleva, E.A., Fedirko, A.V., Shutov, S.A., Derjushkin, D.V., Shapovalov, R.O., Shapovalov, Yu.I. and Shcherbachenko, S.V., 2020. Waters Circulation in the Northern Part of the Black Sea in Summer – Winter of 2018. *Ecological Safety of Coastal and Shelf Zones of Sea*, (1), pp. 69–90. https://doi.org/10.22449/2413-5577-2020-1-69-90 (in Russian).

27. Aleskerova, A.A., Kubryakov, A.A., Goryachkin, Yu.N. and Stanichny, S.V., 2017. Propagation of Waters from the Kerch Strait in the Black Sea. *Physical Oceanography*, (6), pp. 47–57. https://doi.org/10.22449/1573-160X-2017-6-47-57

28. Ivanov, V.A., Katunina, E.V. and Sovga, E.E., 2016. Assessments of Anthropogenic Impacts on the Ecosystem of the Waters of the Herakleian Peninsula in the Vicinity of Deep Drains. *Processes in GeoMedia*, 1(5), pp. 62–68 (in Russian).

29. Bondur, V.G., Ivanov, V.A., Vorobiev, V.E., Dulov, V.A., Dolotov, V.V., Zamshin, V.V., Kondratiev, S.I., Lee, M.E. and Malinovsky, V.V., 2020. Ground-to-Space Monitoring of Anthropogenic Impacts on the Coastal Zone of the Crimean Peninsula. *Physical Oceanography*, 27(1), pp. 95–107. https://doi.org/10.22449/1573-160X-2020-1-95-107

30. Artamonov, Yu.V., Skripaleva, E.A., Fedirko, A.V. and Nikolsky, N.V., 2023. Synoptic Variability of Water Temperature off the Crimea Coast in Summer 2022 Based on the Contact and Satellite Data. *Physical Oceanography*, 30(6), pp. 811–825.

31. Nardelli, B.B., Tronconi, C., Pisano, A. and Santoleri, R., 2013. High and Ultra-High Resolution Processing of Satellite Sea Surface Temperature Data over Southern European Seas in the Framework of MyOcean Project. *Remote Sensing of Environment*, 129, pp. 1–16. https://doi.org/10.1016/j.rse.2012.10.012

32. Rubakina, V.A., Kubryakov, A.A. and Stanichny, S.V., 2019. Seasonal and Diurnal Cycle of the Black Sea Water Temperature from Temperature-Profiling Drifters Data. *Sovremennye Problemy Distantsionnogo Zondirovaniya Zemli iz Kosmosa*, 16(5), pp. 268–281. https://doi.org/10.21046/2070-7401-2019-16-5-268-281 (in Russian).

33. Rubakina, V.A., Kubryakov, A.A. and Stanichny, S.V., 2019. Seasonal Variability of the Diurnal Cycle of the Black Sea Surface Temperature from the SEVIRI Satellite Measurements. *Physical Oceanography*, 26(2), pp. 157–169. https://doi.org/10.22449/1573-160X-2019-2-157-169

34. Borovskaya, R.V., Lomakin, P.D., Panov, B.N. and Spiridonova, E.O., 2008. Structure and Interannual Variability of Characteristics of Inshore Black Sea Upwelling on Basis of Satellite Monitoring Data. *Issledovaniye Zemli iz Kosmosa*, (2), pp. 26–36 (in Russian).

35. Lomakin, P.D., 2018. Upwelling in the Kerch Strait and the Adjacent Waters of the Black Sea Based on the Contact and Satellite Data. *Physical Oceanography*, 25(2), pp. 114–123. https://doi.org/10.22449/1573-160X-2018-2-114-123

About the authors:

Yuri V. Artamonov, Leading Research Associate, Marine Hydrophysical Institute of RAS (2 Kapitanskaya St., Sevastopol, 299011, Russian Federation), Dr.Sci. (Geogr.), **ResearcherID: AAC-6651-2020**, *artam-ant@yandex.ru*

Elena A. Skripaleva, Senior Research Associate, Marine Hydrophysical Institute of RAS (2 Kapitanskaya St., Sevastopol, 299011, Russian Federation), Ph.D. (Geogr.), **ResearcherID: AAC-6648-2020**, *sea-ant@yandex.ru*

Aleksandr V. Fedirko, Junior Research Associate, Marine Hydrophysical Institute of RAS (2 Kapitanskaya St., Sevastopol, 299011, Russian Federation), **ResearcherID: AAC-6629-2020**, *vault102@gmail.com*

Contribution of the authors:

Yuri V. Artamonov – general scientific supervision of the research, setting of study aims and objectives, development of methods and performance of experiments, qualitative analysis of the results and interpretation thereof, discussion of the study results, drawing conclusions

Elena A. Skripaleva – review of literature on the research topic, qualitative analysis of the results and interpretation thereof, processing and description of the study results, discussion of the study results, drawing conclusions, article text preparation and refinement

Aleksandr V. Fedirko – development and debugging of software for experiment data secondary processing, computer implementation of algorithms, chart and diagram construction, participation in discussion of the article

All the authors have read and approved the final manuscript.

Original paper

Hydrochemical Composition
of the Chernaya River (Crimea) in 2012–2023

S. I. Kondratev

Marine Hydrophysical Institute of RAS, Sevastopol, Russia
e-mail: skondratt@mail.ru

Abstract

The paper aims to evaluate hydrochemical composition of the Chernaya River waters, which is the major supplier of fresh water in Sevastopol, as well as to assess the influence of the river runoff on the ecological state of Sevastopol Bay. Flowing from the Chernorechenskoye Reservoir, the Chernaya River crosses the Baydar Valley and on its way takes in several tributaries, not having passed through the reservoir geochemical filter. Then it loses the most of its flow at several water intakes near the village of Khmelnitskoe and turns into a stream. The stream again becomes a relatively full-flowing river after the inflow of circulating water from the treatment facilities near the village of Sakharnaya Golovka, and finally, it discharges into Sevastopol Bay near the Inkerman basin. In order to investigate the transformation of the river waters hydrochemical composition as it moves from the Chernorechenskoye Reservoir to the river mouth, graphs of average concentration for some hydrochemical elements for four hydrological seasons 2012–2023 were constructed for 10 stations located on the river and two conditional stations in the water area of the bay (averaged data for the Inkerman basin and 30 stations of the bay). The waters of the Chernorechenskoye Reservoir and Chernaya River were revealed to be close in composition along the length of almost the entire channel from the outlet to the water intake near the village of Shturmovoe. Further, the composition of the river waters is determined by wastewater. Directly (without taking into account wastewater), the Chernaya River supplies significant amounts of nitrates, silicic acid and ammonium to Sevastopol Bay, but not phosphates, which come with the wastewater.

Keywords: Chernaya River, Crimea, hydrochemical composition, nutrients, carbonate system, Sevastopol Bay

Гидрохимическая структура реки Черной (Крым) в 2012–2023 годах

С. И. Кондратьев

Морской гидрофизический институт РАН, Севастополь, Россия
e-mail: skondratt@mail.ru

Аннотация

Цель статьи – оценка гидрохимического состава вод реки Черной, являющейся основным поставщиком пресных вод в г. Севастополе, а также влияния стока этой реки на экологию Севастопольской бухты. Река Черная, вытекающая из Чернореченского водохранилища, на своем пути пересекает Байдарскую долину, вбирает несколько притоков, не прошедших через геохимический фильтр водохранилища, теряет бóльшую часть своего потока на нескольких водозаборах в районе с. Хмельницкого и превращается в ручей. Вновь становится относительно полноводной рекой после поступления в нее оборотных вод очистных сооружений возле с. Сахарная Головка и наконец впадает в Севастопольскую бухту возле Инкерманского ковша. Чтобы проследить за изменением гидрохимического состава вод реки по мере продвижения от Чернореченского водохранилища до устья, для 10 станций, расположенных на реке, и двух условных станций на акватории бухты (осредненные данные для Инкерманского ковша и 30 станций бухты) были построены графики средних значений концентраций некоторых гидрохимических элементов для четырех гидрологических сезонов 2012–2023 гг. Выявлено, что воды Чернореченского водохранилища и реки Черной сходны по составу на протяжении почти всего русла от выхода на поверхность до водозабора под с. Штурмовым, далее состав вод реки определяют сточные воды. Непосредственно река Черная (без учета сточных вод) поставляет в Севастопольскую бухту значительные количества нитратов, кремнекислоты и аммония; фосфаты поступают со сточными водами.

Ключевые слова: река Черная, Крым, гидрохимический состав, биогенные элементы, карбонатная система, Севастопольская бухта

Introduction

In fact, the Chernaya River flows out of the Skelskaya Cave, almost immediately (two hundred metres from the source) begins to fill the Chernorechenskoye Reservoir (CR), then comes again to the surface through the water intake under the reservoir and flows into the eastern apex of Sevastopol Bay after about 35 km. This river is one of the most important elements of the Sevastopol ecology. Firstly, the Chernaya River is the main external supplier to the bay waters of various hydrochemical components, such as nutrients [1], carbonate system elements [2], trace elements [3], organochlorine compounds [4] and aromatic polycyclic hydrocarbons [5]. Secondly, the waters of the Chernaya River are the main source of fresh water

for the city of Sevastopol, and the quality of the water is deemed satisfactory. In accordance with work [1], a mere 1.7% of the fresh water supplied to Sevastopol fails to meet the requisite sanitary and chemical indicators. This water is drawn from the North Side water supply system.

The influence of the Chernaya River on the hydrochemical composition of the Sevastopol Bay waters has been the subject of considerable scientific investigation [6–8], including in the most recent works [1–5], yet the changes that occur in the composition of waters on their way from the CR to the river mouth have attracted much less attention from researchers. The population of Sevastopol is so accustomed to the fact that the water supply system provides sufficiently clean water (additional purification is still recommended for food use) that they demonstrate interest in water supply problems only when there are interruptions in supply [2] or where the quality of running water is uncertain, as was the case following the dam failure on the Baydarka River in 2006 [3].

In light of the significance of observations pertaining to the impact of the Chernaya River waters on the Sevastopol Bay ecosystem, Marine Hydrophysical Institute (MHI), which initiated its investigation into the hydrological and hydrochemical characteristics of the bay waters towards the end of the 20th century, incorporated the lower Chernaya River waters (from the CR to the Inkerman basin (IB)) into the scope of its study in 2006. The principal findings of the results of the 2006–2011 observations published in [9] indicate that the Chernaya River waters up to the water intake near the village of Shturmovoe exhibit a relatively consistent hydrochemical composition with the CR water, which the surrounding villages have been utilising for food purposes for an extended period without any notable concerns. However, the hydrochemical composition of the water deteriorates significantly between the village of Shturmovoe and the railway bridge across the river.

Thus, the river is conditionally divided into two parts on the basis of water quality. The water from one part is suitable for domestic purposes, while the water from the second part, which contains significant amounts of nutrients, is comparable to phosphorus-containing fertiliser for agricultural needs. All these unfavourable changes in water composition are attributed to the activity of the KOS-3 sewage treatment plant in the village of Sakharnaya Golovka [10], which discharges its wastewater into the river below the water intake near the village of Shturmovoe.

Recent studies devoted to the Chernaya River have addressed the significant issue of water composition alteration during the transition from fresh to saline conditions in the estuary zone between the railway and highway bridges [4, 10–13]. Nevertheless, these studies fail to address the issue of changes in water composition on the route from the reservoir to the IB, which was the objective of the research initiated in 2006 and continued until the present (the most recent survey was conducted in December 2023).

---

[1] Antonova, A., 2017. You Can Drink Tap Water. *Sevastopol'skaja Gazeta*. Online available at: https://sevastopol.press/2017/09/04/vodu-iz-krana-mozhno-pit/ [Accessed: 12 April 2024].

[2] Aleshina, N., 2024. Emergency due to Mud. Sevastopol Remains without Water for the Fourth Day. *KRym.AIF.RU*. Available at: https://krym.aif.ru/society/jkh/chs_iz-za_gryazi_sevastopol_ostayotsya_bez_vody_chetvertye_sutki [Accessed: 12 April 2024].

[3] Ryabov, M., 2006. The Tap Water is Poisoned! *Sevastopol'skaja Gazeta.* Available at: https://sevastopol.press/2006/11/09/voda-otravlena/ [Accessed: 12 April 2024].

This study aims at analysing changes in the hydrochemical composition of the waters of the lower Chernaya River in 2012–2023.

Materials and methods

The findings of the quarterly environmental monitoring of Sevastopol Bay at 36 stations and the lower Chernaya River at 10 stations (Fig. 1), conducted by the MHI Marine Biogeochemistry Department were employed in this study. The sequence of the stations is as follows: *1–0–4–6–5–3–2–2a–7–8–9–10*. Stations *11, 12* were carried out in advance, during the Sevastopol Bay expedition, for details see [15]. From 2012 to December 2023, a total of 36 expeditions were conducted. While surveys were planned in each of the four hydrological seasons, not all of them were carried out. The water samples were transported to a fixed onshore laboratory within a timeframe of 2–3 hours after collection, where they were subjected to immediate analysis. Before analysing dissolved mineral forms of nutrients (silicic acid, phosphates, nitrate, nitrite, ammonium), water samples were pre-filtered through a membrane filter with a pore size of 0.45 µm.

Dissolved oxygen content was determined by the Winkler method [16], mineral forms of nutrients (phosphates, silicon, nitrate and nitrite nitrogen) were analysed photometrically in accordance with work [4].
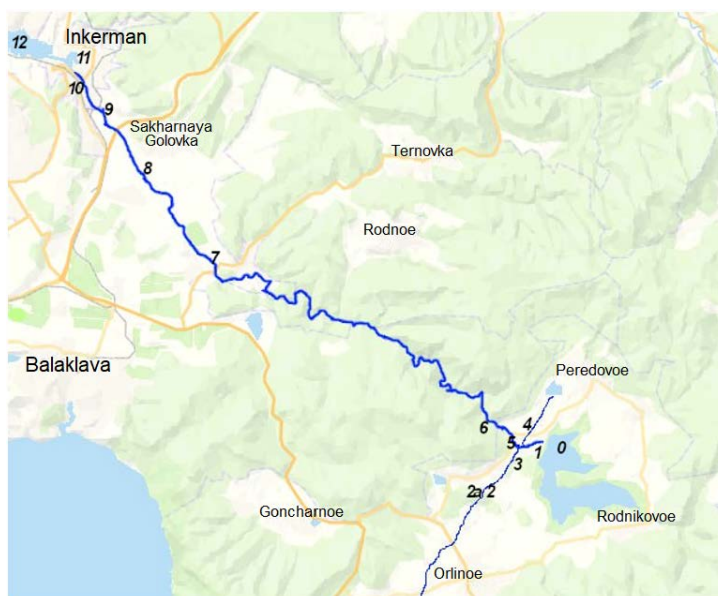
F i g . 1 . Map of stations for sampling water from the River Chernaya. Notations are given in the table below

---

[4] Bordovsky, O.K. and Ivanenkov, V.N., eds., 1978. [*Methods of Hydrochemical Studies of the Ocean*]. Moscow: Nauka, 271 p. (in Russian).

Station number	Coordinates		Reference points
	N	E	
0	44.492033	33.809025	Reservoir surface over the water intake
1	44.490475	33.805073	Water intake under the reservoir
2	44.475604	33.790574	Baydarka River, former pond
2a	44.475604	33.790574	Concrete trough bypassing the pond
3	44.486921	33.794287	Baydarka River, pipe-bridge outside the village of Ozernoe
4	44.492832	33.792845	Urkusta River
5	44.492115	33.792624	Highway bridge of the village Ozernoe– the village of Peredovoe
6	44.496838	33.784174	Gauging station near Krasnaya Skala
7	44.545083	33.662152	Gauging station near the village of Khmelnitskoe
8	44.574922	33.629644	Highway bridge near the village of Shturmovoe
9	44.595650	33.609477	Railway bridge near Inkerman
10	44.605719	33.601888	Highway bridge near Inkerman

Note: Station *11* – the average over three stations of the Inkerman basin, station *12* – the average over 33 stations in Sevastopol Bay.

Ammonium nitrogen was determined using the modified method of Sagi–Solorzano based on the phenol-hypochlorite reaction using sodium nitroprusside and sodium citrate [5]. The pH value was determined potentiometrically in an open cell with calibration by NBS scale buffer solutions; total alkalinity was determined by direct titration with potentiometric termination.

The Grafer programme was employed to plot the figures of sequential changes in the composition of each hydrochemical element when progressing from the CR surface to Sevastopol Bay.

[5] Bordovsky, O.K. and Chernyakova, A.M., eds., 1992. [*Modern Methods of Hydrochemical Studies of the Ocean*]. Moscow: IO AN SSSR, 199 p. (in Russian).

Results

First, we explain the location of stations along the Chernaya River in more detail (Table). Station *0* represents the reservoir surface waters, while st. *1* – the CR bottom waters (water intake under the reservoir, from which the Chernaya River flows out for the second time); further on, the river waters take in two tributaries: the Baydarka River (st. *2*, *3*) and the Urkusta River (St. *4*). Prior to st. *5*, these three rivers are combined. At st. *6*, they have already become a homogeneous mass, with multiple water intakes along the way. The first intake is located near the village of Khmelnitskoe (st. *7*), while the last intake is situated near the village of Shturmovoe (st. *8*). Following the diversion of the Chernaya River through a series of water intakes, a residual stream of water remains. It receives wastewater from KOS-3, which changes the water hydrochemical composition qualitatively to st. *9*. At st. *10*, waters have already become partially distributed marine ones (their salinity is rarely less than 16). Two more stations – *11*, *12* – represent averaged data for surface waters of the Inkerman basin (3 stations) and all Sevastopol Bay (33 stations). Data from some stations in Sevastopol Bay, namely in the Southern Bay apex, where 10–100-fold exceedance of MPC for nitrate and ammonium was constantly observed [17], were not taken into account during averaging.

It is important to note that prior to the formation of the CR, the Chernaya River had a considerable number of tributaries, which now contribute to the CR. The volume of water from these tributaries is comparable to that of Sevastopol Bay. The CR is a geochemical filter, which is why it is inaccurate to suggest that tributaries flow into it. Biochemical processes extract nutrients, and the products of this processing eventually settle to the bottom of the river. This transformation results in a natural self-purification of the waters which can be used for food without additional treatment. All this becomes possible only because the reservoir, due to its strategic importance, is not used as a recreation object at all; there are enough artificially created stanks, ponds and other water bodies for recreation of the population of the nearest villages.

Two principal tributaries of the Chernaya River exhibit a significant distinction. The Urkusta River originates from the pond near the village of Peredovoe, traversing a geochemical filter. In contrast, a comparable filtration system for the Baydarka River was dismantled due to an unanticipated incident in November 2006[3)] and was not subsequently restored. Instead of constructing treatment facilities for the Baydarka River waters and emergency discharge of the CR waters, a concrete trough was constructed to collect rainfall parallel to the Baydarka River bed (st. *2a*). As a result, the Baydarka River, which collects waste from the village of Orlinoe and agricultural lands as it goes, flows untreated into the Chernaya River.

Expected seasonal variations in the distribution of oxygen are observed across stations, with the highest concentrations in winter which gradually decrease in spring and the lowest concentrations in summer which increase in autumn (Fig. 2, *a*). The percentage of oxygen saturation in the waters of the CR and the river at st. *5–7* up to the water intake is consistently maintained at a level of approximately 100%. (Fig. 2, *b*) which indicates a low rate of photosynthesis in the river waters in comparison with surface waters of the CR, the Inkerman basin and the whole bay, oxygen saturation of which reaches ~110% in summer.
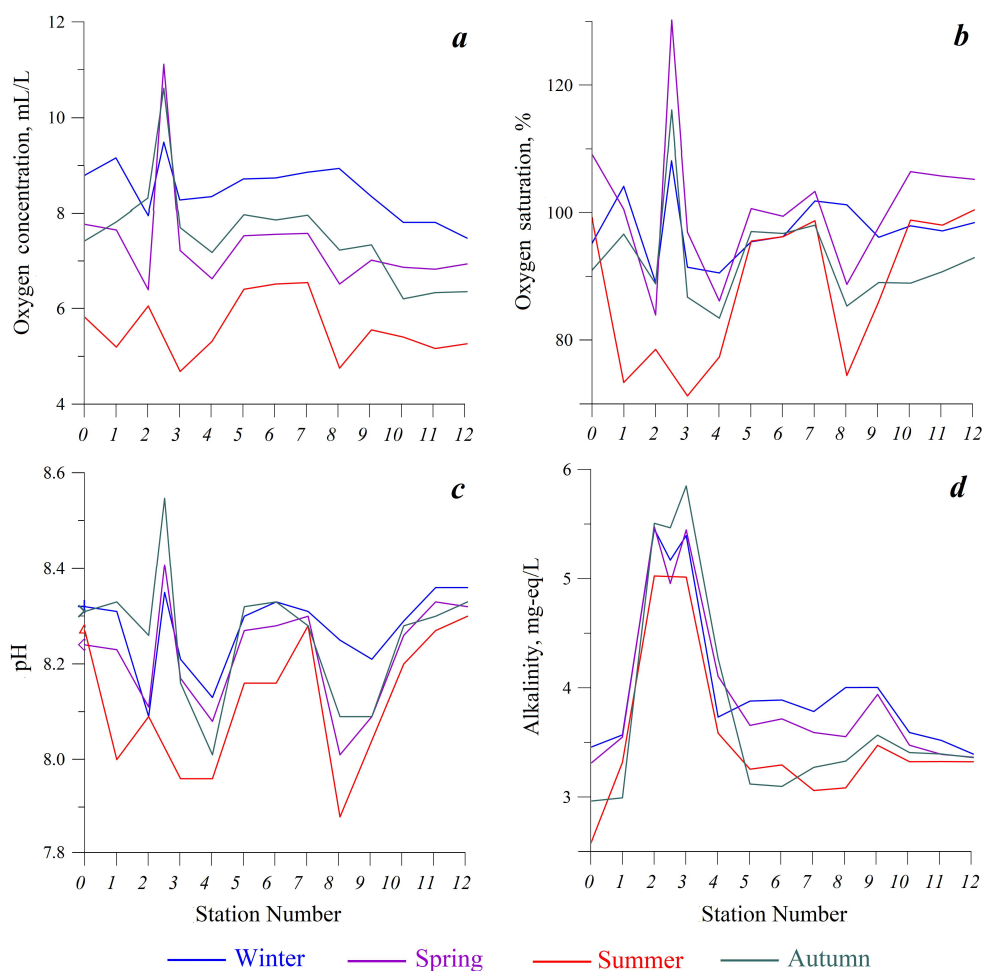
F i g . 2 . Oxygen content (*a*), water oxygen saturation (*b*), pH value (*c*) and total alkalinity value (*d*) at the stations of the lower Chernaya River in 2012–2023

The change in pH value is similar to the pattern of oxygen saturation of waters (Fig. 2, *c*), value 8.3 is typical for all seasons for the surface waters of the CR, st. *5–7*, IB and the bay waters. In summer, however, the pH is somewhat lower than this value.

The tributaries of the Baydarka and Urkusta Rivers exert the most significant influence on the alkalinity value of the river water, with a pH level exceeding 5 mg-eq/L. This results in an increase in the alkalinity of the Chernaya River water following the discharge of the tributaries (Fig. 2, *d*). Seasonal variations of alkalinity demonstrate a distinct pattern, with the highest values observed in winter, subsequent decline in spring and further reduction in summer. Conversely, autumn marks a period of increased alkalinity. Nevertheless, these fluctuations have a negligible impact on the alkalinity of the IB waters, with the average alkalinity of the bay surface waters remaining largely unaltered at ~3.4 mg-eq/L.

Fig. 2 shows that the contribution of wastewater at st. *9* does not change the values of these parameters too much. But the content of elements of the main biogenic cycle is very much influenced by the wastewater appearing at st. *9* (Fig. 3). The phosphate concentration variations are the most contrasting in this respect. In the CR waters, its content is insignificant in all seasons, at the level of 0.1 µM (Fig. 3, *a*). After the inflow of the Baydarka River waters (phosphates are almost absent in the Urkusta River waters (st. *4*) passing through the geochemical filter), the phosphate concentration at st. *5–7* remains about the same as in the CR. And after wastewater inflow, the minimum phosphate concentration at st. *9* becomes higher than 2 µM, which is 20–50 times higher than its content in the CR waters.
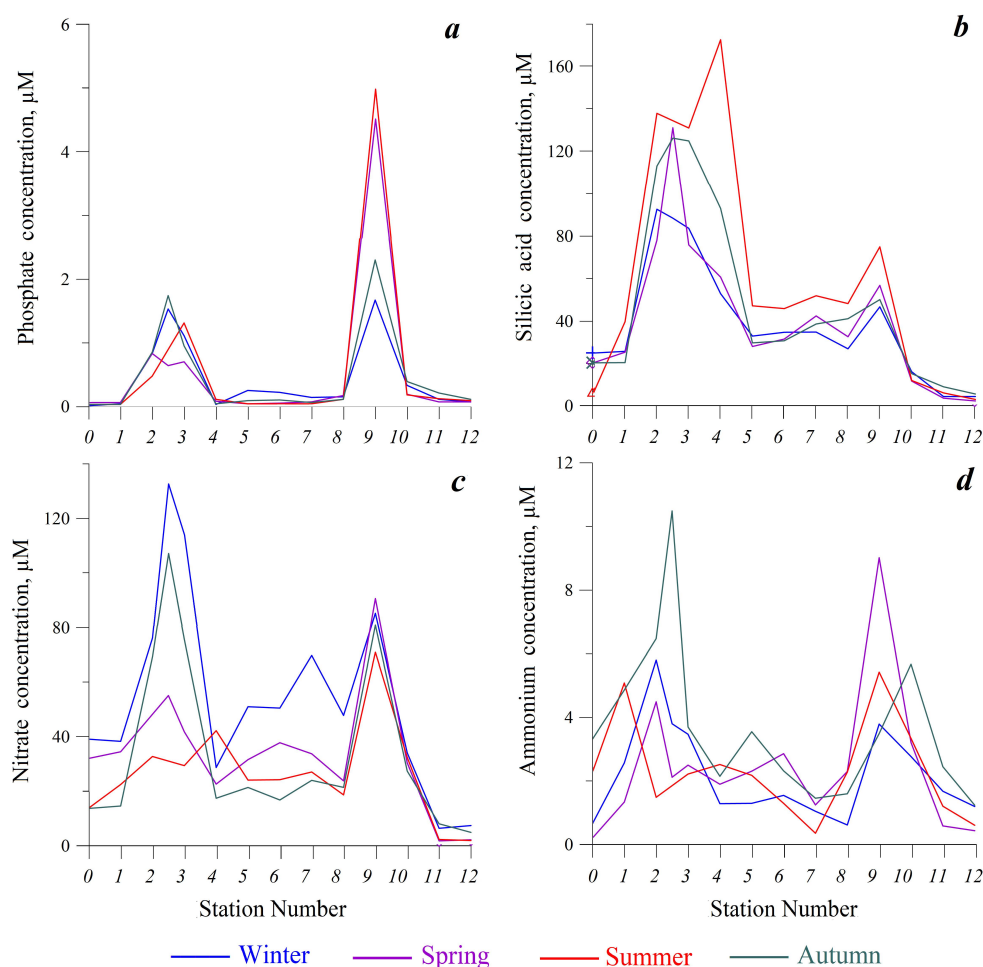
F i g . 3 . Contents of phosphates (*a*), silicic acid (*b*), nitrates (*c*) and ammonium (*d*) at the stations of the lower Chernaya River in 2012–2023

The concentration of silicic acid in the CR waters during the summer months is approximately equivalent to that observed in the waters of the IB and the entire bay, ~ 5 µM (Fig. 3, *b*). In other seasons, the concentration of silicic acid in the CR waters is noticeably higher, at 20 µM. This value increases markedly after the inflow of tributaries containing silicic acids about 5 to 8 times higher than in the CR, ranging from 80 to 160 µM. This results in a slight increase in silicic acid content at st. *5–7*, which then almost doubles at st. *9* after wastewater intake. Thereafter, a monotonic decrease in silicic acid concentration upon contact with seawater at st. *10*, *11*, *12* takes place.

Seasonal variations in nitrate content in the CR waters have been observed, with accumulation during winter, extraction in spring, and increased consumption during summer and autumn. At the same time, nitrate concentration in the CR waters is always higher than in the bay waters (Fig. 3, *c*). The Baydarka River has a nitrate concentration that is 3–4 times higher than that of the CR (it is important to note again that the geochemical filter in the Urkusta River has a similar nitrate concentration to that of the CR). This has a negligible impact on the water composition at st. *5–7* upstream of the water intake. Below the water intake, wastewater inflow leads to a 2–4 times increase in nitrate concentration at st. *9* which then remains at a stable level of 80 µM. The decrease in nitrate content upon contact with seawater is gradual; at st. *10* nitrate concentrations become approximately the same as in the CR, after which they decrease by an order of magnitude in the IB and subsequently throughout the bay.

The dynamics of ammonium content in the CR surface waters are qualitatively opposite to those of nitrate content. During the winter and spring months, when nitrate levels are elevated, ammonium concentrations are typically low, with an average value of less than 0.5 µM (Fig. 3, *d*). In summer, nitrate begins to be consumed during photosynthesis, while ammonium accumulates as a result of decomposition of suspended organic matter (SOM) (SOM decomposition process provides higher ammonium concentrations in the CR bottom waters compared to the surface waters). By autumn, the process of ammonium accumulation in the CR surface waters intensifies (photosynthesis weakens, SOM decomposition continues). It is also noteworthy that while the nitrate concentration in the CR surface and bottom waters is approximately equivalent, ammonium is consistently present at higher levels in bottom waters than in surface ones. It can be assumed that this is caused by the decomposition of deposited SOM near the bottom. Wastewater increases ammonium content at st. *9* predictably, about 2–4 times higher than at st. *5–7*. The decrease in ammonium as well as nitrate concentrations in contact with seawater during the progression from st. *10* to st. *12* is not immediate, but gradual.

Discussion

Among the above results, the main ones should be highlighted: the role of the tributaries of the Chernaya River (the Baydarka and Urkusta Rivers) and the sewage treatment plants in changing the composition of the CR waters; the rate of assimilation of the river waters by the bay seawater.

Figs. 2, 3 demonstrate that the inflow of tributary waters (st. *2–4*) containing significantly more of all nutrients and having higher alkalinity than the CR

waters does not significantly affect the composition of the Chernaya River waters. Only silicic acid content at st. *5–7* (river waters up to the intake) exhibits a notable increase following the inflow of tributary waters. In contrast, the concentrations of other nutrients and alkalinity value remain approximately at the same level as in the CR.

With regard to the waters of wastewater treatment facilities, the impact of which is evident just before the mouth at st. *9*, they contain significantly higher levels of nutrients throughout the year than the waters of the Chernaya River at st. *5–7*: phosphates by 10–100 times, silicic acid, nitrates and ammonium by about 2 times.

Such an increase in concentrations is almost levelled out before the river water enters the IB, the concentrations of all biogenic elements are markedly reduced at st. *10* compared to st. *9*, and the composition of water in the IB is almost the same as in Sevastopol Bay. That is, the main decrease in the content of nutrients and alkalinity value occurs at the river mouth, between st. *9* and st. *10*, where the Chernaya River waters are diluted with marine waters and finally turn into them at st. *10*, where salinity is rarely less than 17. It is no coincidence that this area has attracted increased attention from the scientific community [4, 5, 10–13].

A comparison of the composition of the waters of the CR (st. *0–1*) and the bay (st. *12*) reveals that the waters of the Chernaya River contribute only silicic acid and nitrates to the bay, while phosphates enter the bay exclusively from the waters of the Sakharnaya Golovka wastewater treatment facilities. Furthermore, the effluent from the wastewater treatment facilities contains silicic acid, nitrates and ammonium.

Conclusions

The hydrochemical monitoring of the Chernaya River waters shows the following:

1. The oxygen saturation of the waters of the CR and the lower Chernaya River up to the water intakes is approximately 100% in all seasons, and the pH value is within the range of 8.25–8.30.

2. The total alkalinity of the CR and the Chernaya River exhibits seasonal variations. During the winter and spring months, it is higher than the alkalinity of the Sevastopol Bay waters. Conversely, during the summer and autumn, it is lower.

3. The waters of the CR and the Chernaya River exhibit elevated concentrations of silicic acid and nitrates throughout the year, in comparison to the Sevastopol Bay waters. The ammonium concentrations in the river and bay waters are found to be approximately equivalent.

4. The phosphate content of the reservoir and river waters is approximately equivalent, yet the river subsequently becomes the source of phosphates for the bay following the introduction of wastewater from the treatment plant.

5. The waters of the Baydarka River (a tributary of the Chernaya River), which have not undergone geochemical filtration via the CR, consistently exhibit markedly elevated concentrations of silicic acid, nitrates, ammonium and phosphates as well as a higher alkalinity value than the river waters. This presents a potential risk to the quality of the water supplied to Sevastopol.

REFERENCES

1. Orekhova, N.A., Medvedev, E.V. and Ovsyany, E.I., 2018. Influence of the River Chernaya Water on Hydrochemical Regime of the Sevastopol Bay (the Black Sea). *Ecological Safety of Coastal and Shelf Zones of Sea*, (3), pp. 84–91. https://doi.org/10.22449/2413-5577-2018-3-84-91 (in Russian).

2. Moiseenko, O.G., Khoruzhiy, D.S. and Medvedev, E.V., 2014. Carbonate System in the Chernaya River Waters and in the Zone of the Chernaya River – Sevastopol Bay Biogeochemical Barrier (the Black Sea). *Morskoy Gidrofizicheskiy Zhurnal*, (6), pp. 47–60 (in Russian).

3. Malakhova, L.V., Proskurnin, V.Yu., Egorov, V.N., Chuzhikova-Proskurnina, O.D. and Bobko, N.I., 2020. Trace Elements in the Chernaya River Water and Evaluation of their Income with the Riverine Inflow into the Sevastopol Bay in Winter 2020. *Ecological Safety of Coastal and Shelf Zones of Sea*, (3), pp. 77–94. https://doi.org/10.22449/2413-5577-2020-3-77-94 (in Russian).

4. Malakhova, L.V., Egorov, V.N., Malakhova, T.V., Lobko, V.V., Murashova, A.I. and Bobko, N.I., 2020. Organochlorine Compounds Content in the Components of the Black River Ecosystem and Assessment of their Inflow to the Sevastopol Bay in the Winter Season 2020. *International Journal of Applied and Fundamental Research*, (5), pp. 7–14. https://doi.org/10.17513/mjpfi.13061 (in Russian).

5. Soloveva, O.V., Tikhonova, E.A., Mironov, O.A. and Barabashin, T.O., 2021. Polycyclic Aromatic Hydrocarbons in the Bottom Sediments of the River – Sea Mixing Zone on the Example of the River Chernaya and the Sevastopol Bay (the Black Sea). *Physical Oceanography*, 28(3), pp. 338–347. https://doi.org/10.22449/1573-160X-2021-3-338-347

6. Ovsyany, E.I., Romanov, A.S., Min'kovskaya, R.Ya., Krasnovid, I.I., Ozyumenko, B.A. and Zymbal, I.M., 2001. Basic Polluting Sources of Sea near Sevastopol. In: MHI, 2001. *Ekologicheskaya Bezopasnost' Pribrezhnoy i Shel'fovoy Zon i Kompleksnoe Ispol'zovanie Resursov Shel'fa* [Ecological Safety of Coastal and Shelf Zones and Comprehensive Use of Shelf Resources]. Sevastopol: ECOSI-Gidrofizika. Iss. 2, pp. 138–152 (in Russian).

7. Ivanov, V.A., Ovsyany, E.I., Repetin, L.N., Romanov, A.S. and Ignatyeva, O.G., 2006. *Hydrological and Hydrochemical Regime of the Sebastopol Bay and its Changing under Influence of Climatic and Anthropogenic Factors*. Sevastopol: Marine Hydrophisical Institute NAS of Ukraine, 90 p. (in Russian).

8. Ovsyany, E.I., Artemenko, V.M., Romanov, A.S. and Orekhova, N.A., 2007. The Chernaya River Discharge as a Factor Affecting the Water-Salt Regime Forming and Ecological State of the Sevastopol Bay. In: MHI, 2007. *Ecological Safety of Coastal and Shelf Zones and Comprehensive Use of Shelf Resources*. Sevastopol: MHI. Iss. 15, pp. 57–65 (in Russian).

9. Kondratiev, S.I., 2014. [Study of the Hydrochemical Structure of the Chernaya River (Crimea) in 2006–2011]. In: MHI, 2014. *Ekologicheskaya Bezopasnost' Pribrezhnoy i Shel'fovoy Zon i Kompleksnoe Ispol'zovanie Resursov Shel'fa* [Ecological Safety of Coastal and Shelf Zones and Comprehensive Use of Shelf Resources]. Sevastopol: MHI. Iss. 28, pp. 176–185 (in Russian).

10. Narivonchik, S.V., 2024. Variability of Nutrient Concentration in Waters of the Chernaya River Estuarine Zone (Sevastopol Region). *Ecological Safety of Coastal and Shelf Zones of Sea*, (1), pp. 82–97.

11. Boltachev, A.R., Karpova, E.P. and Danilyuk, O.N., 2010. Peculiarities of thermohaline parameters and ichthyocenosis of the Chernaya River estuary (the Sevastopol Bay). *Marine Ekological Journal*, 9(2), pp. 23–36 (in Russian).

12. Mezentseva, I.V. and Sovga, E.E., 2019. Self-Purification Ability of the Ecosystem of the East Part of the Sevastopol Bay with Respect to Inorganic Nitrogen. *Ecological Safety of Coastal and Shelf Zones of Sea*, (1), pp. 71–77. https://doi.org/10.22449/2413-5577-2019-1-71-77 (in Russian).

13. Rudneva, I. and Shayda, V., 2019. Bioassay of the Estuary Waters of the Chernaya River (Bay of Sevastopol, Black Sea) Using the Brine Shrimp Artemia (Crustacea: Brachiopoda). *Ecosystem Transformation*, 2(3), pp. 76–84. https://doi.org/10.23859/estr-190213

14. Sovga, E.E. and Khmara, T.V., 2020. Influence of the Chernaya River Runoff during High and Low Water on the Ecological State of the Apex of the Sevastopol Bay Water Area. *Physical Oceanography*, 27(1), pp. 28–36. https://doi.org/10.22449/1573-160X-2020-1-28-36

15. Orekhova, N.A. and Varenik, A.V., 2018. Current Hydrochemical Regime of the Sevastopol Bay. *Physical Oceanography*, 25(2), pp. 124–135. https://doi.org/10.22449/1573-160X-2018-2-124-135

16. Carpenter, J.H., 1965. The Chesapeake Bay Institute Technique for the Winkler Dissolved Oxygen Method. *Limnology and Oceanography*, 10(1), pp. 141–143. https://doi.org/10.4319/lo.1965.10.1.0141

17. Kondratev, S.I. and Orekhova, N.A., 2023. Potential Threats to the Ecological State of Water in the Sevastopol Bay. *Lomonosov Geography Journal*, 78(6), pp. 3–14. https://doi.org/10.55959/MSU0579-9414.5.78.6.1 (in Russian).

About the author:

Sergey I. Kondratev, Senior Research Associate, Marine Hydrophysical Institute of RAS (2 Kapitanskaya St., Sevastopol, 299011, Russian Federation), PhD (Chem.), **ORCID ID: 0000-0002-2049-7750**, **ResearcherID: F-8972-2019, Scopus Author ID: 35784380700**, *skondratt@mail.ru*

The author has read and approved the final manuscript.

Original article

Dynamics of Coastal Litter Density on the Beaches of the Northeastern Black Sea Coasts in 2016–2021

V. A. Spirina [1]*, M. P. Pogojeva [1, 2]

[1] *N. N. Zubov State Oceanographic Institute, Moscow, Russia*

[2] *Shirshov Institute of Oceanology of the Russian Academy of Sciences, Moscow, Russia*
* e-mail: Viktoriia_spirina@bk.ru

Abstract

The article presents the results of coastal litter monitoring on the beaches of the Black Sea from 2016 to 2021. The study was conducted on five beaches of the northeastern Black Sea coast, including urban and suburban areas. The Marine Strategy Framework Directive (MSFD) methodology of the European Commission was used for the collection and classification of litter items. During 13 monitoring sessions, a total of 2633 litter items (108 types, 8 categories) were identified, with plastic being the predominant component, averaging 71.7% of the total litter volume. The second predominant category was metal, averaging 8.2% of the found litter. The litter density varied from 47.66 pcs./100 m to 1163 pcs./100 m. The litter density median was 118.26 pcs./100 m on all studied beaches. The inter-annual variability in the litter amount on the beaches shows a decreasing trend in all monitored areas with pronounced peaks in the summer and winter seasons. The main source of the coastal litter pollution was recreational activities, the impact of which was aggravated by lack of developed waste management infrastructure as well as by the proximity of transport routes. The obtained data highlight the necessity of continued monitoring and implementation of measures to reduce pollution, such as improving waste management systems and reducing plastic production and usage. These data can also contribute to legislative and practical initiatives for the protection of the Black Sea marine ecosystems as developed both by the government and people at large.

Keywords: marine litter, marine pollution, marine beach litter, Black Sea, microplastics

For citation: Spirina, V.A. and Pogojeva, M.P., 2024. Dynamics of Coastal Litter Density on the Beaches of the Northeastern Black Sea Coasts in 2016–2021. *Ecological Safety of Coastal and Shelf Zones of Sea*, (4), pp. 39–50.

Динамика плотности берегового мусора на пляжах северо-восточного побережья Черного моря с 2016 по 2021 год

В. А. Спирина [1]*, **М. П. Погожева** [1, 2]

[1] *Государственный океанографический институт имени Н. Н. Зубова, Москва, Россия*

[2] *Институт океанологии имени П. П. Ширшова РАН, Москва, Россия*
***e-mail: Viktoriia_spirina@bk.ru**

Аннотация

Рассмотрены результаты мониторинга берегового мусора на пляжах Черного моря с 2016 по 2021 г. Исследование проводили на пяти пляжах северо-восточного побережья Черного моря, включая городские и пригородные участки. Мусор собирали и классифицировали по методике Рамочной директивы Европейской комиссии по морской стратегии. Всего за время 13 мониторинговых обследований было собрано 2633 частиц мусора из 8 категорий 108 типов. Преобладающим компонентом стал пластик, составляющий в среднем 71.7 % от общего количества мусора. Второй преобладающей категорией стал металл, доля которого в среднем составила 8.2 % от найденного мусора. Плотность пляжного мусора варьировала от 47.66 шт. / 100 м до 1163 шт. / 100 м. Медиана плотности мусора на всех исследуемых пляжах составила 118.26 шт. / 100 м. В межгодовой изменчивости количества мусора на пляжах отмечается тенденция к уменьшению во всех обследуемых районах с явными пиками в летние и зимние сезоны. Основным источником мусорного загрязнения побережья стала рекреационная деятельность, воздействие которой усиливалось из-за отсутствия развитой инфраструктуры по утилизации отходов, а также близости транспортных путей. Полученные данные свидетельствуют о необходимости продолжения мониторинга и принятия мер по снижению загрязнения, таких как улучшение систем управления отходами и уменьшение производства и использования пластика. Эти данные могут использоваться при выработке рекомендаций и практических инициатив по защите морской экосистемы Черного моря как со стороны государства, так и со стороны научного сообщества и обычных граждан.

Ключевые слова: морской мусор, загрязнение моря, загрязнение пляжей, Черное море, микропластик

Introduction

Marine debris pollution of beaches is a growing global problem that requires a comprehensive approach. An important step against marine pollution is continuous monitoring of the scale and dynamics of the problem. Based on analyses of the collected data on the composition, quantity and sources of litter on beaches, effective measures to prevent pollution are developed [1]. Awareness-raising campaigns and improved waste management systems can help to reduce pollution and protect ecosystems and human health [1], [2].

Like any closed body of water, the Black Sea is vulnerable to marine debris pollution. Both terrestrial and marine factors contribute to its accumulation. The terrestrial factors include litter entering the seas from rivers in industrialised countries, uncontrolled landfills, growing tourism, recreational activities, and port activities in coastal cities [1], whereas the marine factors include fishing and intensive shipping [3, 4]. Due to the large-scale circulation of the Black Sea, litter is spreading throughout the basin and this is becoming a growing transborder problem [5].

The main litter component is plastic [6–9]. The widespread use of plastic is due to its utility, availability and demand in all spheres of life. However, there is no enzyme in nature that can degrade this material. Plastic is not evenly redistributed in the environment and thus accumulates in large quantities and affects it negatively [10].

The effects of marine pollution are diverse. Non-degradable plastic often causes death of marine organisms, which may get trapped in nets and plastic substrates or swallow it. Microplastics, derived from larger plastic items, enter food chains, affecting the entire biological cycle [2]. Litter on beaches can affect human health both directly, leading to injuries and cuts, and indirectly through interaction with toxic waste [3]. In addition, polluted beaches lose their attractiveness to tourists, which negatively affects the local economy [4].

The work aims to analyse the qualitative and quantitative composition of the collected litter in order to assess its seasonal variability and to compare the pollution levels of the north-eastern Black Sea coast with other parts of the coast.

---

[1] BSC, 2007. *Marine Litter in the Black Sea Region: a Review of the Problem*. Istanbul: Black Sea Commission Publications, 2007. 160 p.

[2] European Parliament, 2008. *Directive 2008/56/EC of the European Parliament and of the Council of 17 June 2008. Marine Strategy Framework Directive*. Available at: https://eur-lex.europa.eu/legal-content/en/ALL/?uri=CELEX%3A32008L0056 [Accessed: 2 December 2024].

[3] UNEP, 2005. *Marine litter: An analytical overview*. 47 p.

[4] UNEP, 2009. *Marine Litter: A Global Challenge*. 232 p.

Materials and methods

Study area

The study area is located in the north-eastern Black Sea coast (Fig. 1). According to [3], the study area is one of the most polluted parts of the coast.

In addition to the large recreational load, this area is under seasonal spatial and temporal variability of currents, which is one of the main determinants of pollution spreading on the sea coasts and is taken into account when identifying possible sources of marine litter inputs [11].

Two types of beaches were selected for monitoring: urban and suburban ones. The urban beaches are Loo, Primorsky and Sochi Beaches located in resort areas near the central district of the city of Sochi. Loo (84 m long) and Sochi (104 m long) Beaches are pebbly, while Primorsky Beach (128 m long) is sandy.

Vostok and Maly Akhun Beaches are located in the suburbs. The nearby infrastructure is not well-developed, and the proximity of motorways and railways is noted. Near Vostok Beach, forest vegetation prevails. Vostok Beach (87 m long) is sandy, while Maly Akhun Beach (104 m long) is pebbly.

Data collection

Marine litter monitoring was conducted from 2016 to 2021 at five beaches. In order to ensure comparability and data quality, this study used the methodology of the European Commission's Marine Strategy Framework Directive
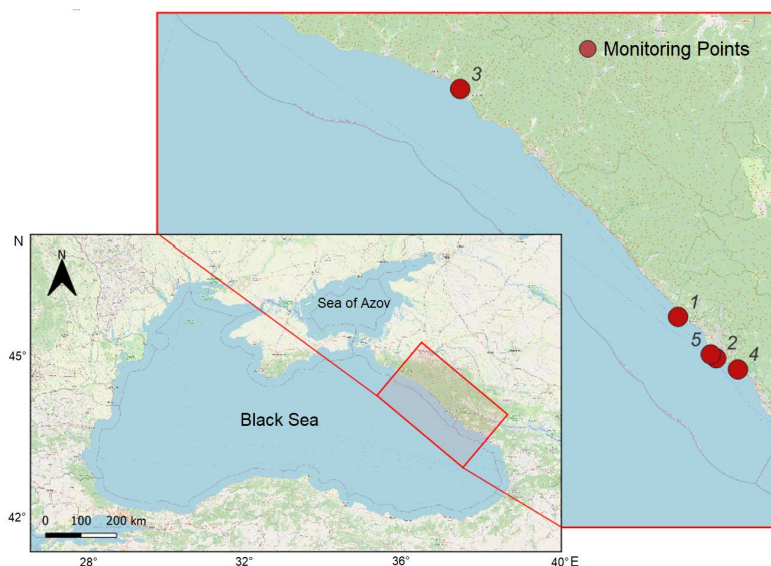
F i g . 1 . Monitoring area. The numbers indicate beaches: *1* – Lo; *2* – Sochi; *3* – Vostok; *4* – Maly Akhun; *5* – Primorsky

(MSFD) [5] to assess marine litter pollution on the north-eastern Black Sea coasts. This strategy aims at the protection and sustainable use of marine ecosystems.

According to the methodology, litter larger than 2.5 cm was collected during the monitoring works on a site about 100 m long and 5 m wide. The found litter was then categorised into a basic list of litter categories and assigned a code number with a letter designation from G1 to G217 according to the chosen methodology. The data was recorded using the Marine Litter Watch mobile application for marine litter monitoring by trained observers using the MSFD methodology.

A total of 108 different types of litter were identified and broken down into the following categories: Plastic, Clothing/Textiles, Glass/Ceramics, Metal, Paper/Cardboard, Engineered Wood, Rubber and Unidentified. The amount of litter per 100 m was then calculated for each beach to allow comparison between the obtained data and to identify the density of litter pollution at each beach during different seasons.

Results

Density and composition

From 2016 to 2021, 13 monitoring surveys were conducted with a total of 2,633 pieces of litter collected. The density of beach litter ranged from 47.66 pieces / 100 m to 1163 pieces / 100 m. The predominant category of litter on all beaches and in all seasons was Plastic, averaging 71.7% of all litter found (Table). The second predominant category was Metal, averaging 8.2% of the litter found.

Maly Akhun Beach

The highest litter concentrations were observed in the summer period of 2020 (245.2 pieces / 100 m) and in the winter period of 2021 (212.5 pieces / 100 m) (Fig. 2).

In summer 2020, 255 litter particles were found. Plastic particles amounted to 168 (65.88%). The most common types were hygiene products (G96) – 22 items, cigarette ends and filters (G27) – 19 items and plastic parts up to 50 cm (G79) – 17 items. The remaining categories were distributed as follows (pcs.): 8 Clothing/Textiles (3.14%), 5 Glass/Ceramics (1.96%), 43 Metal (16.86%), 22 Paper/ Cardboard (8.63%), 5 Wood (1.96%) and 4 Rubber (1.57%) items. In the Metal category, 11 particles were from tin cans (G175) and 10 from bottle caps (G178).

In autumn 2020, 187 litter particles were identified. Of these, 110 items were Plastic (58.82%), 10 were Clothing/Textiles (5.35%), 11 were Glass/Ceramics (5.88%), 22 were Metal (11.76%), 17 were Paper/Cardboard (9.09%), 14 were Wood (7.49%), and 3 were Rubber (1.6%). Cigarette ends and filters also predominated in the Plastic category (G27) – 24 items, and in the category Wood it was engineered wood (G161) – 13 items.

Marine litter density in different seasons

Place of collection	Season	Litter density, pcs./100 m	Proportion of plastic, %	Predominant litter	
				Type	Proportion of the total amount, %
Maly Akhun	Summer 2021	118.27	76.42	Cigarette ends and filters	17.07
Primorsky		47.66	78.69	Cigarette ends and filters	52.46
Maly Akhun	Spring 2021	106.73	71.17	Bottles ≤ 0.5 L	10.81
Primorsky		67.97	85.06	Cigarette ends and filters	37.93
Maly Akhun	Winter 2021	212.5.	62.44	Plastic parts 2.5–50 cm	10.86
Primorsky		78.91	81.19	Cigarette ends and filters	41.58
Maly Akhun	Autumn 2020	179.81	58.82	Cigarette ends and filters	12.83
Primorsky		61.72	56.96	Cigarette ends and filters	34.18
Maly Akhun	Summer 2020	216.35	65.88	Personal hygiene supplies	8.63
Primorsky		75	72.92	Cigarette ends and filters	45.83
Vostok	Summer 2017	151.72	78.03	Cigarette ends and filters	28.03
Sochi	Autumn 2017	224.04	73.82	Cigarette ends and filters	51.07
Loo	Autumn 2016	1163.09	70.28	Cigarette ends and filters	20.57
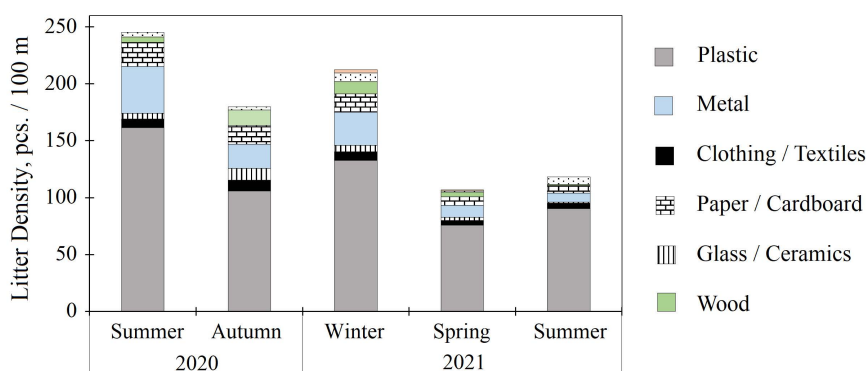
F i g . 2 . Seasonal distribution of marine litter on Maly Akhun Beach

In winter 2021, 221 litter particles were detected. Of these, 138 items were Plastic (62.44%), 8 were Clothing/Textiles (3.62%), 6 were Glass/Ceramics (2.71%), 30 were Metal (13.57%), 17 were Paper/Cardboard (7.69%), 11 were Wood (4.98%), 8 were Rubber (3.62%), and 3 were Other (1.36%). The Plastic category was dominated by unidentifiable plastic particles up to 50 cm (G79) – 24 items, 0.5 litre beverage bottles (G7) – 19 items and pieces of plastic/polystyrene up to 50 cm (G76) – 14 items. In the Metal category, there were 12 items – tin cans (G175).

In spring 2021, a total of 111 litter particles were found. Of these, 79 were Plastic items (71.17%), 4 were Clothes/Textiles (3.60%), 3 were Glass/Ceramics (2.70%), 11 were Metal (9.91%), 8 were Paper/Cardboard (7.21%), 4 were Wood (3.60%), 1 was Rubber (0.9%), and 1 was Other (0.9%). In the Plastic category 0.5 litre beverage bottles prevailed (12 pcs.).

In summer 2021, 123 particles were detected. Of these, 94 were Plastic items (76.4%), 5 were Clothing/Textiles (4.1%), 1 was Glass/Ceramics (0.8%), 8 were Metal (6.5%), 7 were Paper/Cardboard (5.7%), 1 was Wood (0.8%), and 7 were Rubber (5.7%) (Fig. 2). The Plastic category was dominated by cigarette ends and filters (G27) – 21 pcs. and hygiene products (G96) – 10 pcs.

Primorsky Beach

On Primorsky Beach, the highest litter concentrations were also recorded in summer 2020 (75 pcs./100 m) and the winter of 2021 (78.9 pcs./100 m) (Fig. 3).

In summer 2020, 96 marine litter particles were found. Of these, 70 items were Plastic (72.92%), 1 was Clothing/Textiles (1.04%), 6 were Metal (6.25%), 14 were Paper/Cardboard (14.58%), 3 were Wood (3.13%), and 2 were Other (2.08%). The Plastic category was dominated by cigarette ends and filters (G27) – 44 pcs. The Paper/Cardboard category entirely consisted of paper fragments (G156).

In autumn 2020, 79 particles were found. Of these, 45 items were Plastic (56.96%), 2 were Clothing/Textiles (2.53%), 7 were Metal (8.86%), 23 were Paper/Cardboard
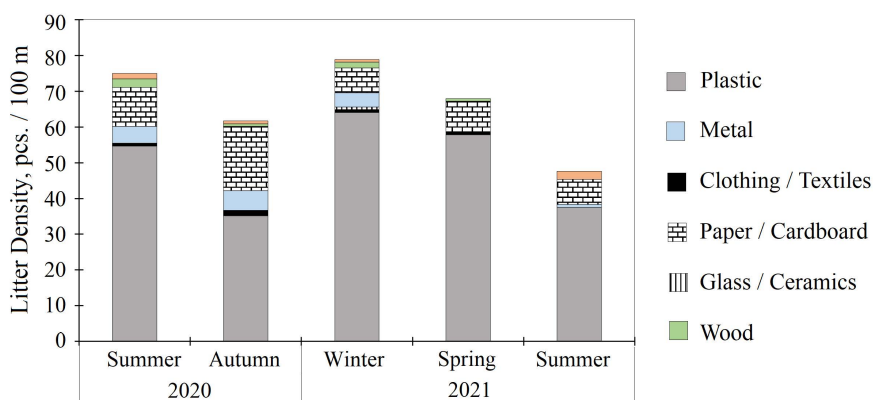
F i g . 3 . Seasonal distribution of marine litter
on Primorsky Beach

(29.11%), 1 was Wood (1.27%), and 1 was Other (1.27%). The category Plastic
was dominated by cigarette ends and filters (G27) – 27 pcs. In the Paper/Cardboard
category, 22 pcs. were paper fragments (G156).

In winter 2021, 101 particles of litter were detected. Of these, 82 items were
Plastic (81.19%), 1 was Clothing/Textiles (0.99%), 1 was Glass/Ceramics (0.99%),
5 were Metal (4.95%), 9 were Paper/Cardboard (8.91%), 2 were Wood (1.98%),
and 1 was Other (0.99%). Cigarette ends and filters in the Plastic category (G27) –
42 pcs.

In spring 2021, 87 particles were detected, of which 74 were Plastic (85.06 %),
1 was Clothing/Textiles (1.15 %), 11 were Paper/Cardboard (12.64 %), and 1 was
Wood (1.15 %). Cigarette ends and filters in the Plastic category (G27) amounted
to 33 pcs.

In autumn 2021, 61 particles were identified. Of these, 48 were Plastic
(78.69%), 1 was Metal (1.64%), 9 were Paper/Cardboard (14.75%), and 3 were
Other (4.92%). Cigarette ends and filters in the category Plastic (G27) amounted to
32 pcs.

Loo Beach

A total of 979 pieces of litter were found on the beach, of which 688 were
Plastic items (70.28%), 13 were Clothing/Textiles (1.33%), 56 were Glass/Ceram-
ics (5.72%), 144 were Metal (14.71%), 58 were Paper/Cardboard (5.92%), 15 were
Wood (1.53%), 3 were Rubber (0.31%) and 2 were Other (0.2%). The predominant
type in the Plastic category was cigarette ends and filters (G27) – 29.2% of all plas-
tic found and 20.5% of all identified litter. Bottles, including fragments, accounted
for (G45) 80.3% of all litter collected in the Glass/Ceramic category. In the Metal
category, the predominant types were bottle caps and tin can tabs (G178), 34%, and
other metal objects less than 50 cm (G198), 22.2%. No predominant type was iden-
tified in other litter categories.
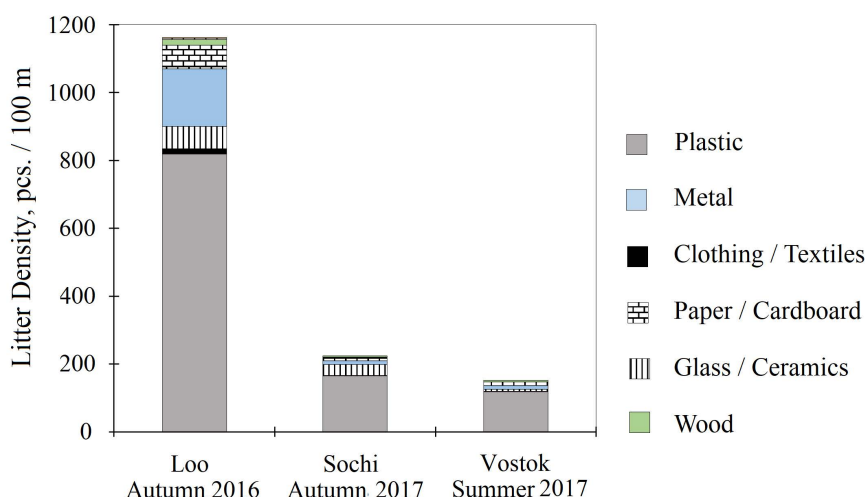
Fig. 4. The density of marine litter on the beaches of Loo, Sochi, Vostok

Sochi Beach

A total of 233 pieces of litter were found on the beach. The distribution by material was as follows: 172 items were Plastic (73.82%), 1 was Clothing/Textiles (0.43%), 34 were Glass/Ceramics (14.59%), 11 were Metal (4.72%), 11 were Paper/Cardboard (4.72%), 4 were Wood (1.72%). The predominant type in the Plastic category was also cigarette ends and filters (G27), 69.2% of all plastic collected and 51% of all litter found. The Glass/Ceramics category consisted of one type of litter, which was bottles, including shards and fragments (14.6% of all litter).

Vostok Beach

On Vostok Beach 132 pieces of litter were found: 103 items were Plastic (78.03%), 1 was Clothes/Textiles (0.76%), 5 were Glass/Ceramics (3.79%), 10 were Metal (7.58%), 9 were Paper/Cardboard (6.82%), 4 were Wood (3.03%). As on the other beaches, cigarette ends and filters (G27) predominated, accounting for 35.9% of litter in this category and 28% of all litter.

Discussion

The results of the work show that the main component of beach litter, registered during the monitoring, was plastic. Its share ranged from 56.96 to 85.06% of the total amount of litter in the monitoring surveys, averaging 71.7%. Similar results were also noted in papers [6–9], where the share of plastic was 71.58, 80.6, 84.3 and 61.65%, respectively.

At the urban Primorsky Beach, paper litter prevailed, in addition to cigarette ends and filters, which may indicate a significant contribution of leisure travellers to the appearance of litter on the beach (proximity of food outlets, including takeaways, advertising leaflets). The following types of litter prevailed on the suburban

Maly Akhun Beach: cigarette ends and filters, drink bottles, plastic fragments 2.5–50 cm large, hygiene products.

The lack of infrastructure and rubbish bins nearby increases the amount and variety of litter on suburban beaches. In addition to recreational activities, Maly Akhun Beach is also affected by the proximity of a motorway, railway and a nearby river, which raises the overall litter density.

During the entire observation period, a total of 424 litter particles were found on urban Primorsky Beach, while on suburban Maly Akhun Beach twice as many particles were detected (867). These differences may be explained by regular clean-ups on the urban beaches and equipped litter disposal sites, which reduces the amount of litter on the beach itself. This study revealed no differences in the composition and amount of litter in terms of the beach type (sandy, pebbly).

When comparing the results of single-season observations at Loo, Sochi and Vostok Beaches, Loo Beach had the highest amount of litter, of which plastic accounts for 70.28%. The beach is remote from the city centre, with the Gorny Vozdukh railway station nearby, and the beach itself is located on a small ledge in the sea. It is likely that due to this location, litter accumulates due to not only recreational impacts, but also to marine litter cast ashore.

The interannual variability of litter density on the studied Black Sea beaches shows a decreasing trend in the amount of litter found in all surveyed areas, with clear peaks in summer and winter. The increase in the litter amount in winter can be attributed to the large number of storm days and litter brought directly by the sea, whereas in summer it can be explained by the increasing number of tourists.

The qualitative composition of litter by season also supports this: in summer, plastic bags, cigarette ends, hygiene products and paper fragments predominated, while in winter, plastic bottles and plastic fragments/details of all sizes prevailed.

The median litter density on all the beaches studied was 118.26 pcs./100 m. According to the data in paper [6], the Black Sea is the most polluted of the four regions studied (median 475 pcs./100 m), followed by the Mediterranean Sea (median 310 pcs./100 m). Less polluted beaches are found in the Baltic Sea (median 71 pcs./100 m) and the north-eastern Atlantic Ocean (average 133 pcs./100 m).

Differences in the median values of this study and study [6] for the Black Sea may be due to the fact that the monitoring works were carried out in different areas and in different seasons. However, the exceeding of the threshold value for marine litter on the coastline (20 pcs./100 m) [7] in each study season and each monitoring survey does indicate a high level of marine litter pollution of the studied beaches.

[6] Šubelj, G. and Veiga, J.M., 2024. *Marine Litter Watch – Europe's Beach Litter Assessment.* ETC BE Report 2024/1. European Topic Centre on Biodiversity and Ecosystems, 25 p. https://doi.org/10.5281/zenodo.12633722

[7] Van Loon, W., Hanke, G., Fleet, D., Werner, S., Barry, J., Strand, J., Eriksson, J., Galgani, F., Grawe, D. [et al.], 2020. *A European Threshold Value and Assessment Method for Macro Litter on Coastlines: Guidance Developed Within the Common Implementation Strategy for the Marine Strategy Framework Directive MSFD Technical Group on Marine Litter.* Publications Office, 26 p. https://doi.org/10.2760/54369

Conclusion

The quantitative and qualitative analyses of marine litter on the north-eastern Black Sea coast allowed comparison of this site with other study regions.

The most polluted beaches were Maly Akhun Beach in 2020, Sochi Beach in 2017 and Loo Beach in 2016, with litter densities of 216.35, 224.04 and 1163.09 pcs./100 m, respectively. The predominant category of litter in all years and in each monitoring survey was Plastic, which accounted for 71.7% of the total identified litter. It is concluded that the study area is one of the most polluted points on the coast of the World Ocean.

Continued monitoring surveys are needed to investigate the general condition of beaches, sources of inputs and transport routes of beach litter as well as to assess the impact thereof, particularly plastic litter, on living organisms and the existing ecosystem as a whole. The obtained data will enable authorities and other stakeholders to take measures to reduce the production of plastic products and improve waste management both on land and in the sea. Regular monitoring surveys of specified representative beaches will help to assess the dynamics of marine litter accumulation in the area as well as to understand the efficiency of the measures taken against pollution in the Black Sea.

REFERENCES

1. Galgani, F., Hanke, G. and Maes, T., 2015. Global Distribution, Composition and Abundance of Marine Litter. In: M. Bergmann, L. Gutow, M. Klages, eds., 2015. *Marine Anthropogenic Litter*. Cham: Springer, pp. 29–56. https:/doi.org/10.1007/978-3-319-16510-3_2

2. Barnes, D.K.A., Galgani, F., Thompson, R.C. and Barlaz, M., 2009. Accumulation and Fragmentation of Plastic Debris in Global Environments. *Philosophical Transactions of the Royal Society B: Biological Sciences*, 364(1526). https:/doi.org/10.1098/rstb.2008.0205

3. Aytan, U., Sahin, F.B.E. and Karacan, F., 2020. Beach Litter on Sarayköy Beach (SE Black Sea): Density, Composition, Possible Sources and Associated Organisms. *Turkish Journal of Fisheries and Aquatic Sciences*, 20(2), pp. 137–145. https:/doi.org/10.4194/1303-2712-v20_2_06

4. Grelaud, M. and Ziveri, P., 2020. The Generation of Marine Litter in Mediterranean Island Beaches as an Effect of Tourism and its Mitigation. *Scientific Reports*, 10, 20326. https:/doi.org/10.1038/s41598-020-77225-5

5. Lechner, A., Keckeis, H., Lumesberger-Loisl, F., Zens, B., Krusch, R., Tritthart, M., Glas, M. and Schludermann, E., 2014. The Danube so Colourful: A Potpourri of Plastic Litter Outnumbers Fish Larvae in Europe's Second Largest River. *Environmental Pollution*, 188, pp. 177–181. http://dx.doi.org/10.1016/j.envpol.2014.02.006

6. Terzi, Y. and Seyhan, K., 2014. Seasonal Changes in the Marine Litter in the Eastern Black Sea Region of Turkey. *Scientific Annals of the Danube Delta Institute*, 20, pp. 77–82. https:/doi.org/10.7427/DDI.20.12

7. Paiu, A., Cândea, M.M., Paiu, R.M. and Gheorghe, A.-M., 2017. Composition and Spatial Distribution of Marine Litter along the Romanian Black Sea Coast. *Cercetări Marine*, 47, pp. 232–239. Available at: https://www.rmri.ro/Home/Downloads/Publications.RecherchesMarines/2017/paper09.pdf [Accessed: 23 November 2024].

8. Simeonova, A., Chuturkova, R. and Yaneva, V., 2017. Seasonal Dynamics of Marine Litter along the Bulgarian Black Sea Coast. *Marine Pollution Bulletin*, (119), pp. 110–118. https:/doi.org/10.1016/j.marpolbul.2017.03.035

9. Terzi, Y. and Seyhan, K., 2017. Seasonal and Spatial Variations of Marine Litter on the South-Eastern Black Sea Coast. *Marine Pollution Bulletin*, 120(1–2), pp. 154–158. https://doi.org/10.1016/j.marpolbul.2017.04.041

10. Yasakova, O.N. and Makarevich, P.R., 2023. *Current State of Phytoplankton in the North-Eastern Black Sea*. Rostov-on-Don: SSC RAS Publishers, 232 p. (in Russian).

11. Haseler, M., Balciunas, A., Hauk, R., Sabaliauskaite, V., Chubarenko, I., Ershova, A. and Schernewski, G., 2020. Marine Litter Pollution in Baltic Sea Beaches – Application of the Sand Rake Method. *Frontiers in Environmental Science*, 8. https:/doi.org/10.3389/fenvs.2020.599978

About the authors:

Viktoria A. Spirina, Junior Research Associate, N.N. Zubov State Oceanographic Institute, Roshydromet, (6 Kropotkinsky Lane, Moscow, 119034, Russian Federation), **ORCID ID: 0009-0006-9786-7904, ResearcherID: JWP-7223-2024**, *Viktoriia_spirina@bk.ru*

Maria P. Pogojeva, Leading Research Associate, Head of Laboratory of marine environment ecological monitoring, N.N. Zubov State Oceanographic Institute, Roshydromet, (6 Kropotkinsky Lane, Moscow, 119034, Russian Federation), **ORCID ID: 0000-0002-4763-2422, ResearcherID: AAK-7811-2020**, *Pogojeva_maria@mail.ru*

Contribution of the authors:

Viktoria A. Spirina – data processing, preparation of the article text and graphic materials

Maria P. Pogojeva – aim and objectives statement, text editing

All the authors have read and approved the final manuscript.

Original paper

Spatiotemporal Changes in Macrophytobenthos in the Western Part of Sevastopol Bay (Black Sea)

N. V. Mironova, T. V. Pankeeva *

A. O. Kovalevsky Institute of Marine Biological Research of RAS, Sevastopol, Russia
* e-mail: tatyanapankeeva@yandex.ru

Abstract

For the first time, the paper presents data on the interannual dynamics of quantitative indicators of macrophytobenthos. A comparative analysis of spatiotemporal changes in the contribution of dominant macrophyte species in the western part of Sevastopol Bay over a 40-year period was performed. Hydrobotanical studies were carried out in the summer period of 1977, 2008 and 2017 on the same transects using standard methods. It was revealed that during the period under study, polydominant phytocommunities were formed in the composition of bottom vegetation, dominated by species inhabiting highly euthrophic environments, with a high proportion of epiphytic algae and an insignificant role of *Gongolaria barbata*. Over the studied period, the lower boundary of macrophyte growth rose and a sharp decrease in macrophytobenthos biomass was registered at a depth of over 5 meters. It was established that changes in the distribution and composition of bottom vegetation in the western part of the bay were caused by its geo-ecological state, which depends on the impact of anthropogenic and natural factors. The construction of hydraulic structures in the bay leads to redistribution of sea grasses growing on soft soils and algae occurring on a hard substrate. It was revealed that after extreme storms, the vegetation cover is predominated by seasonal and annual algae species, with only juvenile *Gongolaria barbata* beds observed at a depth of 0.5–1 m. The obtained results can be used to monitor the ecological situation in the bay and to organize the coastal-marine nature management.

Keywords: coastal zone, bottom vegetation, *Gongolaria barbata*, sea grasses, Black Sea, Sevastopol, Sevastopol Bay

For citation: Mironova, N.V. and Pankeeva, T.V., 2024. Spatiotemporal Changes in Macrophytobenthos in the Western Part of Sevastopol Bay (Black Sea). *Ecological Safety of Coastal and Shelf Zones of Sea*, (4), pp. 51–67.

Original paper

Spatiotemporal Changes in Macrophytobenthos in the Western Part of Sevastopol Bay (Black Sea)

N. V. Mironova, T. V. Pankeeva *

A. O. Kovalevsky Institute of Marine Biological Research of RAS, Sevastopol, Russia
* e-mail: tatyanapankeeva@yandex.ru

Abstract

For the first time, the paper presents data on the interannual dynamics of quantitative indicators of macrophytobenthos. A comparative analysis of spatiotemporal changes in the contribution of dominant macrophyte species in the western part of Sevastopol Bay over a 40-year period was performed. Hydrobotanical studies were carried out in the summer period of 1977, 2008 and 2017 on the same transects using standard methods. It was revealed that during the period under study, polydominant phytocommunities were formed in the composition of bottom vegetation, dominated by species inhabiting highly euthrophic environments, with a high proportion of epiphytic algae and an insignificant role of *Gongolaria barbata*. Over the studied period, the lower boundary of macrophyte growth rose and a sharp decrease in macrophytobenthos biomass was registered at a depth of over 5 meters. It was established that changes in the distribution and composition of bottom vegetation in the western part of the bay were caused by its geo-ecological state, which depends on the impact of anthropogenic and natural factors. The construction of hydraulic structures in the bay leads to redistribution of sea grasses growing on soft soils and algae occurring on a hard substrate. It was revealed that after extreme storms, the vegetation cover is predominated by seasonal and annual algae species, with only juvenile *Gongolaria barbata* beds observed at a depth of 0.5–1 m. The obtained results can be used to monitor the ecological situation in the bay and to organize the coastal-marine nature management.

Keywords: coastal zone, bottom vegetation, *Gongolaria barbata*, sea grasses, Black Sea, Sevastopol, Sevastopol Bay

For citation: Mironova, N.V. and Pankeeva, T.V., 2024. Spatiotemporal Changes in Macrophytobenthos in the Western Part of Sevastopol Bay (Black Sea). *Ecological Safety of Coastal and Shelf Zones of Sea*, (4), pp. 51–67.

Пространственно-временные изменения макрофитобентоса в Севастопольской бухте (Черное море)

Н. В. Миронова, Т. В. Панкеева *

Институт биологии южных морей
имени А.О. Ковалевского РАН, Севастополь, Россия
* e-mail: tatyanapankeeva@yandex.ru

Аннотация

Впервые приведены сведения о межгодовой динамике количественных показателей макрофитобентоса и проведен сравнительный анализ пространственно-временных изменений вклада доминирующих видов макрофитов в западной части Севастопольской бухты за 40-летний период. Гидроботанические исследования выполняли в летний период 1977, 2008 и 2017 гг. на одних и тех же разрезах по стандартной методике. Выявлено, что на протяжении изучаемого периода в составе донной растительности сформировались полидоминантные фитосообщества, где господствуют виды, обитающие в среде с повышенным уровнем эвтрофирования. При этом отмечены высокая доля эпифитирующих водорослей и незначительная роль *Gongolaria barbata*. За исследуемый промежуток времени произошло поднятие нижней границы произрастания макрофитов и зарегистрировано резкое снижение биомассы макрофитобентоса на глубине свыше 5 м. Установлено, что изменения в распределении и составе донной растительности в западной части бухты обусловлены ее геоэкологическим состоянием, которое зависит от воздействия антропогенных и природных факторов. Строительство в бухте гидротехнических сооружений приводит к изменению распространения зарослей морских трав, обитающих на мягких грунтах, и водорослей, встречающихся на твердом субстрате. Выявлено, что после экстремальных штормов в составе растительного покрова преобладают сезонные и однолетние виды водорослей, при этом на глубине 0.5–1 м отмечаются лишь ювенильные слоевища *Gongolaria barbata*. Полученные результаты могут быть использованы для мониторинговых исследований экологической ситуации в бухте, а также при организации прибрежно-морского природопользования.

Ключевые слова: прибрежная зона, донная растительность, морские травы, *Gongolaria barbata*, Черное море, Севастополь, Севастопольская бухта

Introduction

In recent years, a notable increase in the level of eutrophication of the Crimean peninsula coastal zone has been attributed to a number of factors including an increase in the volumes of untreated wastewater, uncontrolled recreational load and active construction on the coast [1–3]. The most significant anthropogenic impact on the ecological state of the coastline is evident in bays and port water areas.

Sevastopol Bay is a water area subject to active economic utilisation. Currently, it functions as a reservoir that receives industrial and domestic wastewater as well as stormwater from the surrounding catchment area. On a daily basis, up to 10,000–15,000 m³ of untreated or conditionally clean water is discharged into the bay resulting in the introduction of a diverse range of chemical compounds of organic and inorganic origin into it [4, 5]. This unfavourable ecological situation in the bay has resulted in significant alterations to the composition and biomass of the macrophytobenthos, with the potential for complete degradation observed in certain areas of the water body.

The current state of the macrophytobenthos in Sevastopol Bay is not well documented [6, 7]. The growth of certain species of macrophytes in the Black Sea, particularly in Sevastopol Bay, was first documented in the works of N. N. Voronikhin in the early 20th century [1, 2]. The author noted that algae and higher aquatic vegetation grow on a particular type of substrate. During the same period, S. M. Pereyaslavtseva made a map of the bay showing the distribution of benthic communities [3]. Later, S. A. Zernov presented a map of the distribution of bottom vegetation in Sevastopol Bay [4]. The author showed that in the early 20th century, the bottom biocenoses of the bay followed the general pattern of the Black Sea biocenoses where the distribution of macrophytobenthos was mainly determined by the substrate (cystosira was found on hard substrates and sea grasses on soft substrates) [4]. The paper suggests that significant changes in the state of biocenoses will occur in the bay under the influence of anthropogenic activities [4]. It is notable that by the 1930s the bay had already been considerably polluted, which resulted in negative changes to the local fauna [8].

The first hydrobotanical survey of macrophytobenthos in Sevastopol Bay was carried out by A. A. Kalugina-Gutnik in 1967 [5]. The materials presented in the work provide an overview of the species composition and calculate the biomass of macrophytes at varying depths across different regions of the bay. Subsequently, in 1977, A. A. Kalugina-Gutnik proceeded with her investigation of the bottom vegetation of the bays situated along the coastline of Sevastopol [9].

It is notable that over the last 40 years, the level of pollution in the bay has fluctuated repeatedly due to a range of socio-economic factors. Therefore, it is necessary to implement a monitoring programme to observe changes in the composition and structure of the macrophytobenthos, which is considered to be a bioindicator of the marine environment state.

---

[1] Voronikhin, N.N., 1908. [On Distribution of Algae in the Black Sea near Sevastopol]. *Botanichesky Zhurnal. Trudy Imperatorskogo Sankt-Peterburgskogo Obshchestva Estestvoispytateley*, (7), pp. 181–198 (in Russian).

[2] Voronikhin, N.N., 1909. [Red Algae (Rhodophyceae) of the Black Sea]. *Trudy Imperatorskogo Sankt-Peterburgskogo Obshchestva Estestvoispytateley*, 40(3–4), pp. 175–356 (in Russian).

[3] Pereyaslavtseva, S.M., 1910. [Materials to Characterize the Black Sea Flora]. In: N. N. Voronikhin, ed., 1910. *Zapiski Imperatorskoy Akademii Nauk*. Saint Petersburg: Imperatorskaya Akademiya Nauk. Vol. 25, iss. 9, pp. 39 (in Russian).

[4] Zernov, S.A., 1913. [On Studying Life of the Black Sea]. In: IAS, 1913. *Zapiski Imperatorskoy Akademii Nauk*. Saint Petersburg: Imperatorskaya Akademiya Nauk. Vol. 32, iss. 1, 304 p. (in Russian).

[5] Kalugina-Gutnik, A.A., 1974. [Bottom Vegetation of Sevastopol Bay]. In: AS USSR, 1974. *Biologiya Morya*. Kiev: Naukova Dumka. Iss. 32, pp. 133–164 (in Russian).

The objective of this study is to identify the distinctive characteristics of the macrophytobenthos distribution interannual dynamics in the western part of Sevastopol Bay over the period 1977–2017.

Materials and methods of study

The length of Sevastopol Bay is approximately 7.5 km, with a maximum width of 1 km (Fig. 1). At the entrance to the bay, the depth reaches 20 m, at the top – 5 m. The bay was formed due to the flooding of the mouth of the Chernaya River during the post-glacial sea level rise. The shores of the bay are characterised by elevated terrain, comprising Sarmatian limestone, and the coastline displays a pronounced indentation. The coastal relief is dissected by gullies, the extensions of which give rise to smaller bays and concavities of the coastline. The shore type can be defined as abrasion-embayed ingression ria [10]. In modern conditions, the coastal zone has been significantly transformed (concreting of the coastline, construction of breakwaters, piers). It is established that in 2022, the untransformed shores of the bay constituted only 1.1 km (3% of the original length) of all the shoreline [11].

Sevastopol Bay is currently classified as a semi-enclosed estuarine-type water area with a relatively slow rate of water exchange [5]. The configuration of the bay renders it susceptible to wave action from the westward direction only. Since the construction of the entrance breakwaters in the late 1970s, the bay has remained largely protected from significant wave action [10]. The hydrochemical structure of the waters in the bay is primarily influenced by natural factors, namely interactions with the atmosphere, freshwater runoff from the Chernaya River into the eastern part of the bay and the inflow of saline marine waters through the entrance strait in its western part [5].

Hydrobotanical surveys in Sevastopol Bay were carried out using lightweight diving equipment and small vessels in July 2017. Macrophyte distribution and biomass were estimated for the coastal zone of the western part of the bay (profiles *1–4*) (Fig. 1). The coordinates of the transects were determined using an Oregon 650 portable GPS receiver (Table 1).

F i g . 1 . Schematic map of the location of hydrobotanical profiles in the western part of Sevastopol Bay (*1* – Cape Konstantinovsky; *2* – Cape Khrustalny; *3* – Cape Slavy; *4* – Monument to Sunken Ships)

T a b l e 1. Coordinates and depth range of hydrobotanical profiles, number of sampled macrophytobenthos in Sevastopol Bay

Profile	Coordinates		Depth, m					Number of samples
	northern latitude	eastern longitude	0.5	1	3	5	7–10	
1	44°37'36"	33°30'44"	+	+	+	+	–	16
2	44°37'1"	33°31'2"	+	+	+	+	+	20
3	44°37'35"	33°31'59"	+	+	+	+	–	16
4	44°37'3"	33°31'29"	+	+	+	+	–	16

Note: dash – no bottom vegetation.

To study the composition of macrophytobenthos, samples were taken according to standard methods [6]. Four 25 × 25 cm survey plots were laid at depths of 0.5, 1, 3, 5, 10 and 15 m and a total of 68 quantitative samples were collected (Table 1). The dominant classification was used to describe the bottom vegetation in accordance with [7]. Shannon diversity index (*H*) was used to analyse the structure of phytocommunities. Algae were identified in accordance with [8], taking into account the latest nomenclature changes (available at: http://www.algaebase.org). Information on the composition and distribution of macrophytobenthos in the bay for 1977 and 2008 was obtained by one of the authors who participated in the collection and processing of material carried out in the summer period in the same areas using a similar methodology.

Results and discussion
The distribution of macrophytobenthos and its dominant macrophyte species in the western part of Sevastopol Bay is characterised on the basis of the conducted studies.

Distribution of bottom vegetation in the bay in 1977. In the estuary of Sevastopol Bay on the northern coastal area at profile *1* (Cape Konstantinovsky) bottom vegetation is registered up to 5 m depth. The maximum total biomass of

[6] Kalugina-Gutnik, A.A., 1969. [Black Sea Benthic Vegetation Survey Using Light-Weight Diving Equipment]. In: AS USSR, 1969. [*Marine Underwater Studies*]. Moscow: Nauka, pp. 105–113 (in Russian).

[7] Kalugina-Gutnik, A.A., 1975. [*Phytobenthos of the Black Sea*]. Kiev: Naukova Dumka, 248 p. (in Russian).

[8] Zinova, A.D., 1967. [*Field Guide to Green, Brown and Red Algae of the Southern Seas of the USSR*]. Leningrad: Nauka, 397 p. (in Russian).

macrophytes was recorded at a depth of 3 m. At depths of 0.5 and 1 m, the quantitative index was slightly lower, while at a depth of 5 m, the biomass decreased sixfold (Table 2). *Gongolaria barbata* (Stackhouse) Kuntze (= *Cystoseira barbata*) was the most abundant species observed in the depth range studied, representing a significant proportion (Fig. 2). The macrophytobenthos included *Cladophora albida* (Nees) Kütz. and *Ulva rigida* L. The presence of epiphytic algae was not identified. The diversity index values by depth ranged widely from 0.07 to 1.48. Its low values at depths of 1 and 3 m are explained by the fact that almost pure vegetation of *Gongolaria barbata* was recorded at these depths (Table 2).

T a b l e 2 . Changes in the total biomass of macrophytobenthos, percentage of its dominant and epiphytic macrophyte species, diversity index (H) in Sevastopol Bay by depth and years

Profile	Depth, m	Year	Total biomass of macrophytes, g·m^{-2}	Proportion, %		H
				Gongolaria barbata	Epiphytic	
1	0.5	1977	1608.4 ± 422.3	88	0	1.42
		2008	1088.9 ± 251.5	0	5	2.19
		2017	992.2 ± 302.1	63	3	1.58
	1	1977	1382.6 ± 214.9	95	0	0.31
		2008	1425.4 ± 396.4	0	11	1.99
		2017	422.6 ± 58.1	73	15	1.41
	3	1977	2249.8 ± 92.5	99	0	0.07
		2008	361.6 ± 92.6	0	5	2.52
		2017	424.3 ± 31.9	44	27	2.19
	5	1977	370.1 ± 117.7	84	0	1.48
		2008	296.5 ± 58.8	0	6	2.10
		2017	18.6±7.7	18	26	2.39
	7	2008	63.1 ± 18.7	20	23	3.37
2	0.5	1977	38.8 ± 5.2	0	0	0.64
		2008	360.2 ± 40.4	0	4	2.03
		2017	744.7 ± 330.3	70	9	1.76
	1	1977	375.0 ± 128.9	0	0	0
		2008	120.5 ± 60.2	3	6	2.54
		2017	1224.3 ± 135.5	80	17	1.24

Profile	Depth, m	Year	Total biomass of macrophytes, g·m⁻²	Proportion, %		H
				Gongolaria barbata	Epiphytic	
2	3	1977	623.8 ± 45.1	0	0	0
		2008	537.1 ± 194.4	39	2	2.31
		2017	1310.2 ± 431.9	45	48	1.86
	5	1977	600.9 ± 145.3	0	0	0.65
		2008	399.3 ± 141.3	79	14	1.29
		2017	306.3 ± 67.3	55	25	1.85
	10	2008	50.0 ± 2.9	38	1	2.32
	7	2017	13.1 ± 6.4	72	0	1.57
3	0.5	1977	623.3 ± 97.3	0	0	0.15
		2008	789.9 ± 343.9	55	3	2.11
		2017	4699.6 ± 1206.9	86	12	0.84
	1	1977	588.5 ± 128.2	0	0	0
		2008	253.3 ± 112.8	0	1	1.03
		2017	5063.6 ± 346.6	87	7	0.88
	3	1977	689.9 ± 130.7	0	0	0
		2008	202.7 ± 75.9	0	2	0.49
		2017	2322.8 ± 363.1	79	4	1.06
	5	1977	200.7 ± 76.9	0	0	0.97
		2008	228.4 ± 33.3	0	0	0.05
		2017	1.2 ± 0.54	0	0	1.23
4	0.5	1977	917.0 ± 122.4	0	0	0.77
		2008	955.9 ± 284.7	52	6	2.59
		2017	5483.0 ± 1536.9	87	8	0.97
	1	1977	1602.6 ± 127.4	0	0	0.02
		2008	1406.2 ± 431.1	55	22	2.26
		2017	3416.2 ± 1039.5	85	6	0.89
	3	1977	$1079.0 \pm 543,7$	0	0	0.82
		2008	616.1 ± 172.1	50	4	2.06
		2017	1863.7 ± 327.0	39	10	1.91
	5	2008	270.9 ± 64.0	76	3	1.27
		2017	655.2 ± 135.5	32	39	2.42

In the estuary of Sevastopol Bay, *Ulva rigida* was the dominant species in the southern coastal area at profile *2* (Cape Khrustalny), occurring at depths of 0.5–3 m (Fig. 2). The total biomass of macrophytes in this range exhibited a 16-fold increase with increasing depth (Table 2). *Zostera noltei* Hornem predominated
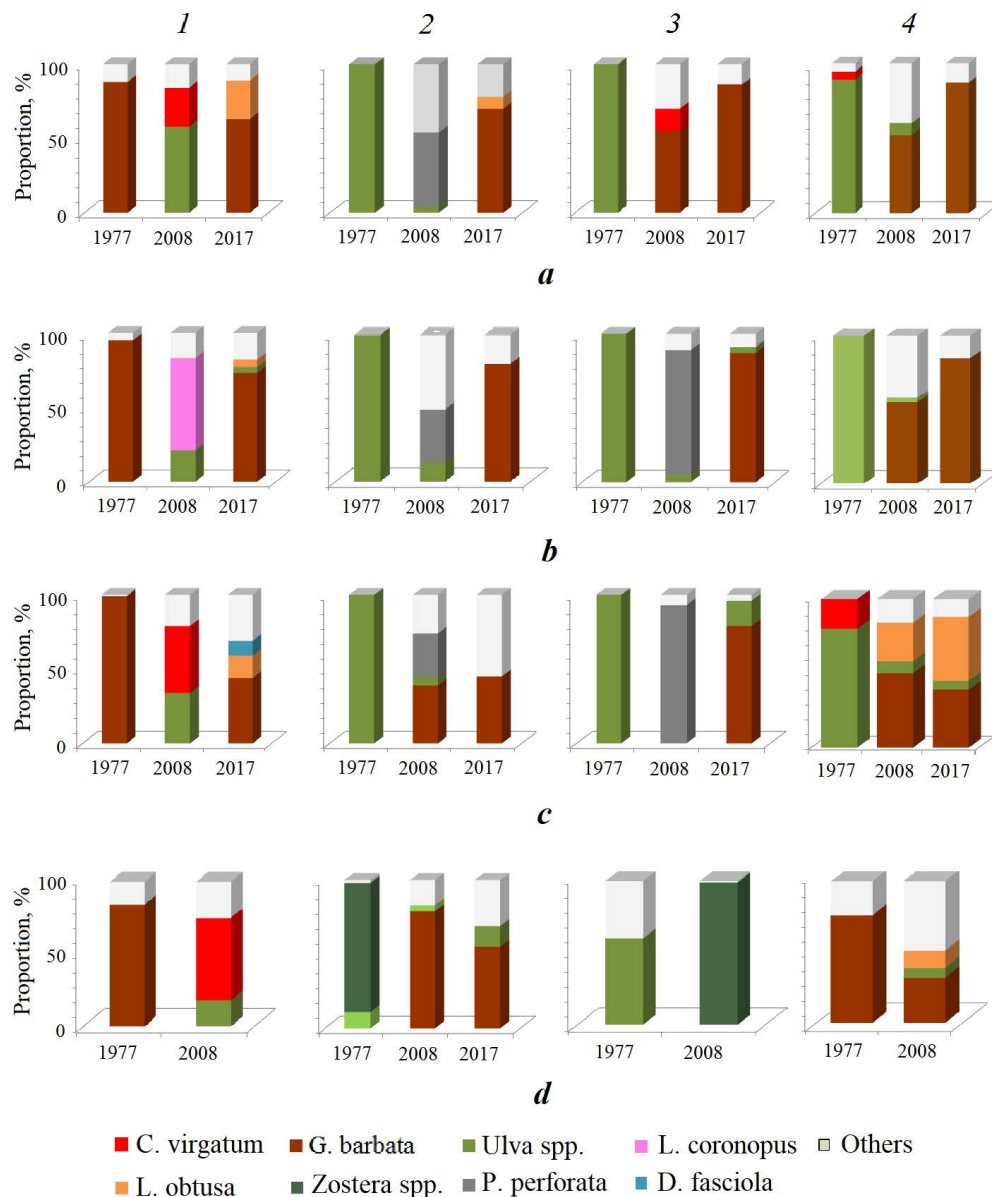
F i g . 2 . Change in the proportion of dominant macrophyte species by profile and years at the depth of 0.5 m (*a*), 1 m (*b*), 3 m (*c*) and 5 m (*d*) (*1* – Cape Konstanti-novsky; *2* – Cape Khrustalny; *3* – Cape Slavy; *4* – Monument to the Sunken Ships)

at a depth of 5 m. *Ulva rigida* was noted among sea grasses. Epiphytes were absent. The diversity index values were low (0–0.65), indicating a monodominant structure of the phytocommunity.

Along the way further into the bay along the northern coastline, *Ulva rigida* exhibited a dominant presence at depths of 0.5–5 m at profile *3* (Cape Slavy) (Fig. 2). The total biomass of macrophytes exhibited minimal variation at depths of 0.5–3 m, demonstrating a notable decrease of approximately threefold at a depth of 5 m (Table 2). It is indicative that the macrophytobenthos is represented by accumulations of *Ulva rigida* at depth of 1–3 m, whereas *Ulva* sp. and *Bryopsis hypnoides* Lamour were noted in its composition at depths of 0.5 m and 5 m, respectively. The diversity index values provide insight into the dominant species within the algal community.

Further inland along the southern coastline of the bay, *Ulva rigida* was also dominant at depths of 0.5–3 m at profile *4* (Monument to the Sunken Ships) (Fig. 2). The maximum total biomass of macrophytes was recorded at a depth of 1 m, while at depths of 0.5 and 3 m, this index was found to be 1.7–1.5 times lower. Representatives of *Ceramium* were found in the composition of bottom vegetation at all depths. The diversity index values varied by depth from 0.03 to 0.82.

Distribution of bottom vegetation in the bay in 2008. At profile *1*, the dominant species at a depth of 0.5 m were *Ulva intestinalis* L., *U. rigida* and *Ceramium virgatum* Roth (Fig. 2). The composition of bottom vegetation also included *Callithamnion corymbosum* (Smith) Lyngb., *Ceramium diaphanum* (Lightf.) Roth. The dominant species at a depth of 1 m were *Laurencia coronopus* J. Ag. and *Ulva intestinalis*. *Ulva rigida*, *Ceramium virgatum* and species of *Cladophora* were also recorded at this depth. The depth range of 3–5 m was dominated by *Ceramium virgatum* and *Ulva rigida*. The proportion of these species exhibited considerable variation, with values ranging between 45–57 and 18–20% of the total macrophyte biomass, respectively. The total macrophyte biomass at these depths exhibited minimal variation (Table 2). It is significant that the contribution of *Ulva intestinalis* to the total macrophyte biomass decreased from 35 to 1% as the depth increased from 0.5 to 5 m. At a depth of 7 m, the total macrophyte biomass was found to be relatively low (Table 2). *Gongolaria barbata* and *Ulva rigida* dominated there. Epiphytic algae were abundant at this depth. Among them, the predominant ones were *Ceramium virgatum*, *Ectocarpus confervoides* (Roth) Le Jolis, *Laurencia coronopus* and *Vertebrata subulifera* (C. Ag.) Kütz. The diversity index values indicate a complex polydominant community structure with a high contribution of associated species and epiphytic algae.

At profile *2*, *Palisada perforata* (Bory) K.W. Nam dominated at depths of 0.5–1 m, with its proportion decreasing in this range with increasing depth from 50 to 36% of the total macrophyte biomass (Fig. 2), which also decreased threefold (Table 2). The composition of bottom vegetation included *Gelidium crinale* (Hare ex Turner) Gaillon, *Ulva intestinalis*, *U. rigida*, *Callithamnion corymbosum.* The representatives of *Cladophora* were found in both lithophytic and epiphytic forms. *Gongolaria barbata* and *Palisada perforata* predominated at a depth of 3 m. *Cladophoropsis membranacea* (Ag.) Börg., *Gelidium crinale*, *Ulva rigida* were

also abundant in the composition of the macrophytobenthos. At depths of 5–10 m, *Gongolaria barbata* dominated, the proportion of which decreased by half with increasing depth, and the total biomass of macrophytes decreased by a factor of eight (Table 2). Under the cover and among the *Gongolaria barbata* beds, *Ulva rigida* was observed at a depth of 5 m, while *Cladostephus spongiosus* (Huds.) C. Ag., *Laurencia coronopus* and *Cladophora laetevirens* (Dillw.) Kütz were recorded at a depth of 10 m. Such deepwater species as *Zanardinia typus* (Nardo) P. C. Silva, *Carradoriella elongata* (Huds.) Savoie & G.W. Saunders., *Nereia filiformis* (J. Ag.) Zanard. were found in the composition of bottom vegetation at depths of 5–10 m. The greatest development of epiphytic synusia occurred at a depth of 5 m. *Vertebrata subulifera* and *Stilophora tenella* (Esper) P. C. Silva dominated among epiphytic algae. The diversity index values indicate a high proportion of associated species in the phytocommunity structure.

At profile *3*, *Gongolaria barbata* predominated at a depth of 0.5 m (Fig. 2). *Ceramium virgatum*, *Carradoriella denudata* (Dillw.) Savoie et G. W. Saunders, species of *Cladophora* and *Ulva* were abundant in the composition of the macrophytobenthos. *Palisada perforata* dominated at depths of 1–3 m, with this species accounting for 84–93% of the total macrophyte biomass. With increasing depth, the contribution of *Cladophora laetevirens* increased from 1 to 5% and that of *Ulva rigida* decreased from 5 to 1% of total macrophyte biomass. *Zostera marina* was dominant at a depth of 5 m. The contribution of epiphytic algae at all investigated depths was insignificant (Table 2). The diversity index values varied in a wide range and depended on the complexity of the community structure.

At profile *4*, *Gongolaria barbata* dominated at depths of 0.5–5 m (Fig. 2). The maximum total macrophyte biomass was recorded at a depth of 1 m, while at a depth of 0.5 m, this parameter was observed to be 1.5 times lower, and at depths exceeding 1 m, it decreased by a factor of two and five at depths of 3 and 5 m, respectively (Table 2). *Ulva rigida*, *Cladophoropsis membranacea* were found in the composition of bottom vegetation at all investigated depths. A high proportion of *G. crinale* and *Dermocorynus dichotomus* (J. Ag.) Gargiulo Morabito and Manghisi was observed at depths of 0.5–1 m, while at a depth of 3 m – the lithophytic form *Laurencia obtusa* (Huds.) J. V. Lamour., and at a depth of 5 m – *Zanardinia typus*. The contribution of *Cladophora laetevirens* decreased from 9 to 1% with increasing depth in the studied range. Epiphytes were most abundant at a depth of 1 m. *Vertebrata subulifera* and species of *Cladophora* dominated among them. High diversity index values indicate a polydominant community structure.

Distribution of bottom vegetation in the bay in 2017. In the estuary of Sevastopol Bay, bottom vegetation was recorded up to a depth of 5 m at profile *1*. *Gongolaria barbata* dominated at depths of 0.5–3 m (Table 2). The proportion of this species was observed to be at its maximum at a depth of 1 m, with a subsequent decrease in abundance with increasing depth, occurring at a rate of two and four times. The total macrophyte biomass exhibited a decrease of over 50 times with increasing depth. *Dictyota fasciola* (Roth) Howe was found in the macrophytobenthos composition at all investigated depths (Fig. 2). The proportion of this species at depths of 0.5–1 m exhibited a range of 2–4%, while at depths of 3–5 m, it showed a notable increase to 10–28% of the total macrophyte biomass.

The lithophytic form *Laurencia obtusa* was observed among *Gongolaria barbata* thickets at a depth of 0.5 m; at greater depths, this species was found as an epiphyte. *Cladophora serisea* (Huds.) Kütz. was abundant at a depth of 5 m. The contribution of epiphytic algae exhibited a notable increase with increasing depth. The shift in the diversity index suggests that the community structure becomes increasingly complex with increasing depth.

At profile *2*, *Gongolaria barbata* was predominant at depths of 0.5–5 m (Fig. 2). The total macrophyte biomass exhibited a significant increase, approximately two-fold, with an increase in depth from 0.5 to 3 m (Table 2). With further increase in depth this indicator decreased more than fourfold, and at a depth of 7 m, bottom vegetation was practically absent. The proportion of the dominant species at depths of 0.5–1 m varied from 70 to 80% and decreased at depths of 3–5 m to 45–55% of the total macrophyte biomass. Green algae of *Cladophora* and *Ulva* were found in the macrophytobenthos at all depths among *Gongolaria barbata*. Deepwater species *Nereia filiformis* and *Carradoriella elongata* were recorded at depths of 3–5 m. The contribution of epiphytes increased from 9 to 17% with increasing depth (0.5 and 1 m) and decreased from 48 to 25% of total macrophyte biomass with further depth (3 and 5 m). Among the epiphytic algae, the predominant one was *Vertebrata subulifera*. The diversity index by depth varied from 1.24 to 1.86.

At profile *3*, bottom vegetation was found down to a depth of 3 m (Table 2). *Gongolaria barbata* dominated at these depths (Fig. 2). The total macrophyte biomass at depths of 0.5–1 m was found to be considerable (from 4699.6 ± 1206.9 to 5063.6 ± 346.6 g·m^{-2}) and decreased twofold at a depth of 3 m, whereas at a depth of 5 m, macrophytobenthos was practically absent. The composition of the macrophytobenthos exhibited a notable increase in the proportion of *Ulva rigida* with increasing depth, from 1% to 17%. Conversely, the contribution of epiphytic algae demonstrated a significant decrease from 12% to 4% of the total macrophyte biomass. The epiphytes were dominated by *Shacelaria cirrhosa* (Roth) C. Ag. *Dictyota fasciola*, *Ulva rigida* and *Carradoriella elongata* occurred sporadically at a depth of 5 m. The diversity index at a depth of 0.5–3 m exhibited a narrow range (0.84–1.06) suggesting the dominance of a single species.

At profile *4*, *Gongolaria barbata* was predominant at depths of 0.5–5 m. The total biomass of macrophytes decreased eightfold with increasing depth in the studied range, and the proportion of the dominant species decreased almost threefold (Table 2). *Cladophora laetevirens* and *Ulva rigida* were noted in the composition of bottom vegetation at all depths. *Ulva* was sporadic at depths of 0.5–1 m, and at depths of 3–5 m, its proportion increased up to 6–7% of the total macrophyte biomass (Fig. 2). The lithophytic form *Laurencia obtusa* was abundant at a depth of 3 m, whereas this species epiphytised on *Gongolaria barbata* at a depth of 5 m. The greatest concentration of epiphytic algae was observed at a depth of 5 m, with significantly lower levels recorded at depths of 0.5–3 m. The most prevalent species among the epiphytes was *Vertebrata subulifera*. The diversity index values indicate that the community structure becomes more complex with increasing depth.

In the late 1970s, the western part of Sevastopol Bay was a water area that had been significantly affected by human activities. A notable proliferation of green algae was observed in the studied part of the bay (profiles *2–4*) during the specified period, with *Ulva rigida* exhibiting a marked dominance. This species

is characteristically found in water with a high level of pollution from domestic sewage. It seems probable that the species composition of the macrophytobenthos has been affected by the sewage outlet from the north side urban development since 1964. Furthermore, a fish farm was situated in the vicinity of Severnaya Bay, and its operations also had a deleterious effect on benthic biocenoses. Thus, it is shown in [8] that in areas where ships and other vessels are moored, the concentration of organic and ammonium nitrogen in bottom sediments is found to be 1.5 and 5 times higher, respectively, than in the open sea.

During the construction period of the northern part of the breakwater at profile *1*, the macrophytobenthos is represented mainly by *Gongolaria barbata* (84–99% of the total macrophyte biomass), a cenosis-forming species of the Black Sea coastal zone (Table 2). Although partial water exchange with the open sea still occurred at this site in 1977, the total biomass of macrophytes at depth was 3–10 times lower than in the same year at the open coast of Omega Bay where the proportion of *Cystoseira* spp. also reached 95–98% [9].

Over the past more than 30 years (1977–2008), the composition of dominant macrophyte species has changed significantly in the studied area of the bay. At profiles *2–4*, where *Ulva* species had dominated in 1977, *Gongolaria barbata* became dominant at some depths in 2008 (Table 2). The shift in dominant species is likely indicative of a decline in water pollution. The aforementioned assumption is supported by the studies outlined in monograph [12]. The findings demonstrate that by the conclusion of the 20th century, the concentration levels of phosphates and biogenic elements indicating primarily the release of sewage and storm water were noticeably lower than in the period 1974–1983. Furthermore, it was observed that the concentration of phosphate was 16 times lower during the period 1998–1999 than it was during the 1970s.

Monograph [8] states that the concentration of such persistent organic pollutants of bottom sediments as petroleum hydrocarbons and chloroform bitumoid exhibited a slight increase in 1979–1985 in comparison to the period 1997–2000 (328–999 and 451–507 mg/100 g; 0.82–2.7 and 1.21–1.25 g/100 g). It has been established [13] that in the central part of Sevastopol Bay, in the bottom sediments at a depth of 5 to 20 cm, a zone of extremely high concentration of polychlorinated biphenyls (PCBs) was formed reaching concentrations of up to 600 ng·g^{-1} (per dry weight). The concentration of PCBs in the surface layer of bottom sediment in this area was observed to be slightly lower (from 200 to 450 ng·g^{-1}), which resulted in the authors reaching the conclusion that the anthropogenic pollution of the bay had been reduced.

In June 2009, macrozoobenthos sampling was conducted at stations distributed throughout the bay. The quality of the environment in the vicinity of the Monument to Sunken Ships (profile *4*) was evaluated as "good" according to the M-AMBI index. In contrast, the quality at other stations (central and eastern parts of the bay) was classified as "moderate" or "poor" [14]. According to a number of researchers, the environmental situation of Sevastopol Bay improved during the late 1990s and early 2000s. However, this was not the result of environmental protection actions, but rather due to a reduction in the volume of sewage from industrial enterprises as a consequence of their cessation of operations as well as a decrease in oil pollution due to a reduction in the naval fleet [8, 12]. Nevertheless, the proliferation of algae

(*Ulva intestinalis*, *U. rigida*, *Cladophora laetevirens*, *Cl. serisea Ceramium virgatum*, *C. diaphanum*, *Callithamnion corymbosum*, *Carradoriella denudata*, *Ectocarpus confervoides*), which inhabit water with increased eutrophication, has become a pervasive phenomenon in the study areas, thus indicating the presence of pollutants in the bay.

It is characteristic that the construction of the northern (250 m long) and southern (500 m long) parts of the breakwater at the entrance to the bay has changed the longshore drift of deposits [11]. This provides an explanation for the change of substrate in some areas of the western part of the bay. As posited by the authors, the initial accumulations manifested in the form of sandbanks in both Severnaya and Aleksandrovskaya Bays. The influx of sand into the first bay has ceased entirely, while in the second bay, only residual fragments of sandbanks remain [11]. It is likely that the absence of soft substrates is responsible for the disappearance of sea grasses (*Zostera noltei*) in the area of Cape Khrustalny (profile *2*), which were previously (1977) recorded at a depth of 5 m. In 2008, algae species growing exclusively on hard substrate were found at this profile at this depth. At the same time, minor accumulations of *Zostera marina* appeared at a depth of 5 m near Cape Slavy (profile *3*).

It is possible that the distribution and composition of macrophytobenthos in the western part of the bay in 2008 were influenced by the effects of the storm. It is established that active storm activity results in the degradation and destruction of coastal biocenoses. For instance, following the most intense storm on record in 1992, a comprehensive decimation of benthic vegetation was documented in the Kara Dag region at depths of 0–10 m [15]. In November 2007, an extreme storm was recorded in the Black Sea area, with wind speeds reaching 27–32 m·s⁻¹ and wave heights of up to 4 m [16]. It has previously been demonstrated that this storm had a negative impact on the macrophytobenthos in Laspi Bay [17]. It is well documented that the most intensive growth of macrophytes in the Black Sea occurs during the spring and summer months [8]. Probably, that is why the bottom vegetation in the coastal zone of this part of Sevastopol Bay in summer 2008 was characterised by a high species mosaic, with annual algae species (*Ceramium* spp., *Cladophora* spp.) occurring en masse in the macrophytobenthos composition. During that period, algae of *Laurencia* (*L. coronopus*, *L. obtusa, L. papillosa = Palisada perforata*) were abundant in the studied areas of the bay (Fig. 2). It is known that the active growth of these species begins under intense sunlight and with the beginning of warming of the water column [18]. It is possible that the storm-destroyed *Gongolaria barbata*, with its thalli growing rather slowly, was originally replaced by the beds of representatives of *Laurencia* [8] [18]. Thus, in the water area of profile *2* (Cape Khrustalny), *Gongolaria barbata* seedlings only were recorded at depths of 0.5–1 m and only at depths of 3–5 m, the proportion of this species was 39–79% of the total macrophyte biomass (Table 2).

The results of studies conducted in 2017 indicate that the western part of Sevastopol Bay is characterised by a decrease in the quantitative indicators of macrophytobenthos in the lower sublittoral zone. This trend is observed in other areas of the Black Sea coastline that have experienced an increase in eutrophication [19, 20]. The aforementioned trend precipitates a series of catastrophic outcomes in the bays.

Thus, in the area of Cape Konstantinovsky (profile *1*), at a depth of 5 m, the total macrophyte biomass decreased 20-fold and the proportion of *Gongolaria barbata* decreased 5-fold from 1977 to 2017 (Table 2). During the same period, the total biomass of macrophytes at the same depth exhibited a decrease of over two orders of magnitude in the area of Cape Slavy (profile *3*). The remaining study areas also showed a decrease in the contribution of *Gongolaria barbata* from 2008 to 2017.

It is notable that at the present time, epiphytic algae (*Vertebrata subulifera*, species of *Cladophora*) are prevalent in the macrophytobenthos at all profiles of the western part of the bay. This is attributed to their high competitive ability determined by their resistance to changing environmental conditions, rapid growth and effective assimilation of excessive amounts of organic and mineral elements [9].

It can be reasonably deduced that the changes in the composition of the bottom vegetation in the western part of Sevastopol Bay are likely the result of a combination of natural factors and human economic activity:

– the geo-ecological situation in the bay, associated with high anthropogenic load, has led to the fact that the dominant role in the composition of macrophytobenthos belonged to species growing in the environment with an increased level of pollutants, with a high proportion of epiphytic algae, while the contribution of *Gongolaria barbata* is decreasing. In addition, a sharp decrease in the quantitative indicators of the vegetation component at depths greater than 5 m is observed. The diversity index values indicate a complex polydominant structure of phytocommunities;

– the construction of hydraulic structures in the bay, which have altered the longshore drift of deposits, has resulted in the redistribution of sea grasses growing on soft soils and algae occurring on hard substrates;

– increase in storm intensity affects the state of benthic communities negatively. It is revealed that after extreme storms, the vegetation cover is characterised by significant species mosaic and is predominated by seasonal and annual algae species, with only juvenile *Gongolaria barbata* beds observed at depths of 0.5–1 m.

Conclusion

The distribution of macrophytobenthos biomass and its constituent dominant macrophyte species by depth and years (1977, 2008 and 2017) in the western part of Sevastopol Bay was illustrated.

A comparative analysis of spatiotemporal changes in the contribution of dominant macrophyte species in the western part of Sevastopol Bay over a 40-year period was performed.

It was revealed that during the period under study, polydominant phytocommunities were formed in the composition of bottom vegetation, dominated by species inhabiting highly euthrophic environments, with a high proportion of epiphytic algae and an insignificant role of *Gongolaria barbata*. A sharp decrease in the quantitative indicators of macrophytobenthos at a depth of more than 5 m is a distinctive feature, accompanied by an upward shift in the lower boundary of the macrophyte growth.

---

[9] Minicheva, G.G., 1990. [Predicting the Phytobenthos Structure Using Algal Surface Indicators]. *Botanichesky Zhurnal*, 75(11), pp. 1611–1618 (in Russian).

It was established that changes in the distribution and composition of bottom vegetation in the western part of Sevastopol Bay were caused by its geo-ecological state, which depends on the impact of anthropogenic and natural factors.

The obtained results can be used to monitor the ecological situation in the bay and to organize the coastal and marine nature management.

References

1. Ovsyany, E.I., Romanov, A.S., Min'kovskaya, R.Ya., Krasnovid, I.I., Ozyumenko, B.A. and Zymbal, I.M., 2001. Basic Polluting Sources of Sea near Sevastopol. In: MHI, 2001. *Ekologicheskaya Bezopasnost' Pribrezhnoy i Shel'fovoy Zon i Kompleksnoe Ispol'zovanie Resursov Shel'fa* [Ecological Safety of Coastal and Shelf Zones and Comprehensive Use of Shelf Resources]. Sevastopol: ECOSI-Gidrofizika. Iss. 2, pp. 138–152 (in Russian).

2. Gruzinov, V.M., Dyakov, N.N., Mezenceva, I.V., Malchenko, Y.A., Zhohova, N.V. and Korshenko, A.N., 2019. Sources of Coastal Water Pollution near Sevastopol. *Oceanology*, 59(4), pp. 523–532. https://doi.org/10.1134/S0001437019040076

3. Verzhevskaya, L.V. and Minkovskaya, R.Ya., 2020. Structure and Dynamics of Anthropogenic Load on the Coastal Zone of the Sevastopol Region. *Ecological Safety of Coastal and Shelf Zones of Sea*, (2), pp. 92–106. https://doi.org/10.22449/2413-5577-2020-2-92-106 (in Russian).

4. Slepchuk, K.A. and Sovga, E.E., 2018. Eutrophication Level of the Eastern Part of the Sevastopol Bay on the Basis of Numerical Modeling Of E-TRIX Index. *Ecological Safety of Coastal and Shelf Zones of Sea*, (2), pp. 53–59. https://doi.org/10.22449/2413-5577-2018-2-53-59 (in Russian).

5. Sovga, E.E., Mezentseva, I.V. and Khmara, T.V., 2021. Natural-Climatic and Anthropogenic Factors Determining the Self-Purification Capacity of Shallow-Water Marine Ecosystems in Relation to Reduced Nitrogen Forms. *Ecological Safety of Coastal and Shelf Zones of Sea*, (3), pp. 23–36. https://doi.org/10.22449/2413-5577-2021-3-23-36 (in Russian).

6. Evstigneeva, I.K. and Tankovskaya, I.N., 2008. [Current State and Variability of Macrophytobenthos of the Ushakova Balka Botanical Nature Monument (Black Sea, Sevastopol Region)]. In: B. N. Panov, 2008. *Current Problems of the Azov-Black Sea Region Ecology: Materials of IV International Conference, 8–9 October 2008, Kerch, YugNIRO*. Kerch: YugNIRO Publishers', pp. 92–98 (in Russian).

7. Evstigneeva, I.K., Evstigneev, V.P. and Tankovskaya, I.N., 2019. Structural and Functional Characteristics of the Black Sea Macrophytobenthos in Regions with Different Wind-Wave Conditions. *Water and Ecology: Challenges and Solutions*, (2), pp. 82–91. https://doi.org/10.23968/2305-3488.2019.24.2.82-91 (in Russian).

8. Mironov, O.G., Kirjukhina, L.N. and Alyomov, S.V., 2003. *Sanitary-Biological Aspects of the Sevastopol Bays Ecology in XX Century*. Sevastopol: ECOSI-Gidrofizika, 185 p. (in Russian).

9. Kalugina-Gutnik, A.A., 1982. Changes in Benthic Vegetation in the Sevastopol Bay from 1967 to 1977. *Ecology of the Sea*, 9, pp. 48–62 (in Russian).

10. Goryachkin, Yu.N. and Dolotov, V.V., 2019. *Sea Coasts of Crimea*. Sevastopol: Colorit, 256 p. (in Russian).

11. Efremova, T.V. and Goryachkin, Yu.N., 2023. Morphodynamics of the Sevastopol Bays under Anthropogenic Impact. *Ecological Safety of Coastal and Shelf Zones of Sea*, (1), pp. 31–47.

12. Pavlova, E.V. and Shadrin, N.V., eds., 1999. *Sevastopol Aquatory and Coast: Ecosystem Processes and Services for Human Society*. Sevastopol: Akvavita Publ., 290 p. (in Russian).

13. Malakhova, L.V., Malakhova, T.V. and Egorov, V.N., 2019. [Bottom Sediments of Marine and Fresh Water Bodies of the Crimea as a Depot of Persistent Organic Pollutants]. In: O. A. Shpyrko, V. V. Khapaev, S. I. Rubtsova [et al.], eds., 2019. [*Lomonosov Readings 2019: Annual Scientific Conference of Moscow State University. Sevastopol, 3–4 April 2019*]. Sevastopol: MSU Branch in Sevastopol, pp. 209–210 (in Russian).

14. Osadchaya, T.S., Alyomov, S.V., Tikhonova, E.V., Konsulova, T., Todorova, V. and Shtereva, G., 2010. [Features of Spatial Distribution of Petroleum Hydrocarbons and Structure of Macrozoobenthos of Sevastopol and Varna Bays]. *Monitoring Systems of Environment*, (13), pp. 247–255 (in Russian).

15. Kostenko, N.S., Dyky, E.A. and Zaklezky, A.A., 2008. Long-Term Changes in Cystoseira Phytocenosis of Karadag Natural Reserve (Crimea, Black Sea). *Marine Ekological Journal*, 7(3), pp. 25–36 (in Russian).

16. Dotsenko, S.F. and Ivanov, V.A., 2011. Marine Hazards in the Azov-Black Sea Region. In: MHI, 2011. *Ekologicheskaya Bezopasnost' Pribrezhnykh i Shel'fovykh Zon i Kompleksnoe Ispol'zovanie Resursov Shel'fa* [Ecological Safety of Coastal and Shelf Zones and Comprehensive Use of Shelf Resources]. Sevastopol: ECOSI-Gidrofizika. Iss. 24, pp. 209–218 (in Russian).

17. Pankeeva, T.V. and Mironova, N.V., 2019. Spatiotemporal Changes in the Macrophytobenthos of Laspi Bay (Crimea, Black Sea). *Oceanology*, 59(1), pp. 86–98. https://doi.org/10.1134/S0001437019010168

18. Evstigneeva, I.K., 1983. Seasonal Dynamics of *Laurencia* Cenopopulation Structure in the Sevastopol Bay. *Ecology of the Sea*, 14, pp. 56–62 (in Russian).

19. Milchakova, N.A., Mironova, N.V. and Ryabogina, V.G., 2011. [Marine Plant Resources]. In: V. N. Eremeev, A. V. Gaevskaya, G. E. Shulman and Ju. A. Zagorodnyaya, eds., 2011. *Biological Resources of the Black Sea and Sea of Azov*. Sevastopol: ECOSI-Gidrofizika. Ch. 4, pp. 117–139 (in Russian).

20. Mironova, N.V. and Pankeeva, T.V., 2020. Spatio-Temporal Changes in the Macrophytobenthos of Kruglaya Bay. *South of Russia: Ecology, Development*, 15(2), pp. 125–139. https://doi.org/10.18470/1992-1098-2020-2-125-139 (in Russian).

About the authors:

Nataliya V. Mironova, Senior Research Associate, A.O. Kovalevsky Institute of Biology of the Southern Seas of RAS (2 Nakhimov Av., Sevastopol, 299011, Russian Federation), PhD (Biol.), **ResearcherID: AAC-9421-2022, ORCID ID: 0000-0001-7110-7081**, *dr.nataliya.mironova@yandex.ru*

Tatyana V. Pankeeva, Senior Research Associate, A.O. Kovalevsky Institute of Biology of the Southern Seas of RAS (2 Nakhimov Av., Sevastopol, 299011, Russian Federation), PhD (Geogr.), **ResearcherID: AAC-8694-2022**, **ORCID ID: 0000-0002-8933-6103**, *tatyanapankeeva@yandex.ru*

Contribution of the authors:

Nataliya V. Mironova – processing of macrophytobenthos samples (1977, 2008, 2017), analysis and description of the study results, preparation of the article text, selection, systematisation and analysis of literature sources

Tatyana V. Pankeeva – selection, systematisation and analysis of literature sources, preparation of the article text, cartographic materials and references

All the authors have read and approved the final manuscript.

Original paper

Distribution of Polychaetes of the Family Dorvilleidae (Annelida) on the Shelf of Crimea

N. A. Boltachova*, E. V. Lisitskaya

A.O. Kovalevsky Institute of Biology of the Southern Seas of RAS, Sevastopol, Russia
**e-mail: boltachova@ibss.su*

Abstract
In recent decades, the interest in polychaetes of the Dorvilleidae family, adapted to exist in marginal biotopes (cold methane seeps, hydrothermal vents, sulphide sediments) has increased. The work aims to analyze the ecological characteristics, distribution and quantitative representation of Dorvilleidae in the Black Sea. The study materials were samples of macrozoobenthos on the Black Sea shelf in 2010–2019, taken with an Okean-50 bottom grab ($S = 0.25$ m^2), and benthos samples, taken in the coastal areas of Crimea in 1997–2023 with a diving bottom grab ($S = 0.04$ m^2). Three species of the family Dorvilleidae were recorded in the northern Black Sea: *Dorvillea rubrovittata* (Grube, 1855)*, Schistomeringos rudolphii* (Delle Chiaje, 1828), *Protodorvillea kefersteini* (McIntosh, 1869)*. Their bathymetric range was limited to the photic zone (up to 50 m). *D. rubrovittata* occurred mainly in the biotope of hard substrates fouling and formed relatively large aggregations (up to 438 ind.·m^{-2}) in underwater channels and caves. The species was first found by us in the northwestern part of the Black Sea. *S. rudolphii* was recorded in small quantities (2–300 ind.·m^{-2}) along the entire Crimean coast. This species was found mainly on shell substrates and among macrophytes. *P. kefersteini* was recorded in almost the entire northern part of the Black Sea (excluding the Caucasian coasts) on sandy-shell substrates with varying degrees of siltation. It is a mass species, and its density reached significant values in some areas. In Kruglaya Bay (Sevastopol area), a stable population of this species with the highest occurrence (up to 88 %) and density (up to 13,215 ind.·m^{-2}) was recorded for a long time. The supposed reason for this is the formation in Kruglaya Bay of large assemblages of bacteria and microalgae, which are a forage base for *P. kefersteini*.

Keywords: Polychaeta, Dorvilleidae, *Protodorvillea kefersteini,* Kruglaya Bay, Black Sea

Распространение полихет семейства Dorvilleidae (Annelida) на шельфе Крыма

Н. А. Болтачева*, Е. В. Лисицкая

Институт биологии южных морей имени А. О. Ковалевского РАН, Севастополь, Россия
*e-mail: boltachova@ibss.su

Аннотация

В последние десятилетия возрос интерес к полихетам семейства Dorvilleidae, приспособленным к существованию в маргинальных биотопах – в холодных метановых сипах, гидротермальных источниках, сульфидных осадках. Целью настоящей работы являлся анализ экологических особенностей, распространения и количественной представленности Dorvilleidae в Черном море. Материалом для исследований послужили сборы макрозообентоса на Черноморском шельфе в 2010–2019 гг., выполненные с помощью дночерпателя «Океан-50» (S = 0.25 м^2), а также сборы бентоса в прибрежных районах Крыма в 1997–2023 гг. с использованием водолазного дночерпателя (S = 0.04 м^2). В северной части Черного моря зарегистрированы три представителя Dorvilleidae: *Dorvillea rubrovittata* (Grube, 1855)*, Schistomeringos rudolphii* (Delle Chiaje,1828), *Protodorvillea kefersteini* (McIntosh, 1869)*. Батиметрический диапазон их обитания ограничивается фотической зоной (до 50 м). *D. rubrovittata* встречался преимущественно в биотопе обрастания твердых субстратов, относительно большие скопления (до 438 экз.·м$^{-2}$) образовывал в подводных канала и гротах. Видвпервые обнаружен нами в северо-западной части Черного моря. *S. rudolphii* зарегистрирован в небольших количествах (2–300 экз.·м$^{-2}$) вдоль всего побережья Крыма. Этот вид встречался преимущественно на ракушечных грунтах и среди макрофитов. *P. kefersteini* отмечен почти во всей северной части Черного моря (за исключением кавказских берегов) на песчано-ракушечных грунтах с разной степенью заиления. Это массовый вид, его плотность в отдельных районах достигала значительных величин. В бухте Круглой (район Севастополя) в течение длительного времени регистрировали устойчивую популяцию этого вида с наиболее высокими показателями встречаемости (до 88 %) и плотности (до 13 215 экз.·м$^{-2}$). Предполагаемая причина этого – образование в бухте Круглой больших скоплений бактерий и микроводорослей, которые являются кормовой базой для *P. kefersteini*.

Ключевые слова: Polychaeta, Dorvilleidae, *Protodorvillea kefersteini,* бухта Круглая, Черное море

Introduction

The polychaetes of the family Dorvilleidae are widespread in the world ocean. In the 1970s, eight genera of this family were known [1]. Further studies of ecosystems, including deep-sea ones, in the zones of hydrothermal, methane and other seeps, led to the discovery of many new representatives of Dorvilleidae adapted to existence in these marginal biotopes. Notably, these polychaetes have been observed to dominate the macrozoobenthos community in cold methane seeps, hydrothermal vents, whale bone accumulations and sediments within the oxygen minimum zone [2]. Dorvilleids exhibit a remarkable tolerance to sulfides and these polychaeteshave been identified in sulfide sediments found in both shallow waters and polluted estuaries [2–4]. Dorvilleidaeare regarded as opportunistic species capable of colonising diverse habitats characterised by the presence of organic matter and heavy metals [2]. Observations have revealed that certain Dorvilleidae species form substantial aggregations in areas of intensive fish aquaculture, with their abundance also increasing in proximity to mussel farms. Consequently, these species can be utilised as indicators of the aquaculture impact on the surrounding biota [1)][5].

To date, researchers have documented more than 200 species belonging to 31 genera of Dorvilleidae. Of these, three genera are known to occur in the Black Sea [2)] [6–8], namely *Protodorvillea kefersteini* (McIntosh, 1869)*, Dorvillea rubrovittata* (Grube, 1855)*, Schistomeringos rudolphii* (Delle Chiaje, 1828) and *Schistomeringos neglecta* (Fauvel, 1923). The latter species is listed for the Bosporus outlet area of the Black Sea and the coasts of Bulgaria and apparently belongs to the complex of species inhabiting the zone of action of the waters of the Sea of Marmara [3)] [9]. The first three species are listed for many areas of the Black Sea [4)] [9–13], however, there is little data on their distribution and occurrence in different biotopes. No representatives of Dorvilleidae have been recorded in the Sea of Azov [8, 14, 15].

Given the increased interest in this polychaete family, a more detailed analysis of the ecological characteristics, distribution and quantitative representation of Dorvilleidae in the Black Sea becomes relevant, which is the aim of this paper.

[1)] Ross, J., McCarty, A., Davey, A., Pender, A. and MacLeod, C., 2016. *Understanding the Ecology of Dorvilleid Polychaetes in Macquarie*. Fisheries Research and Development Corporation, 2016. Available at: https://www.imas.utas.edu.au/__data/assets/pdf_file/0010/905752/2014-038-DLD-Dorvs.pdf [Accessed: 2 December 2024].

[2)] Bobretsky, N., 1870. [Materials for the Black Sea Fauna. Annelidae (Annelida, Polychaeta)]. In: KOE, 1870. *Zapiski Kievskogo Obshchestva Estestvoispytateley*. Vol. 1, iss. 2, pp. 188–274 (in Russian).

[3)] Rullier, F., 1963. Les Annélides Polychètes du Bosphore, de la Mer de Marmara et de la Mer Noire, en Relation avec Celles de la Méditerranée. *Rapports et Procès-Verbaux des Réunions Commission Internationale pour l'Exploration Scientifique de la Mer Méditerranée*. Monaco. Vol. 17, pp. 161–260.

[4)] Bondarenko, A.S., 2012. [*Ecology of Polichetes of the Northeastern Black Sea*]. Extended Abstract of PhD Thesis. Sevastopol, 23 p. (in Russian).

Materials and methods

The macrozoobenthos samples from R/V *Professor Vodyanitsky* expeditions (cruises Nos. 64, 68, 70, 72, 75, 84, 86, 90, 96, 108) in 2010–2019 served as the present study material. The work was performed on the shelf of the northern part of the Black Sea from the coast of Romania to the Caucasian coast (Tuapse area) as well as in the Sea of Azov off the coast of Crimea. The stations were carried out in the depth range from 10 to 137 m. The salinity levels in the Black Sea ranged from 16.89 to 18.47‰ and in the Azov Sea, they fluctuated between 12.53 and 15.22‰ during the sampling. Collected from 291 stations, the materials obtained from the bottom grab samples were utilised. Bottom sediments were collected employing an Okean-50 bottom grab, with a capture area of 0.25 m². The collected sediments were then subjected to sieve washing, with the smallest mesh size employed being 1 mm.

Materials from benthic surveys carried out in the coastal areas of Crimea by the Benthos Ecology Department of IBSS from 1997 to 2023 were also utilised in the analysis. A series of studies were conducted in a number of locations throughout the region, including Karkinit Bay, Lake Donuzlav, the bays of Sevastopol, the Kara Dag water area and Feodosia Bay. In addition, a number of underwater caves of both natural and artificial origin in southeastern and southwestern Crimea were also investigated [16]. In 2005, year-round macrozoobenthos surveys were conducted at two stations (6–7.5 m depth) in the western part of Kruglaya Bay. Samples from loose substrates were taken with a diving bottom grab (S = 0.04 m²), typically in two repetitions. Material was collected from hard surfaces using a frame (S = 0.04 m²) with a silk bolting cloth bag sewn to it. A total of 440 stations, with a depth range of 0–25 m, were carried out. The collected material was then subjected to sieve washing, with the sieves having a mesh diameter of 0.5 mm. Following this, all specimens were fixed in 4% neutralised formalin. Taxonomic identification of polychaetes was facilitated by the utilisation of literature data [5] [7].

Results and discussion

During the course of the study focused on cruise materials (on loose substrates at a depth of more than 10 m), dorvilleids were identified at 52 out of 291 stations in the Black Sea. Conversely, no dorvilleids were recorded in the Sea of Azov (21 stations). *P. kefersteini* was recorded at 30 stations, *S. rudolphii* – at 19 and *D. rubrovittata* – at three stations (Fig. 1). Thus, dorvilleids are relatively rare species on soft bottoms in the open sea, with only *P. kefersteini* demonstrating 10% occurrence, while *S. rudolphii* and *D. rubrovittata* have 6.5 and 1% occurrence, respectively. The maximum density of dorvilleids reached 704 ind.·m⁻².

In the Crimean coastal area (1–22 m depth), dorvilleids were found in almost all areas on soft bottoms and in fouling (Fig. 1). Their density exhibited significant fluctuations within broad limits, consistently being higher in comparison to areas in the open sea. Representatives of this family were also found in underwater caves and channels.

---

[5] Vinogradov, K.A. and Losovskaya, G.V., 1968. The Type of Segmeted Worms – Annelida. In: F. D. Mordukhay-Boltovskoy, ed., 1968. *Field Guide for the Black Sea and Sea of Azov Fauna.* Kiev: Naukova Dumka. Vol. 1: Free-Living Invertebrates, pp. 251–405 (in Russian).
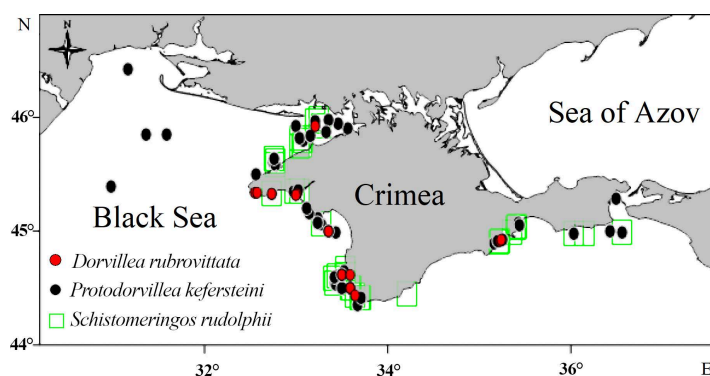
F i g . 1 . Distribution of Dorvilleidae in the northern part of the Black Sea

Dorvillea rubrovittata

D. rubrovittata is an Atlantic-Mediterranean species [1, 7, 17]; in the Black Sea, it is indicated for the Bosporus outlet area of the Black Sea, the coasts of Turkey and Bulgaria [7, 9] and also found [6] off the coasts of the Caucasus and Crimea [7, 18, 19]. This species is considered to be relatively rare, with documented occurrences in minimal numbers on the shell and in the fouling of rocks and stones at a depth of 0–50 m [5] [7, 9]. It has not been recorded off the coast of Romania [10] and is generally found in the northwestern Black Sea (NWBS) [4] [20, 21].

In our samples, *D. rubrovittata* (Fig. 2, *a*) was found in open sea areas only near the western shores of Crimea and in Karkinit Bay at a depth of 14–30 m on shell substrates. Its density was 4–16 ind.·m^{-2} (Fig. 1).

In the coastal shallow water area, the species was recorded in rock and stone fouling in the areas of Kara Dag, Tarkhankut and Donuzlav. In the bays of Sevastopol, it was found in the fouling of oyster farm cages [22]. In these biotopes, its abundance did not exceed 13 ind.·m^{-2}. Higher density values of D. rubrovittata were recorded on the walls of underwater caves in the areas of Balaklava and KaraDag
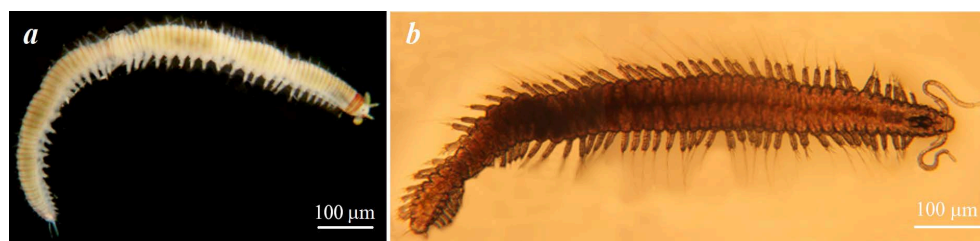
F i g . 2 . *Dorvillea rubrovittata* (*a*); *Protodorvillea kefersteini* (*b*)

---

[6] Yakubova, L.I., 1930. [List of Archiannelidae and Polychaeta of Sevastopol Bay of the Black Sea]. *Izvestiya AN SSSR. Series 7. Physical and Mathematical Division*, (9), pp. 863–881 (in Russian).

(up to 125 ind.·m^{-2} at a depth of 2 m). In the underground Balaklava canal in the fouling of concrete walls at a depth of 2 m, the maximum values of this indicator were recorded – up to 438 ind.·m^{-2}. Conditions in the canal differ from other biotopes due to poor hydrodynamics and low light levels.

It is evident that *D. rubrovittata* is prevalent along the Black Sea coast of Crimea. The species has been recorded predominantly in the fouling biotope of hard substrates, with relatively large aggregations observed in areas of reduced hydrodynamics.

Schistomeringos rudolphii

S. rudolphii is widespread in the Atlantic Ocean (European and American coasts), the Mediterranean Sea and is also indicated for parts of the Pacific and Indian Oceans [1, 7, 9, 17]. There are isolated records of this species in the Black Sea. The species has been recorded in the Bosporus outlet area of the Black Sea [2], the coasts of Turkey and Bulgaria [8–10, 13]. There are also two indications of *S. rudolphii* for the Caucasus coasts [11, 15]. In Crimea, the species was found only in Sevastopol Bay on sandy-shell substrates among Zostera roots [6, 7]. The next occurrence of *S. rudolphi* was also recorded near Sevastopol at the end of the 20th century [23]. The first records of this species in the northwestern Black Sea date back to the end of the 20th and beginning of the 21st century, when it was found [4] in the shallow waters of Yagorlyk, Tendra and Karkinit Bays [12].

In our materials, *S. rudolphii* was recorded in open sea areas on soft bottoms along the entire Crimean coast (Fig. 1). The species was found at depths of 10–45 m, with one occurrence at a depth of 88 m. The maximum density values were recorded in the Karkinit Bay (240 ind.·m^{-2}) and the Kerch pre-strait area (210 ind.·m^{-2}) at depths of 20 and 34 m, respectively.

In coastal samples, *S. rudolphii* was found at a depth of 2–22 m at some stations on the eastern and southern coasts of Crimea (Feodosia Bay, Kara Dag area, Laspi Bay), in many bays of southwestern Crimea and also in Lake Donuzlav. The density of these polychaetes was relatively low, but sometimes it reached 300 ind.·m^{-2} (Laspi Bay, 13 m depth) [24]. The species was discovered to inhabit a variety of substrates, yet it was most frequently observed in association with shell substrates and among macrophytes (Fig. 3).

It has been observed that *S. rudolphii* is present in Donuzlav and Kruglaya Bay, where it has been recorded inhabiting areas of algae fam. Characeae and sea grasses *Potamogeton* and *Zostera*, growing on silty substrates at a depth of 2–7 m. The species has also been found in small numbers (8–50 ind.·m^{-2}) in the fouling of the walls of caves and underground Balaklava canal.

Protodorvillea kefersteini

P. kefersteini is an Atlantic-Mediterranean species indicated for the North American and European coasts, widely distributed in the seas of the Mediterranean basin [1, 9, 17]. The distribution of *P. kefersteini* has been documented in nearly all areas of the Black Sea [7–10, 13]. However, it did not occur in the NWBS until

[7] Pereyaslavtseva, S.M., 1891. [Additions to the Black Sea Fauna]. In: *Kharkov University, 1891. Trudy Obshchestva Ispytateley Prirody at the Kharkov University*. Vol. 25, pp. 235–274 (in Russian).
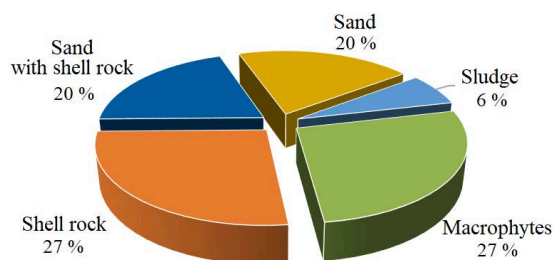
F i g . 3 . Occurrence of *Schistomeringos rudolphii* on different sediments

almost the beginning of the 21st century [20]. The first detection of this species refers to the pseudomeiobenthos of Yagorlyk Bay [12]. In subsequent years, *P. kefersteini* was identified in the shallow waters of Tendra and Karkinit Bays. No records of the species have been found in other NWBS areas [4] [25]. It is likely that the species inhabits the shores of the Caucasus, its occurrence is known off the coast of the Taman Peninsula [26]. *P. kefersteini* has been documented as a species that is abundant in certain Crimean coastal areas, as well as in the coastal waters of Bulgaria [6, 7].

In open sea areas, we encountered *P. kefersteini* (Fig. 2, *b*) in almost the entire northern part of the Black Sea, with the exception of the Caucasian coasts (Fig. 1). The species was recorded at depths of 12–45 m, with a single occurrence off the Southern Coast of Crimea at a depth of 94 m. *P. kefersteini* was predominantly found on sandy-shell substrates, with occasional instances of silty substrates. Its density was found to vary from 4 to 464 ind.·m^{-2}.

The species was recorded in the majority of the coastal shallow water areas of Crimea that were the subject of the study, with the areas in question being located along the eastern and southern coasts (Kerch pre-strait area, Feodosia Bay, Kara Dag water area, Laspi Bay), off southwestern Crimea as well as in Karkinit Bay and Lake Donuzlav. *P. kefersteini* was recorded at a depth of 1–17 m on sandy-shell substrates with different degrees of siltation. Its density varied within large limits and in some areas reached such significant values as 1200 ind.·m^{-2} (Laspi Bay, 13 m depth, sandy-shell substrate) and 4975 ind.·m^{-2} (Kara Dag water area, Experimental mussel farm area, 7 m depth, silty sand).

P. kefersteini was recorded in all bays and gulfs under study off the coast of southwestern Crimea, and during the summer surveys its occurrence and average density varied considerably in different areas (Table).

In the abovementioned areas, the occurrence of *P. kefersteini* did not generally exceed 50% and in Kazachya Bay, it was 50% with relatively low average density 62 ind.·m^{-2}. An exception was observed in Kruglaya Bay, where the occurrence was 88% and the average density was 2514 ind.·m^{-2}. Herewith, the maximum density of the species (13,215 ind.·m^{-2}) was recorded in summer 2004 (4 m depth, coarse sand). Work carried out in the bay in 1990 also recorded relatively high levels

Quantitative parameters of *P. kefersteini* distribution at coastal areas of southwestern Crimea

Study area	Occurrence, %	Mean density, ind.·м$^{-2}$
Balaklava Bay	18	10
Sevastopol Bay	6	4
Kruglaya Bay	**88**	**2514**
Streletskaya Bay	9	233
Kazachya Bay	50	62
Cape Fiolent	33	217
Coast near the village of Lyubimovka	10	76
Donuzlav Lake	24	9

of *P. kefersteini*, with its occurrence of 40% and average density of 280 ind.·m^{-2} [27]. According to our data obtained in 2013 in Kruglaya Bay, the maximum density of the species in May was 11,288 ind.·m^{-2}, and in November, it reached 13,375 ind.·m^{-2} (5–6 m depth at sampling stations, coarse sand), with the average density being 2893 ind.·m^{-2}.

Thus, in Kruglaya Bay, the population of *P. kefersteini* has been recorded for many years and it has always been characterised by high density. It is hypothesised that the high abundance of this species during summer surveys is due to recruitment of juveniles. It is further assumed that the Black Sea is the breeding ground for *P. kefersteini* during the summer season as mature individuals were found in June [7]. Seasonal surveys carried out in 2005 in Kruglaya Bay showed that the species is present in the benthos throughout the year in significant numbers, reaching a maximum in July (Fig. 4).

It is evident that high density values of this species are also present in other Black Sea areas. In the Taman Peninsula, the average density of *P. kefersteini* was recorded as 320 ind.·m^{-2} [26], near Kara Dag – 445 ind.·m^{-2}, with its maximum of 2000 ind.·m^{-2} [7]. Along the Bulgarian coast, *P. kefersteini* is categorised as a mass
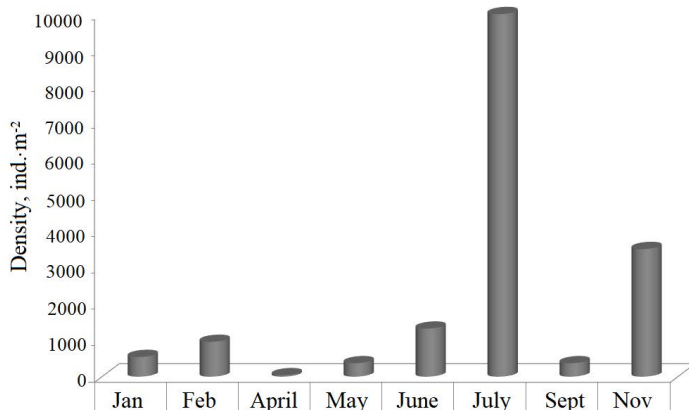
F i g . 4 . Seasonal dynamics of *P. kefersteini* density
in Kruglaya Bay(2005)

species, exhibiting an average density of 556 ind.·m^{-2} in specific biocenoses, with
its maximum of 6200 ind.·m^{-2} [6].

Consequently, the population of *P. kefersteini* in Kruglaya Bay exhibited re-
markably elevated quantitative indices over an extended period when compared
to all other areas under study. This prompts the question of the underlying causes
of this phenomenon. The following hypothesis is proposed.

P. kefersteini belongs to small species of the family Dorvilleidae, which are
characterised by feeding on microalgae and bacterial film, which is possible due to
the peculiarities of their mouth apparatus structure [4]. It can be assumed that
the forage supply of this species is extremely high in Kruglaya Bay.

Kruglaya Bay is located within the Sevastopol municipal boundaries and expe-
riences a high recreational load. During the summer and autumn period, elevated
concentrations of organic nitrogen and phosphorus, in addition to nitrates, have
been recorded in the sea water. This observation is corroborated by long-term data
[28]. Studies have shown that the ammonium nitrogen content in bottom sediments
of Kruglaya Bay is about 10 times higher than in the sediments of the open sea
[27]. It can be hypothesised that the elevated level of organic pollution in Kruglaya
Bay contributes to the augmentation of the polychaete forage base and is a contrib-
uting factor to the mass development of *P. kefersteini* in this water area.

It should also be noted that the bays of Sevastopol are characterised by the pres-
ence of jet gas emissions (cold gas seeps) caused by methane flow from the deep
sediment layers into the surface substrate horizons. Seeps in this area were regis-
tered at shallow depths (from 11–12 m) [29]. The presence of methanotrophic
microorganisms forming bacterial mats has been demonstrated in the area sur-
rounding jet gas outlets [30]. Evidence has been found which suggests the presence
of jet gas emissions in the Kruglaya Bay area [31]. In other regions of the world

ocean, research conducted on methane seeps ecosystems has revealed the prevalence of dorvilleids within these environments. These organisms are particularly abundant in the bacterial mats that proliferate around the seeps, with their abundance reaching up to 92% of the total macrofauna [3, 32]. There is evidence to suggest that certain members of the family Dorvilleidae consume chemosynthetic bacteria as part of their diet [4]. It has been hypothesised that the dorvilleids assemblages observed in proximity to methane seeps can be attributable to the forage specialisation of these polychaetes on specific prokaryotes [2, 3]. Assuming the presence of bacterial mats in Kruglaya Bay, formed around jet gas emissions, and their role as a forage source for *P. kefersteini*, it can be deduced that the development of a stable population of the species within this water area is a consequence.

Conclusion

Three species of the family Dorvilleidae were recorded in the northern Black Sea during the study: *Dorvillea rubrovittata* (Grube, 1855)*, Schistomeringos rudolphii* (Delle Chiaje, 1828), *Protodorvillea kefersteini* (McIntosh, 1869)*. All of the above species are considered to be fairly widespread; however, their bathymetric range is limited to the photic zone (up to 50 m). This can be related to their feeding habits, which are specialised on micro- and macrophytes. The data obtained suggest that the distribution of dorvilleids in the Azov-Black Sea basin is also influenced by water salinity. It can be hypothesised that the salinity of 17–18‰, which is typical of the Black Sea, is a limiting factor for dorvilleids. To date, no species of dorvilleids has been found in the Sea of Azov, despite the recent increase in its salinity (up to 15‰) and pontization of the fauna. This can be indicative of the rarity of dorvilleids in the NWBS where coastal areas can be subject to desalination processes.

D. rubrovittata is a common species on the Black Sea coasts of Crimea. It occurs mainly in the biotope of hard substrates fouling and forms relatively large aggregations in areas with poor hydrodynamics and low light levels (underwater channels and caves), where its density reached 438 ind.·m^{-2}. The species was first found by us in the northwestern part of the Black Sea.

S. rudolphii was previously considered rare in the Black Sea, with only isolated occurrences documented. In the present study, the species was recorded in low numbers (2–300 ind.·m^{-2}) on soft bottoms along the entire Crimean coast. The species was most frequently found on shell substrates and among macrophytes. In Lake Donuzlav, *S. rudolphii* was observed to be widespread in areas of algae fam. Characeae and sea grasses *Potamogeton* and *Zostera*.

P. kefersteini was recorded in almost the entire northern part of the Black Sea (excluding the Caucasian coasts) on sandy-shell substrates with varying degrees of siltation. It is a mass species and its density reached significant values in some areas. In Kruglaya Bay (Sevastopol area), a stable population of this species with the highest occurrence (up to 88 %) and density (up to 13,215 ind.·m^{-2}) was recorded

for a long time. The features of Kruglaya Bay are as follows: firstly, there is an increased level of organic pollution, and secondly, there is the presence of jet gas emissions around which bacterial mats can form. It is hypothesised that this leads to the formation of large assemblages of bacteria and microalgae which are a forage base for *P. kefersteini*.

REFERENCES

1. Jumars, P.A., 1974. A Generic Revision of the Dorvilleidae (Polychaeta), with Six New Species from the Deep North Pacific. *Zoological Journal of the Linnean Society*, 54, pp. 101–135.https://doi.org/10.1111/j.1096-3642.1974.tb00794.x

2. Levin, L.A., Ziebis, W., Mendoza, G.F., Bertics, V.J., Washington, T., Gonzalez, J., Thurber, A.R., Ebbe, B. and Lee, R.W., 2013. Ecological Release and Niche Partitioning under Stress: Lessons from Dorvilleid Polychaetes in Sulfidic Sediments at Methane Seeps. *Deep Sea Research Part II: Topical Studies in Oceanography*, 92, pp. 214–233. https://doi.org/10.1016/j.dsr2.2013.02.006

3. Levin, L.A., Ziebis, W., Mendoza, G.F., Growney, V.A., Tryon, M.D., Brown, K.M., Mahn, C., Gieskes, J.M. and Rathburn, A.E., 2003. Spatial Heterogeneity of Macrofauna at Northern California Methane Seeps: Influence of Sulfide Concentration and Fluid Flow. *Marine Ecology Progress Series*, 265, pp. 123–139. https://doi.org/10.3354/meps265123

4. Jumars, P.A., Dorgan, K.M. and Lindsay, S.M., 2015. Diet of Worms Emended: An Update of Polychaete Feeding Guilds. *Annual Review of Marine Science*, 7, pp. 497–520. https://doi.org/10.1146/annurev-marine-010814-020007

5. Paxton, H. and Davey, A., 2010. A New Species of Ophryotrocha (Annelida: Dorvilleidae) Associated with Fish Farming at Macquarie Harbour, Tasmania, Australia. *Zootaxa*, 2509, pp. 53–61. https://doi.org/10.5281/zenodo.196027

6. Marinov, T.M., 1990. *The Zoobenthos from the Bulgarian Sector of the Black Sea*. Publishing House of the Bulgarian Academy of Sciences, Sofia, 195 p.

7. Kiseleva, M.I., 2004. *Polychaetes (Polychaeta) of the Azov and Black Seas*. Apatity: Print. Kola Science Centre RAS, 409 p. (in Russian).

8. Kurt Şahin, G. and Çinar, M.E., 2012. A Check-List of Polychaete Species (Annelida: Polychaeta) from the Black Sea. *Journal of the Black Sea / Mediterranean Environment*, 18(1), pp. 10–48. Available at: https://www.researchgate.net/publication/251572749_A_checklist_of_polychaete_species_Annelida_Polychaeta_from_the_Black_Sea [Accessed: 21 November 2024].

9. Marinov, T.M., 1977. *Polychaeta. Fauna Bulgarica*. Sofia: Publishing House of the Bulgarian Academy of Sciences. Vol. 6, 258 p.

10. Surugiu, V., 2005. Inventory of Inshore Polychaetes from Romanian Coast (Black Sea). *Mediterranean Marine Science*, 6(1), pp. 51–73. https://doi.org/10.12681/mms.193

11. Frolenko, L.N., 2008. [Current Characterization of Zoobenthos of the Northeastern Part of the Black Sea]. In: AzNIIRKh, 2008. [*The Main Problems of Fisheries and Protection of Fish-ery Water Bodies of the Azov and Black Sea Basin: Collected Papers (2006–2007)*]. Rostov-on-Don: AzNIIRKh, pp. 180–188 (in Russian).

12. Vorobyova, L.V., 1999. [*Meiobenthos of the Ukrainian Shelf of the Black and Azov Seas*]. Kiev: Naukova Dumka, 300 p. (in Russian).

13. Çinar, M.E. and Erdoğan-Dereli, D., 2023. Polychaetes (Annelida: Polychaeta) off Kıyıköy (Black Sea, Türkiye) with Descriptions of Three New Species. *Zootaxa*, 5383(4), pp. 537–560. https://doi.org/10.11646/zootaxa.5383.4.6

14. Volovik, S.P., Korpakova, I.G., Barabashin, T.O. and Volovik, G.S., 2010. [*Fauna of Water and Coastal-Water Ecosystems of the Azov-Black Seas Basin*]. Krasnodar: AzNIIRKH, 251 p. (in Russian).

15. Kiseleva, M.I., 1981. [*Soft-Bottom Benthos of the Black Sea*]. Kiev: Naukova Dumka, 165 p. (in Russian).

16. Sergeeva, N.G., Tarariev, Y.S., Gorbunov, R.V., Revkov, N.K., Boltachova, N.A., Samokhin, G.V., Shcherbich, A.M., Kirin, M.P., Mironyuk, O.A. [et al.], 2021. First Researches of the Underwater Ecosystem Communities of an Underground Channel Built in 1950s (Balaklava Bay, Sevastopol) *Ecologica Montenegrina*, 39, pp. 30–45. https://doi.org/10.37828/em.2021.39.4

17. Dauvin, J.-C., Dewarumez, J.-M. and Gentil, F., 2003. Liste Actualisée des Espèces d'Annélides Polychètes Présentesen Manche. *Cahiers de Biologie Marine*, 44, pp. 67–95.

18. Vinogradov, K.A., 1949. On the Fauna of Annelid Worms (Polychaeta) of the Black Sea. In: K. A. Vinogradov, ed., 1949. *Trudy Karadagskoy Biologicheskoy Stantsii*. Lvov: Izd-vo Akademii Nauk SSSR. Iss. 8. 84 p. (in Russian).

19. Milovidova, N.Yu., 1966. [Bottom Biocenoses of Novorossiysk Bay. In: V. A. Vodyanitsky, ed., 1966. [*Distribution of the Benthos and Biology of Benthic Fauna in the Southern Seas*]. Kiev: Naukova Dumka, pp. 90–101. (in Russian).

20. Vinogradov, K.A., Losovskaya, G.V., Kaminskaya, L.D., 1967. Short Overview ofthe Specific Composition of the Invertebrate Fauna of the Northwestern Part of the Black Sea (by Systematic Groups). In: K. A. Vinogradov, ed., 1967. *Biology of the Northwestern Part of the Black Sea*. Kiev: Naukova Dumka, pp. 177–201 (in Russian).

21. Kovalishina, S.P. and Kachalov, O.G., 2015. Macrozoobenthos of Zernov's Phyllophora Field in May–June 2012 year. *Scientific Issue Ternopil Volodymyr Hnatiuk National Pedagogical University Series: Biology*, 3–4(64), pp. 309–313 (in Russian).

22. Lisitskaya, E.V. and Boltachova, N.A., 2023. Taxonomic Composition of Polychaete Worms in the Mussel-Oyster Farm Area (the Black Sea, Sevastopol). *Ecological Safety of Coastal and Shelf Zones of Sea*, (1), pp. 113–123. https://doi.org/10.29039/2413-5577-2023-1-113-123

23. Kiseleva, M.I., 1988. A Characteristic of Benthos Changes of Many Years in the Littoral Zone of the Area of Sevastopol. *Ecology of the Sea*, 28, p. 26–32 (in Russian).

24. Revkov, N.K. and Boltacheva, N.A., 2022. Restoration of the Biocoenosis of the Black Sea Scallop Flexopecten glaber (Bivalvia: Pectinidae) off the Coast of Crimea (Laspi Area). *Ecological Safety of Coastal and Shelf Zones of Sea*, (4), pp. 90–103.

25. Bondarenko, O. and Vorobyova, L., 2023. Influence the North-Western Part of the Black Sea Habitat Factors on the Meiobenthic Polychaetes. *Turkish Journal of Fisheries and Aquatic Sciences*, 23(9), TRJFAS22222. https://doi.org/10.4194/TRJFAS22222

26. Terentev, A.S. and Semik, A.M., 2019. Macrozoobentos of Tuzla Spit (Kerch Strait) During the Summer of 2013. *Ekosistemy*, 20, pp. 82–91. (in Russian).

27. Boltachova, N.A., Revkov, N.K., Bondarenko, L.V., Makarov, M.V. and Nadolny, A.A., 2022. Benthic Fauna of the Kruglaya Bay (Black Sea, Crimea). Part II: Taxonomic Composition and Quantitative Characteristics of Macrozoobenthos in the Soft-Bottom Biotope. *Proceedings of the T.I. Vyazemsky Karadag Scientific Station – Nature Reserve of the Russian Academy of Sciences*, 7(2), pp. 3–22 (in Russian).

28. Pavlova, E.V., Murina, V.V. and Kuphtarkova, E.A., 2001. Chemical and Biological Studies in the Omega Bay (the Black Sea, Sevastopol). In: MHI, 2001. *Ekologicheskaya*

Bezopasnost' Pribrezhnoy i Shel'fovoy Zon i Kompleksnoe Ispol'zovanie Resursov Shel'fa [Ecological Safety of Coastal and Shelf Zones and Comprehensive Use of Shelf Resources]. Sevastopol: ECOSI-Gidrofizika. Iss. 2, pp. 159–176 (in Russian).

29. Egorov, V.N., Artemov, Yu.G. and Gulin, S.B., 2011. *Methane Seeps in the Black Sea: Environment-Forming and Ecological Role*. Sevastopol: ECOSI-Gidrofizika, 405 p. (in Russian).

30. Egorov, V.N., Pimenov, N.V., Malakhova, T.V., Artemov, Yu.G., Kanapatsky, T.A. and Malakhova, L.V., 2012. Biogeochemical Characteristics of Methane Distribution in Sediment and Water at the Gas Seepage Site of Sevastopol Bays. *Marine Ekological Journal*, 11(3), pp. 41–52 (in Russian).

31. Egorov, V.N., Gulin, S.B., Artemov, Yu.G. and Guseva, I.A., 2005. Stream Seepage in Offshore Area of Sevastopol. *Scientific Issue Ternopil Volodymyr Hnatiuk National Pedagogical University Series: Biology*, (4), pp. 80–82 (in Russian).

32. Levin, L.A., 2005. Ecology of Cold Seep Sediments: Interactions of Fauna with Flow, Chemistry and Microbes. In: R. N. Gibson, R. J. A. Atkinson and J. D. M. Gordon, eds., 2005. *Oceanography and Marine Biology*. CRC Press. Vol. 43, pp. 1–46.

About the authors:

Natalya A. Boltachova, Leading Research Associate, A.O. Kovalevsky Institute of Biology of the Southern Seas of RAS (2 Nakhimov Av., Sevastopol, 299011, Russian Federation), PhD (Biol.), **ORCID ID: 0000-0003-0618-1992, Scopus Author ID: 36149089700**, *nboltacheva@mail.ru*

Elena V. Lisitskaya, Senior Research Associate, A.O. Kovalevsky Institute of Biology of the Southern Seas of RAS (2 Nakhimov Av., Sevastopol, 299011, Russian Federation), PhD (Biol.), **ORCID ID: 0000-0002-8219-4616, Scopus Author ID: 6504112143, ResearcherID: T-1970-2017**, *e.lisitskaya@gmail.com*

Contribution of the authors:

Natalya A. Boltachova – study problem statement, analysis of composition and abundance of polychaetes of the family Dorvilleidae in the benthos, preparation of graphical materials

Elena V. Lisitskaya – analysis of the distribution of representatives of the family Dorvilleidae in fouling, manuscript editing

All the authors have read and approved the final manuscript.

Original paper

Estimation of Macrofouling of the Water Intake Tunnel of the Vladivostok CHP-2 Using Laser Technologies

S. I. Maslennikov [1, 2], A. Yu. Zvyagintsev [1], A. A. Begun [1]*

[1] *A.V. Zhirmunsky National Scientific Center of Marine Biology FEB RAS, Vladivostok, Russia*

[2] *Far Eastern Federal University, Ayaks, Russkiy Island, Russia*
* *e-mail: andrejbegun@yandex.ru*

Abstract

For the first time, an accurate quantitative survey of macrofouling in the underground water intake tunnel of the Vladivostok combined heat and power plant (CHP-2) was carried out using laser technologies to develop a strategy for protecting the seawater cooling system from biological damage. In the tunnel biofouling, 91 species of invertebrates belonging to various taxonomic groups were found. The maximum development of macrofouling was established in the lower part of the water intake tunnel with the dominance of the Pacific mussel *Mytilus trossulus*. In the fouling of the tunnel upper part, a quantitative predominance of attached polychaete worms of the genus *Hydroides* was noted. For the concrete sections of the tunnel, the maximum values of the mass of silt biodeposits were recorded, while the steel sections were characterized by calcareous biodeposits. It was noted that the total raw biomass of tunnel macrofouling was 35–50 times greater than the biomass of macrofouling organisms. This difference indicates the predominant role of meiobenthos and microperiphyton organisms in the formation of the fouling community. The differences in the species richness and quantitative indicators of fouling of the tunnel in 2015 compared to 2001 are shown. Thus, the macrofouling estimation of the water intake tunnel of the Vladivostok CHP-2 allows concluding about the need for a comprehensive strategy for protecting the cooling system from marine fouling. Such a strategy is assumed to combine physical methods and other technological methods.

Keywords: macrofouling, water intake tunnel, polychaete worms, different feet crustaceans, bivalve mollusks, biomass, laser technologies

For citation: Maslennikov, S.I., Zvyagintsev, A.Yu., and Begun, A.A., 2024. Estimation of Macrofouling of the Water Intake Tunnel of the Vladivostok CHP-2 Using Laser Technologies. *Ecological Safety of Coastal and Shelf Zones of Sea*, (4), pp. 81–94.

Оценка макрообрастания водозаборного туннеля ТЭЦ-2 Владивостока с применением лазерных технологий

С. И. Масленников [1, 2], А. Ю. Звягинцев [1], А. А. Бегун [1]*

[1] *Национальный научный центр морской биологии им. А. В. Жирмунского ДВО РАН, Владивосток, Россия*

[2] *Дальневосточный федеральный университет, п. Аякс Приморского края, о. Русский, Россия*

* e-mail: andrejbegun@yandex.ru

Аннотация

Впервые проведена точная количественная съемка макрообрастания подземного водозаборного туннеля ВТЭЦ-2 с применением лазерных технологий для разработки стратегии защиты от биологических повреждений системы охлаждения морской водой. В составе биообрастания туннеля обнаружен 91 вид беспозвоночных, принадлежащих к различным таксономическим группам. Установлено максимальное развитие макрообрастания в нижней части водозаборного туннеля с доминированием тихоокеанской мидии *Mytilus trossulus*. В обрастании верхней части туннеля отмечено количественное преобладание прикрепленных многощетинковых червей рода *Hydroides*. На бетонных участках туннеля зарегистрированы максимальные значения массы илистых биоотложений, в то время как для стальных участков были характерны известковые биоотложения. Отмечено, что общая сырая биомасса макрообрастания туннеля больше биомассы макрообрастателей в 35–50 раз. Это разница свидетельствует о преобладающей роли организмов мейобентоса и микроперифитона в формировании сообщества обрастания. Показаны различия видового богатства и количественных показателей обрастания туннеля в 2015 г. по сравнению с 2001 г. Таким образом, проведенная оценка макрообрастания водозаборного туннеля ВТЭЦ-2 позволяет сделать вывод о необходимости комплексной стратегии защиты системы охлаждения от морского обрастания, заключающейся в сочетании физических методов и других технологических приемов.

Ключевые слова: макрообрастание, водозаборный туннель, многощетинковые черви, разноногие раки, двустворчатые моллюски, биомасса, лазерные технологии

Introduction

The proliferation of fouling communities in the techno-ecosystems of cooling ponds of power plants gives rise to a variety of biological disturbances that impinge upon the operational efficacy of the equipment. Marine fouling includes a wide variety of organisms capable of attaching to the hard surface of underwater substrates. The aforementioned fouling agents can be classified into two main categories: microfouling (bacteria, protozoa, microscopic fungi and microalgae that form biofilms or mucus) and macrofouling (seaweeds, bivalves, such as oysters and mussels, crustaceans, bryozoans, hydroids and ascidians). The most significant challenges are observed in the cooling systems of industrial facilities, which include power plant intakes [1–3]. Estimated financial impact of the combined effects of waterway fouling and marine biodamage is estimated to be in the millions of dollars [1]. In recent decades, a notable trend has been observed in industrialised countries to relocate combined heat and power plants and industrial facilities to the coastline. To illustrate, in the United States, over one-third of all power plants are situated in close proximity to the sea shore. In the 1970s, the average daily intake of seawater by these stations already amounted to the billions of litres [2].

Techno-ecosystems of power plants with seawater cooling systems have been studied quite intensively in recent decades in the world practice [4, 5], though it is notable that such studies are not frequently conducted in Russia (or the former USSR) [6]. In addition to macrofouling, changes in the quantitative structure of phytoplankton (as the initial link in the trophic network) were detected when passing through the cooling system of the power plant. The microalgae community of the waterway exhibited a high abundance of benthic forms under an anomalous lengthening of the summer and autumn vegetation season [7].

Previous works on this problem are covered in detail in monograph [8], which focuses on the study of cooling ponds in power plants, with a case study of the Vladivostok combined heat and power plant (CHP-2) (hereinafter referred to as the Vladivostok CHP-2). The data on the composition, quantitative distribution and distinctive formation of fouling communities on different substrates in the cooling system were obtained. On the basis of the research into the biological features of main macrofouling species, recommendations were developed regarding the adjustment of tunnel heat treatment terms and the depth of water intake installation.

In 2015, the research team of the A.V. Zhirmunsky Institute of Marine Biology of the Far Eastern Branch of the Russian Academy of Sciences (currently NSCMB FEB RAS), together with specialists from Far Eastern Federal University, continued comprehensive long-term studies of the fouling community of the Vladivostok CHP-2 water intake tunnel. This is stipulated by the inefficiency of annual heat treatment of tunnels and manual cleaning of fouling during the dewatering process. A period of 14 years has elapsed from the initial survey of the marine techno-ecosystem

---

[1] WHOI, 1952. *Marine Fouling and Its Prevention.* Menasha: George Banta Publishing Co., 388 p. doi:10.1575/1912/191

[2] Young, C.-S., 1971. *Thermal Discharges into the Coastal Waters of Southern California.* Los Angeles, 30 p. Available at: https://ftp.sccwrp.org/pub/download/DOCUMENTS/ TechnicalReports/0003_ ThermalDischarges.pdf [Accessed: 24 November 2024].

of the Vladivostok CHP-2 to the present study. During this time, regular thermal treatment and mechanical fouling cleaning in conjunction with tunnel dewatering have been conducted. In this regard, it was necessary to re-examine the species composition of the fouling of a water intake tunnel with different hydrodynamic conditions in different parts of the tunnel, with the aim of obtaining accurate data on the quantitative distribution of macrofouling.

Thus, the objective of this study is to accurately assess the distribution of macrofouling organisms in the Vladivostok CHP-2 water intake tunnel using a laser rangefinder. To the best of our knowledge, such tools have not previously been employed in the study of biofouling of water intake tunnels in power plants.

Material and methods

The water intake tunnel of the Vladivostok CHP-2 starts in the water intake basin in Sukhoputnaya Bay of Ussuri Bay and consists of a 250 m long steel pipe with an inner diameter of 1.5 m (Fig. 1, *c*, *d*; Fig. 2, *a*), which extends to a 970 m long concrete underground tunnel with an inner diameter of 2 m (Fig. 1, *d*; Fig. 2, *b–f*). The tunnel runs in hard rock beneath a Vladivostok neighbourhood and also ends with a steel pipe with an internal diameter of 1.5 m exiting the power plant site (Fig. 1, *c*, *d*). The vertical distance between the pumping station and the power plant is 42 m. Water from the pumping station is fed into the tunnel via four rotating steel meshes with a mesh diameter of 3 mm. The water flow velocity in the tunnel is 2 m/s, the whole cycle of water passing through the tunnel is about 2 min. Water temperature increases by 5–6 °C when passing through the CHP cooling system [6]. Heated seawater is discharged from the CHP into the River Obyasneniya and further into the Zolotoy Rog Bay apex.

Macrofouling samples were collected on 5 May 2015 during the tunnel dewatering from a 10 × 10 cm area that had been previously marked with a steel frame (Fig. 2, *a–f*). Samples were taken with a 10 cm blade scraper from the bottom, side and top of the pipe in three repetitions. The distance between sampling points was measured using a Leica DISTO A8 laser rangefinder, a modern professional model with an integrated digital viewfinder that permits measurements to be taken even when the laser point is not visible when directed at the measurement object. The inbuilt tilt sensor extends the scope of application of the instrument significantly as it can be used to measure inclination and horizontal position, to perform indirect measurements in cases when one of the measurement points does not reflect the laser beam.

Quantitative data on total raw biomass were obtained by weighing sample bags and further conversion to specific gravity. This approach encompasses all elements that enter the sampler including silt deposits which are typically excluded from laboratory treatment and discharged via drainage systems during the washing of samples. This method makes it possible to take into account the mass not only of macrofouling but also of biodeposits present on the substrate, as well as microperiphyton, detritus and faecal lumps of fouling organisms. Samples were processed in the IBM FEB RAS Laboratory of Ecology of Shelf Communities according to the generally accepted methodology [8].
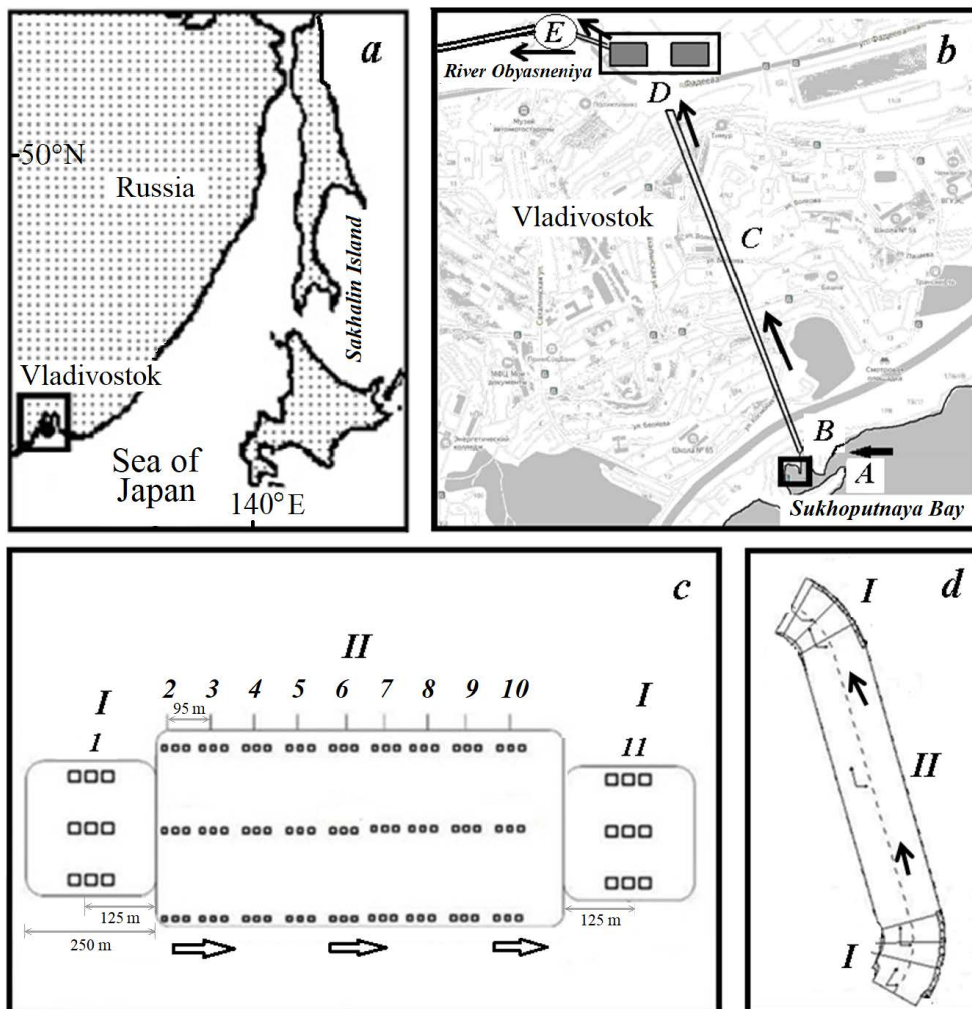
F i g . 1 . Map-scheme of the study area and the structure of the water intake of the combined heat and power plant (CHP-2) in Vladivostok: *a* – map of the study area; *b* – scheme of the location of the water intake and water movement on the map: *A* – Sukhoputnaya Bay, *B* – pumping station, *C* – concrete tunnel, *D* – CHP-2, *E* – discharge channel; *c, d* – scheme of the structure of the water intake tunnel and plan-scheme of the material sampling route: I – steel pipe, II – concrete pipe. The arrows indicate the direction of water movement in the tunnel and beyond it, the squares are stations of macrofouling sampling (*1–11*)

F i g . 2 . The sampling process and general view of fouling of the water intake tunnel of CHP-2 in its different sections: *a* – beginning of the tunnel inspection, *b* – fouling by sessile polychaete worms of the genus *Hydroides*, *c* – test cleaning of the wall to assess the fouling intensity, *d* – mussel fouling, *e* – continuous mussel fouling of the tunnel, *f* – oyster fouling on the tunnel bottom

Species identification was carried out by I.L. Alalykina, Research Associate (polychaetes), and N.L. Demchenko, Research Associate (amphipods), of the above mentioned laboratory. Digital maps of distribution of biofouling quantitative characteristics inside the tunnel were constructed by N.L. Demchenko, Research Associate, using Surfer cartographic package for data modeling and analysis, creation of three-dimensional maps and models and their visualisation.

Results

An inspection of the CHP-2 water intake tunnel revealed a gradual decrease in the amount of fouling on the tunnel walls from st. *1* to st. *10* (Fig. 1, *c*). The general pattern of fouling in the tunnel appeared to be focal with the Pacific mussel *Mytilus trossulus* (A. Gould, 1850) and the giant oyster *Magallana gigas* (Thunberg, 1793) predominating. The initial sections of the water pipeline, constructed from steel, display a range of intensities of mussel fouling. The length of the mussel flaps is less than 30 mm, indicating that the fouling is approximately 15 to 17 months old. As the distance from the intake and pumping station increases, the intensity of the mussel fouling decreases, and the fouling community becomes dominated by the oyster (Fig. 2, *d – f*).

The taxonomic composition of tunnel fouling in 2015 was characterised by a fairly high diversity of invertebrates (Fig. 3, *b*). Fig. 4 shows the distribution dynamics of total raw fouling biomass along the tunnel. Raw fouling biomass tends to increase at the beginning of the tunnel on the concrete substrate. The biomass decreases sharply in the middle of the tunnel and increases again on the steel substrate at the end of the tunnel.

In contrast to the pattern of distribution of total raw biomass of macrofouling in the tunnel, the indices of total biomass of fouling organisms after desktop processing of samples exhibit a slightly different trend (Fig. 4). Therefore, the maximum value of total biomass is recorded at the beginning of the tunnel at st. *1*, after which it decreases significantly, reaches a plateau, and then exhibits a slight increase at st. *10*. In contrast, the relationship between total raw biomass and the other variables is inverse. The biomass of bivalves is dominated by that of the mussel, with the oyster representing the second-largest group. The mussel is the dominant species in the lower part of the tunnel, while the oyster exhibits a competitive advantage at several stations in the middle part of the tunnel.
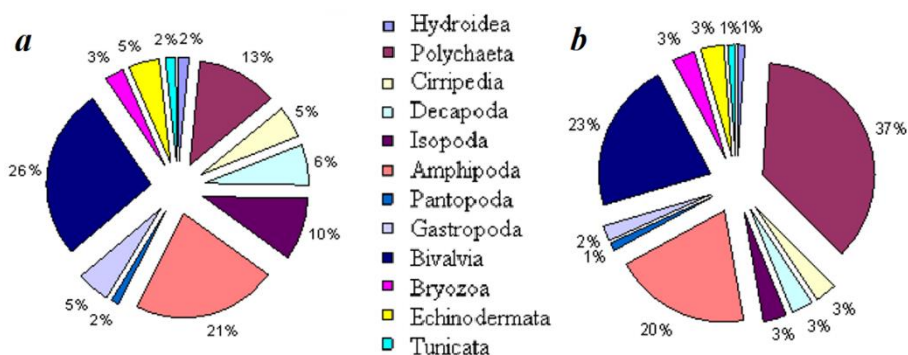
F i g . 3 . Taxonomic composition of fouling of the CHP-2 water intake tunnel in 2001 (*a*) and in 2015 (*b*)
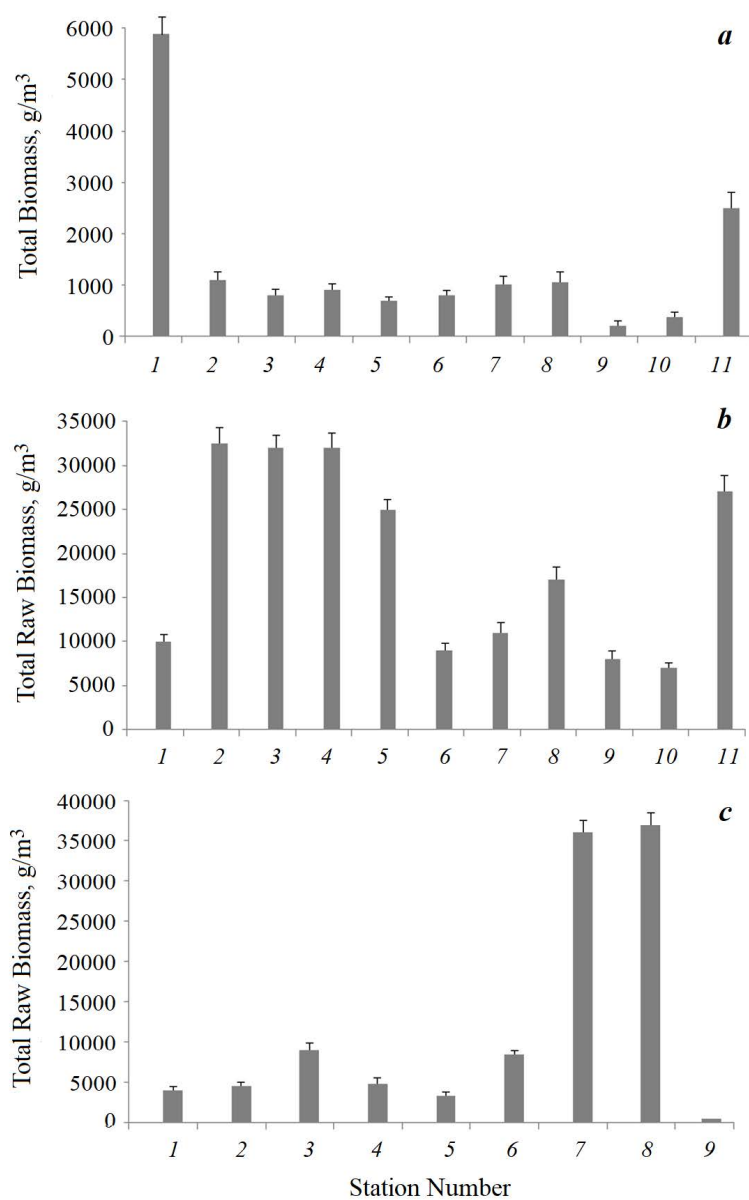
F i g . 4 . Distribution dynamics of total biomass (*a*) and total raw biomass (*b, c*) of macrofouling of the water intake tunnel of CHP-2 in different years: *a, b* – 2015, *c* – 2001

A significant discrepancy has been observed between the raw sample biomass and the macrofouling biomass, with a ratio of these values ranging from 35 to 50 (Fig. 4, *a*, *b*). This suggests that meiobenthos and microperiphyton (and their by-products) play a significant role in the formation of the community of organisms. The influx of clean seawater creates optimal conditions for their proliferation, facilitating their establishment among the macroorganisms of the tunnel fouling community. In previous studies, the quantitative role of meiofauna and microperiphyton in the intake tunnels of power plants with seawater cooling was not taken into account.

The data obtained made it possible to estimate the distribution of macrofouling of different tunnel sections, biomass and settlement density of background-forming species (Fig. 5). Different feet crustaceans predominate in settlement density along almost the entire length of the tunnel, with the exception of st. *10*. A comparable trend is evident in the case of bivalves with regard to biomass.
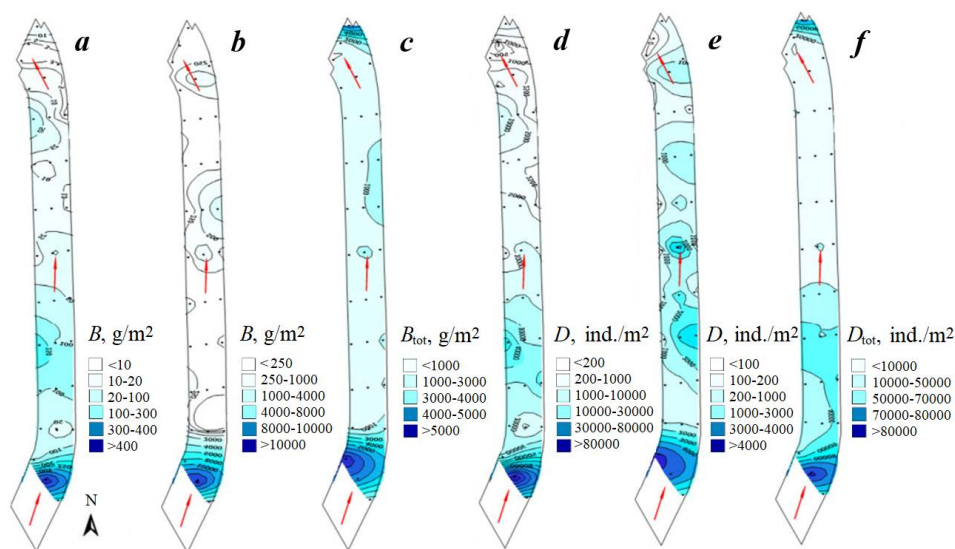
F i g . 5 . Distribution diagram of groups of organisms that provide maximum density and biomass in the biofouling community of the CHP-2 water intake tunnel: biomass *B* of Amphipoda (*a*) and Bivalvia (*b*), total macrofouling biomass B_{tot} (*c*), density *D* of Amphipoda (*d*) and Bivalvia (*e*), total macrofouling density D_{tot} (*f*). The red arrows indicate the water flow

Discussion

A comparison of the taxonomic composition of the Vladivostok CHP-2 tunnel macrofouling for 2001 and 2015 showed that the total number of species increased by almost a third over the 14 years, with 63 and 91 species, respectively (Fig. 3). The prevalence of the most abundant macrofouling species exhibits a general trend, with bivalve mollusks, polychaete worms and different feet crustaceans demonstrating the greatest species diversity. Concurrently, the number of polychaete species exhibited a fourfold increase in 2015 relative to the 2001 survey data. The ratio of other groups of fouling species remained relatively constant.

In 2001, an increase in total raw biomass at the beginning of the tunnel, as in 2015, was not observed. However, a notable increase was recorded in the turning area at the last stations as well as in the zone of increased flow turbulence, specifically the transition from the steel pipe to the concrete tunnel and vice versa.

The results of the assessment indicate the focal character of distribution of macrofouling organisms in the Vladivostok CHP-2 water intake tunnel. Such a mosaic in the distribution of quantitative abundance of fouling was observed both in 2001 [8] and in 2015. Main accumulations of background-forming fouling species are observed in different hydrodynamic conditions of the tunnel sections, namely, in the areas of tunnel bending (turning) under conditions of increased turbulence. A notable decrease in fouling biomass was observed in the central section of the tunnel, with a subsequent increase on the steel substrate at the end of the tunnel. This phenomenon can be attributed to the narrowing of the passage, increased flow turbulence in this section and a reduction in siltation. The cross-sectional area of the steel pipe is 25% smaller than that of the concrete tunnel. It is in the transition areas that the greatest difference in the quantitative indicators of the fouling community was observed.

The spatial distribution of fouling organisms on the inner side of the tunnel is related to the peculiarities of water movement, which is one of the main factors determining the distribution of animals on natural and man-made substrates [8]. It is notable that microvortex motions, otherwise known as microscale turbulence, occupy a distinctive position in this context. Despite the relatively simple geometry of the Vladivostok CHP-2 water intake tunnel, the water motion within it exhibits a complex pattern. This includes the formation of areas of local concentration of tangential stresses, whirlpool zones and transverse circulations, which give rise to a corkscrew-like motion. This is well illustrated in the figure scheme presented in monograph [8].

A more precise estimation of the quantitative macrofouling of the intake tunnel using a laser rangefinder revealed a greater degree of fouling in the tunnel in 2015 compared to the findings of the 2001 study. In 2001, oyster fouling in the tunnel was observed to occur only sporadically. By 2015, however, the fouling community had become a continuous settlement of giant oysters. This community does not lend itself well to physical cleaning methods because oysters are more resistant to elevated water temperatures and oxygen-free abiotic conditions. A particular threat to the tunnel's techno-ecosystem is the climax bivalve mollusk community involving the Pacific mussel. The removal of the mollusks could potentially lead to

a disruption in the stable operation of the cooling system. At the time of the 2015 works, the risk of the mussel and oyster flaps falling into the condenser tubes was considerable. Given the flow capacity in the Vladivostok CHP-2 tunnel, mussel flaps can break off unimpeded, and this probability increases as the mollusks grow.

The 2015 research findings suggest that the regular thermal treatment of the power plant tunnels is not an efficacious approach. Even if such substantial fouling is eradicated through thermal treatment, the aggregation of vast quantities of inert detritus (the shells of mollusks and barnacles, and the calcareous structures of tubeworms) can result in an increase in surface irregularities, thereby facilitating the recurrence of fouling.

In order to minimise the risks of biodamage to the power plant cooling system as a result of fouling by fouling organisms, it is necessary to implement an integrated strategy combining physical protection methods and other technological implementations. Such methods include the utilisation of fully environmentally sound contemporary techniques, such as self-polishing antifouling coatings [9]. The efficacy of such coatings is contingent upon the minimisation of adhesion between the fouling agent and the surface, which is achieved through the utilisation of low surface energy and elastic modulus. The method of pulse supply of 35% hydrogen peroxide and iron salts [6] or ozonation of water during the period of mass settlement of mollusks can also be employed. The method can be easily automated, obviating the need for human intervention.

It is pertinent to highlight the recent development of a ground stand, a controlled water flow facility, which can be utilised for the assessment and validation of the characteristics of protective coatings on substrates under examination, including antifouling and anti-corrosion coatings [10]. Semi-autonomous robots for laser technology of surface cleaning, currently under development by researchers at Institute of Automation and Control Processes FEB RAS, have the potential to be employed as environmentally sound methods to protect structures operating in aquatic environments from biofouling [3] [11, 12]. The robotised complex of laser cleaning of underwater surfaces of ships and offshore structures, which allows to remove biofouling, can also be used for cleaning of CHP water intakes from biofouling [13, 14]. Furthermore, Chinese specialists are currently implementing a shock-wave method to eliminate mussel fouling, which has been demonstrated to have an excellent antifouling effect on the cooling system surfaces [15].

It is imperative that, concurrently with the application of antifouling coatings, the operational parameters of the power plant are adjusted during the period of intensive macrofouling organism settlement which spans from May to September. They consist of continuous operation of each cooling system tunnel for no more than two months during the specified season. Following this, a shutdown and dewatering period of one to two weeks is initiated to eradicate macrofouling

---

3) Kulchin, Yu.N., 2020. [Development of Research of Laser Technologies and their Practical Applications in the Russian Far East]. *Lazer-Inform*, (10), pp. 1–11 (in Russian).

at the earliest stages of community formation. The proposed technique has the potential to replace the costly heat treatment process, although it can be employed in conjunction with the latter to minimise the time required for CHP tunnel maintenance. It is possible to continue this practice during winter months without heat treatment application.

Conclusion

For the first time, a quantitative survey of macrofouling in the underground water intake tunnel of the Vladivostok CHP-2 was carried out using laser technologies. A macrofouling community was identified as being present throughout the inner surface of the tunnel, exhibiting a predominantly focal distribution. In the tunnel fouling, 91 species of invertebrates belonging to various taxonomic groups were found. The most prevalent species among them in terms of density were representatives of the crustacean order Amphipoda, while in terms of biomass, the bivalve mollusks *Mytilus trossulus* and *Magallana gigas* were most abundant. The greatest degree of macrofouling development in the lower part of the intake tunnel, with a quantitative prevalence of *M. trossulus*, was identified. Additionally, a notable prevalence of attached polychaete worms with their hard calcareous structures was observed in the upper part of the water intake.

The degree of tunnel fouling was found to be higher in 2015 than in 2001, and significant differences were identified in species composition and quantity. Under conditions of increased turbulence, the main accumulations of background-forming macrofouling species were observed in the area of the steel pipe bending. The waterway steel sections exhibited the highest biomass of hard deposits, whereas the concrete sections were characterised by a quantitative dominance of silt biodeposits.

A notable discrepancy was observed in the quantitative indices of total raw biomass of tunnel macrofouling and macrofouling biomass (with a ratio of 35 to 50 times). In light of the findings, recommendations are put forth for the development of environmentally sound physical methods of protection of power plant cooling systems from marine fouling in conjunction with other technological approaches.

REFERENCES

1. Li, T., Liu, S., Huang, L., Huang, H., Lian, J., Yan, Y. and Lin, S., 2011. Diatom to Dinoflagellate Shift in the Summer Phytoplankton Community in a Bay Impacted by Nuclear Power Plant Thermal Effluent. *Marine Ecology Progress Series*, 424, pp. 75–85. https://doi.org/10.3354/meps08974

2. Choi, K.-H., Kim, Y.-O., Lee, J.-B., Wang, S.-Y., Lee, M.-W., Lee P.-G., Ahn, D.-S., Hong, J.-S. and Soh, H.-Y., 2012. Thermal Impacts of a Coal Power Plant on the Plankton in an Open Coastal Water Environment. *Journal of Marine Science and Technology*, 20(2), pp. 187–194. https://doi.org/10.51400/2709-6998.1837

3. Protasov, A.A., Sylaieva, A.A., Novoselova, T.N., Gromova, Yu.F., Morozovskaya, I.A. and Stepanova, T.I., 2017. Nuclear Power Plant Technoecosystem: 18 Years of Hydrobiological Observations. *Journal of Siberian Federal University. Biology*, 10(4), pp. 459–484. https://doi.org/10.17516/1997-1389-0045

4. Masilamoni, G., Jesudoss, K.S., Nandakumar, K., Satapathy, K.K., Azariah, J. and Nair, K.V.K., 2002. Lethal and Sub-Lethal Effects of Chlorination on Green Mussel *Perna viridis* in the Context of Biofouling Control in a Power Plant Cooling Water System. *Marine Environmental Research*, 53(1), pp. 65–76. https://doi.org/10.1016/s0141-1136(01)00110-6

5. Venkatesan, R. and Murthy, P.S., 2008. Macrofouling Control in Power Plants. In: H. C. Flemming, P. S. Murthy, R. Venkatesan and K. Cooksey, eds., 2008. *Marine and Industrial Biofouling*. Berlin, Heidelberg: Springer, pp. 435–446. https://doi.org/10.1007/978-3-540-69796-1_14

6. Zvyagintsev, A.Y., Poltarukha, O.P. and Maslennikov, S.I., 2015. Fouling on Technical Water Supply Marine Systems and Protection Method Analysis of Fouling on Water Conduits (Analytical Review). *Water: Chemistry and Ecology*, (1), pp. 30–51 (in Russian).

7. Begun, A.A. and Maslennikov, S.I., 2021. Influence of the Technical Ecosystem of the Electric Power Plant (Vladivostok) on the Phytoplankton of the Japanese Sea. *Water Resources*, 48(3), pp. 404–412. https://doi.org/10.1134/S0097807821030052

8. Zvyagintsev, A.Yu. and Moshchenko, A.V., 2010. *Marine Techno-Ecosystems of Power Plants*. Vladivostok: Dalnauka, 343 p. (in Russian).

9. Nurioglu, A.G., Esteves, A.C.C. and de With, G., 2015. Non-Toxic, Non-Biocide-Release Antifouling Coatings Based on Molecular Structure Design for Marine Applications. *Journal of Materials Chemistry B*, 32, pp. 6547–6570. https://doi.org/10.1039/C5TB00232J

10. Zvyagintsev, A.Yu., Maslennikov, S.I., Tsvetnikov, A.K., Begun, A.A. and Grigoryeva, N.I., 2021. Study of Fouling Communities Succession Under Conditions of the Device of Controlled Water Flow. *Marine Biological Journal*, 6(1), pp. 17–33. https://doi.org/10.21072/mbj.2021.06.1.02

11. Kulchin, Yu.N., Zvyagintsev, A.Yu., Subbotin, E.P., Maslennikov, S.I. and Begun, A.A., 2015. Perspectives and Technical-Economic Aspects of Elaboration of New Methods of Controlling Biofouling on the Maritime Transport. *Vestnik of Far Eastern Branch of Russian Academy of Sciences*, (6), pp. 96–102 (in Russian).

12. Veiko, V.P., Kishalov, A.A., Mutin, T.Yu. and Smirnov, V.N., 2012. Laser Cleaning: Aspects of Industrial Application. *Scientific and Technical Journal of Information Technologies, Mechanics and Optics*, (3), pp. 50–54 (in Russian).

13. Kulchin, Yu.N., Nikitin, A.I. and Subbotin, E.P., 2020. Laser Underwater Cleaning of Hulls of Sea Vessels. *Applied Photonics*, 7(4), pp. 86–101 (in Russian).

14. Bogdanov, E.V. and Budnikov, K.O., 2023. Laser Cleaning and Protection of Ship Hulls and Ships from Corrosion. *Morskoy Vestnik*, (1), pp. 54–56. https://doi.org/10.56192/18123694_2023_1_54 (in Russian).

15. Ge, H., Wang, H. and Gao, Z., 2019. Control of Mussel *Mytilus galloprovincialis* Lamarck Fouling in Water-Cooling Systems Using Plasma Discharge. *Water Science and Technology*, 80(6), pp. 1125–1133. https://doi.org/10.2166/wst.2019.361

About the authors:

Sergey I. Maslennikov, Senior Research Associate, A. V. Zhirmunsky National Scientific Center of Marine Biology, Far Eastern Branch of Russian Academy of Sciences (17 Palchevsky Str., Vladivostok, 690041, Russian Federation), Ph.D. (Biol.), **ORCID ID: 0000-0003-4776-0624**, *721606@mail.ru*

Aleksandr Yu. Zvyagintsev, Leading Research Associate, A. V. Zhirmunsky National Scientific Center of Marine Biology, Far Eastern Branch of Russian Academy of Sciences (17 Palchevsky Str., Vladivostok, 690041, Russian Federation), D.Sc. (Biol.), *ayzvyagin@gmail.com*

Andrey A. Begun, Research Associate, Senior Research Associate, A. V. Zhirmunsky National Scientific Center of Marine Biology, Far Eastern Branch of Russian Academy of Sciences (17 Palchevsky Str., Vladivostok, 690041, Russian Federation), Ph.D. (Biol.), **ORCID ID: 0000-0002-8383-796X**, *andrejbegun@yandex.ru*

Contribution of the authors:

Sergey I. Maslennikov – study conduction, critical analysis of the materials related to the fundamental side of the research, graphical interpretation of the results

Aleksandr Yu. Zvyagintsev – concept development, study problem statement, processing of macrofouling samples, description of the study results, qualitative analysis of the results and their interpretation

Andrey A. Begun – study conduction, quantitative processing of samples and analysis of the results, article editing

All the authors have read and approved the final manuscript.

Original paper

The Ability to Accumulate and Transform Diesel Fuel by Green Algae *Ulva lactuca* of the Barents Sea

G. M. Voskoboinikov *, L. O. Metelkova, D. O. Salakhov, E. O. Kudryavtsteva

Murmansk Marine Biological Institute of RAS, Murmansk, Russia
* e-mail: grvosk@mail.ru

Abstract

The article presents the results of experiments on the ability of the green alga *Ulva lactuca* to absorb and transform diesel fuel from marine water for 5 and 10 days. The original marine water contained 0.62 mg/L of petroleum hydrocarbons, which is about 12 maximum permissible concentrations (MPC). During the experiment with the addition of 20 mg/L of diesel fuel (400 MPC) to the water, the absorption of the introduced hydrocarbons was observed in the experimental tanks without algae. Apparently, they were absorbed by water microorganisms. On the 5th day of the experiment, the petroleum hydrocarbons concentration in the water decreased by 40% and amounted to 12 mg/L (240 MPC). When ulva thalli were added to the water, the total content of petroleum hydrocarbons in the water on the 5th day decreased by 86% (to 2.8 mg/L), and on the 10th day, it increased (to 4.2 mg/L). A slight increase in the concentration of diesel fuel hydrocarbons in water indicates a reverse process of releasing hydrocarbons absorbed by ulva into water. In the experiment with the addition of diesel fuel to the water at a concentration of 10 mg/L, the content of hydrocarbons in algae tissues on the 5th and 10th days was recorded at the level of 0.6 mg/g. The marker ratio of $\sum$n-alkanes / $\sum$ petroleum products in ulva during the experiment was 0.2. A decrease in this indicator to 0.18 on the 10th day of the experiment indicates the beginning of the transformation of the hydrocarbons chemical structure. When 20 mg/L of diesel fuel (400 MPC) were added to the water, this indicator on the 5th and 10th days was 0.25 and 0.28, respectively, indicating an active process of hydrocarbon absorption by the algae surface, which was not yet complete by the 10th day. The experiment results allow us to conclude that *U. lactuca* is able to absorb and transform petroleum hydrocarbons and participates in the bioremediation of coastal waters.

Keywords: *Ulva lactuca*, Barents Sea, diesel fuel, petroleum product accumulation, petroleum product destruction, pollution tolerance

Способность к аккумуляции и трансформации дизельного топлива у зеленой водоросли *Ulva lactuca* Баренцева моря

Г. М. Воскобойников *, **Л. О. Метелькова, Д. О. Салахов, Е. О. Кудрявцева**

Мурманский морской биологический институт РАН, Мурманск, Россия
* e-mail: grvosk@mail.ru

Аннотация

Оценена способность зеленой водоросли *Ulva lactuca* к поглощению и трансформации дизельного топлива из морской воды в ходе экспериментов длительностью 5 и 10 сут. Исходная морская вода содержала 0.62 мг/л нефтяных углеводородов (около 12 ПДК). В ходе эксперимента с добавлением в воду дизельного топлива 20 мг/л (400 ПДК) в опытных емкостях без водорослей наблюдался процесс поглощения введенных углеводородов, по-видимому, микроорганизмами, обитающими в воде. На пятые сутки опыта концентрация нефтяных углеводородов в воде снизилась на 40 % и составила 12 мг/л (240 ПДК). При добавлении в воду талломов ульвы валовое содержание нефтяных углеводородов в воде на пятые сутки уменьшилось на 86 % (до 2.8 мг/л), а на десятые сутки увеличилось (до 4.2 мг/л). Незначительное увеличение концентрации углеводородов дизельного топлива в воде говорит об обратном процессе высвобождения поглощенных ульвой углеводородов в воду. В опыте с добавлением в воду дизельного топлива в концентрации 10 мг/л содержание нефтяных углеводородов в тканях водорослей на пятые и десятые сутки было зарегистрировано на уровне 0.6 мг/г. Маркерное соотношение ∑н-алканов/∑нефтепродуктов у ульвы в течение эксперимента равнялось 0.2. Снижение этого показателя до 0.18 на десятые сутки опыта свидетельствует о начале трансформации химической структуры углеводородов. При добавлении в воду дизельного топлива 20 мг/л (400 ПДК) этот показатель на пятые и десятые сутки составил 0.25 и 0.28 соответственно, что указывает на активное поглощение углеводородов поверхностью водорослей, которое к десятым суткам еще не завершилось. На основании результатов экспериментов делается вывод о способности *U. lactuca* к поглощению и трансформации нефтяных углеводородов и ее участию в биоремедиации прибрежных акваторий.

Ключевые слова: *Ulva lactuca*, Баренцево море, дизельное топливо, аккумуляция нефтепродуктов, деструкция нефтепродуктов, толерантность к загрязнению

Introduction

In recent years, interest in the possible role of macrophyte algae in bioremediation of coastal waters from petroleum products (PP) has increased. This is caused by the information obtained about the ability of algae not only to accumulate PP on the surface of the thallus, but also to absorb and further transform and incorporate PP into the metabolism of cells. The described processes are carried out largely due to hydrocarbon-oxidising bacteria (HOB), which are present in large numbers on the surface of macroalgae, especially in petroleum-contaminated coastal waters [1, 2]. The objects of research on the effect of PP on algae as well as the role of algae in environmental bioremediation were mainly representatives of brown algae, such as laminaria and fucus algae, which constitute the main phytomass in the coastal area of the Barents Sea [1] [3, 4]. A smaller amount of data on the aforementioned subject has been obtained for green algae, although the literature suggests that they also have some tolerance to petroleum contamination [5–7]. Earlier in our experiments on the influence of diesel fuel (DF) on the early stages of *Ulva lactuca* development it was shown that at DF concentration of 5 mg/L (100 MPC) in water, a slowdown of seedlings development on the 20th day of the experiment was observed, at 25 mg/L (500 MPC) – on the 10th day and at 50 mg/L (1000 MPC) toxicant content, the death of seedlings was observed on the 5th day of the experiment [8]. In experiments on the effect of DF on the species *U. intestinalis*, closely related to *Ulva lactuca*, it was observed that the addition of DF to the medium at a concentration of 1–5 mg/L (20–100 MPC) did not result in the death of algae, but rather caused a decrease in photosynthetic activity and content of photosynthetic pigments. The addition of DF in the range of 50 to 150 mg/L (1000–3000 MPC) to the environment has been observed to induce gradual and irreversible changes in algae, ultimately resulting in plant death. It has been demonstrated that at a concentration of 150 mg/L, the mortality of algae occurs within three days of the experiment [9]. To date, the literature contains no information on the range of tolerance of adult *Ulva lactuca* thalli to DF, nor on the ability of *Ulva lactuca* to absorption and transform the toxicant.

Ulva lactuca is a species of green algae that is cosmopolitan in distribution. It was relatively rarely found in the Barents Sea until recently, now being observed to spread actively along the Eastern Murman littoral zone [10]. Diesel fuel is one of the most common marine toxicants due to the fact that it is used by marine transport as well as by coastal heating plants (CHP) [11].

---

[1] Stepanyan, O.V., 2003. [*Morpho-Functional Changes in Algal Macrophytes of the Barents Sea under the Influence of Oil and Oil Products*]. Doctoral Dissertation. Murmansk, 146 p. (in Russian).

The aim of our study is to obtain information on the absorption and transformation of PP by *U. lactuca* tissues, changes in the algae occurring at the cellular level at 10 and 20 mg/L DF content in seawater and *U. lactuca* possible role in bioremediation. The article uses materials of the paper abstracts of the White Sea Student Scientific Session of SPbU [2].

Material and methods

In August 2023, *Ulva lactuca* thalli without any indications of reproduction and water were sampled on the littoral of the Zelenetskaya Bay of the Barents Sea in the area of the seasonal biostation of Murmansk Marine Biological Institute of RAS (69°07′09″ N, 36°05′35″ E). Experiments were performed in a thermostated space at 8–10 °C with constant illumination of 150 µmol m^{-2}·s^{-1}, 24L:0D photoperiod (polar day period), and aeration of the aquatic environment. The water used for the experiment with a salinity of 33 ‰ was subjected to filtration through a cotton-gauze filter and subsequently cooled to a temperature of 8–10 °C. A total of 18 experimental tanks were utilised in the study (three control tanks with algae, three control tanks without algae, six experimental tanks with algae and six experimental tanks without algae (three for each concentration)). Each tank contained 2 L of prepared water, to which 10 and 20 mg/L of summer diesel fuel (200 and 400 MPC, respectively) were added. Adult thalli of *U. lactuca*, with a mass of 5 g each, were placed in the tanks where the algae were to be located, three specimens per one experimental tank. The tanks were aerated by an air compressor.

All experimental tanks were tightly closed with a lid in order to avoid loss of DF volatile fractions. DF concentrations were chosen to determine tolerance to the toxicant and to analyse morphological changes in *U. lactuca*. At the very beginning (day 0), on the 5th and 10th days of the experiment, algae samples were collected and examined by gas chromatography/mass spectrometry for the PP content. Throughout the experiment, samples of algae not exposed to PP were studied as a control sample. Water was analysed for DF content in the initial sample, control one and after the DF addition in the presence and absence of algae in the water. Each water and algae analysis was carried out in three repetitions. The sample and instrumental analysis process preparation was carried out based on the EPA 8270 methodology detailed in previous studies [12]. In order to analyse changes in algae under the influence of PP occurring at the cellular level, 1 cm^2 cuttings were made from thalli and placed in Eppendorf tubes with fixative. Prefixation was carried out with 2.5% glutaric aldehyde on a cacodylate buffer (c-c-b) with 1.5% tannin added to the fixative, and postfixation was carried out with 1% OsO$_4$ (osmium oxide (VIII)) on a similar buffer. The osmotic pressure of both fixatives was adjusted to the osmotic pressure of seawater in the environment (1100 mOsm) using sucrose. Fixation took place at a temperature of 0…+5 °C according to the following scheme: prefixation with glutaric aldehyde for 18 h, washing of c-c-b in two shifts

[2] Kudryavtseva, E., Salahov, D. and Voskoboynikov, G.M., 2024. The Ability of the Green Algae Ulva Lactuca to Purify Seawater from Diesel Fuel. In: SPbU, 2024. [*White Sea Student Scientific Session. Paper Abstracts. 1–2 February 2024, Saint Petersburg*]. Saint Petersburg: Svoe Izdatelstvo, p. 50 (in Russian).

of 6 h, postfixation with OsO_4 for 18 h. Then the material was prepared for viewing in the electron microscope JEM-100C (manufactured by JEOL) according to generally accepted methods [3].

Results and discussion

Light-optical and electron-microscopic observations revealed that the thalli of U. lactuca, collected from a habitat where the PP concentration was 0.62 mg/L (12 MPC), exhibited no significant differences in cell ultrastructure when compared to previously studied thalli of ulva algae inhabiting waters with PP content ranging from 0.1–0.2 mg/L (2–4 MPC) observed in most of the studied bays of the Kola Bay and Eastern Murman coasts of the Barents Sea. All selected thalli were viable under control conditions until the conclusion of the experiment. No destructive changes in cell morphology were observed. Chloroplasts contained single-channel pyrenoids (letter P in Fig. 1, *a*), predominantly immersed; a large number of starch granules were detected (letter K in Fig. 1, *a*), indicating that photosynthesis was well underway (Fig. 1, *a*).

This was also confirmed by the bright green colour of thalli of the control variant which remained until the end of the experiment. At the same time, heterogeneity was observed in the cell structure on the control variant ulva cuttings at all experimental periods: the cells differed in the degree of photosynthetic apparatus development, partial volume of reserve substance. It should be noted that the same heterogeneity was observed when studying the ultrastructure of ulva cells in natural and experimental conditions in our earlier studies [13]. On the fifth day in both variants of the experiment with DF at concentrations of 10 and 20 mg/L, about 90% of cells in the ulva thalli showed no signs of damage, the thalli retained a homogeneous green colour. However, if in the control variant and in the variant with introduced DF at a concentration of 10 mg/L pyrenoids were present in the majority of chloroplasts, then under DF exposure at a concentration of 20 mg/L, pyrenoids were detected only in chloroplasts in only 30–40% of the cells (Fig. 1, *b*), which can indicate a decrease in the activity of photosynthetic apparatus functioning in the majority of ulva cells. On the 10th day of the experiment, following the introduction of DF (10 mg/L) into the water, no alterations were observed in the structure of the majority of thalli cells (up to 70%). However, a small proportion of cells at this concentration, as well as the majority of the ulva cells (up to 80%) at 20 mg/L, exhibited a minimal amount of organised structures: cytoplasm remnants were localised near the envelope and chloroplasts were not detected (Fig. 1, *d*). Starch grains were present in the cells, but in much smaller amounts than in the cells of the control variant and at the previous stage (5 days) of the experiment. A large number of bacteria were detected on the outside of the cell envelope (Fig. 1, *c*, *d*). In addition, a small proportion of the thalli cells were characterised by an intact structure.

---

[3] Weakley, B., 1972. *A Beginner's Handbook in Biological Electron Microscopy*. London, Edinburg: Churchill Livingstone Publ., 240 p.
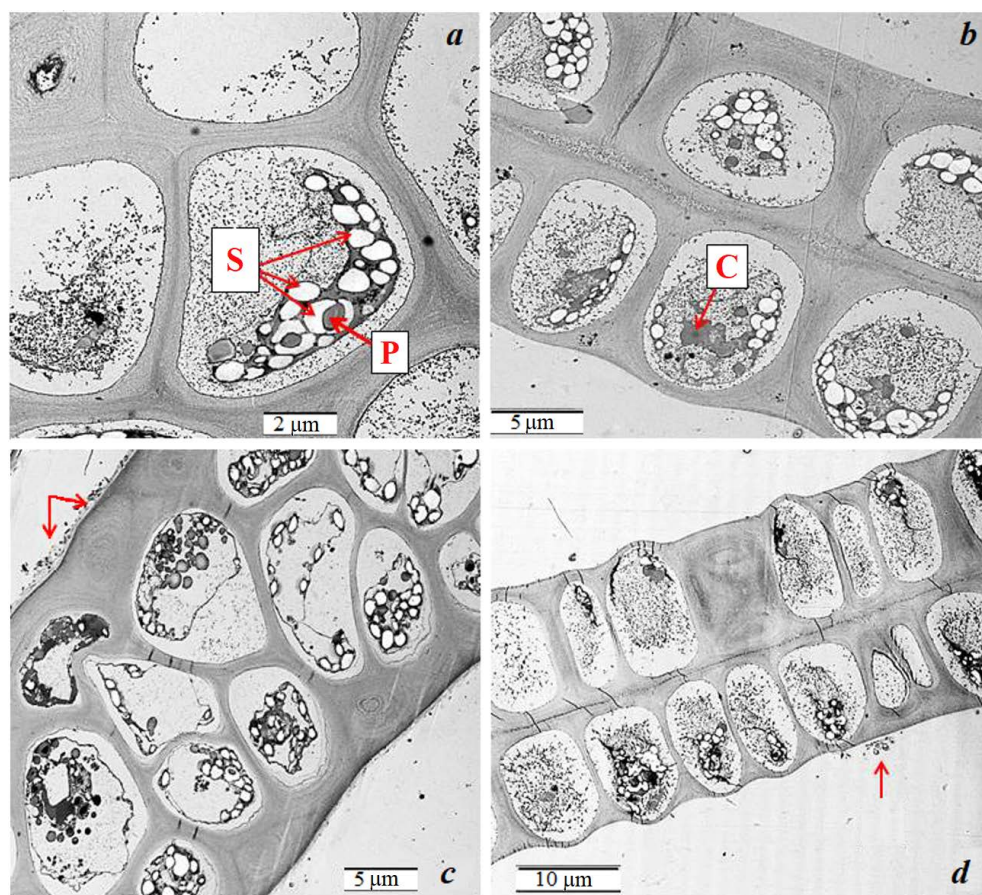
F i g . 1 . Changes in *Ulva lactuca* cells in the experiment: *a* – control for 0 days; *b* – 5 days of the experiment at 10 mg/L (200 MPC) diesel fuel (DF); *c* – 5 days of the experiment at 20 mg/L (400 MPC) DF; *d* – 10 days of the experiment at 20 mg/L (400 MPC) DF. Notations: P – pyrenoid, S – starch granules, C – core. Arrows indicate bacteria on the thallus periphery

The results of the water samples demonstrated that during the experiment with the addition of DF to water at a concentration of 20 mg/L (without ulva), destruction and absorption of the introduced hydrocarbons (IH) occurred, apparently by microorganisms present in the water. On the fifth day of the experiment the PP concentration in water decreased by 40% and made 12 mg/L. The bioremediation ability of microorganisms was noted earlier in studies with other algae species [1]. In the case of the ulva sample addition to the water, the gross PP content in the water decreased by 86% to 2.8 mg/L on the 5th day and increased slightly (to 4.2 mg/L)

on the 10th day. An increase in the PP concentration in water on the 10th day is indicative of a reverse process, i.e. the release of absorbed IH into water. This can be reflected in the change (partial destruction) of the cell membrane system observed in electron microscopic photographs. A similar result was recorded in earlier studies on the effect of crude oil hydrocarbons on the green algae *Acrosiphonia arcta* [14]. The values of the index reflecting the degree of transformation of hydrocarbons (∑n-alkanes/∑PP) remained high enough (> 0.2) throughout the experiment, i. e. the processes of absorption/release of such a quantity of IH (20 mg/L) take place without significant transformation. When DF is added at a concentration of 20 mg/L, a time interval of 10 days is likely to be inadequate for observing substantial alterations in the structure of petroleum IH, both with and without the involvement of microalgae and ulva.

Fig. 2 shows changes in the concentration of alkanes and gross content of petroleum products in *Ulva lactuca* tissues.

F i g . 2 . Mass fraction of n-alkanes in the tissues of the *Ulva lactuca* during the experiment with the addition of DF: *a* – 10 mg/L (200 MPC); *b* – 20 mg/L (400 MPC)

Initially, the algal sample (control, day 0) contained 0.540 mg/g PP, of which C_9–C_{30} n-alkanes were 0.1 mg/g. The sample was characterised by an increased content of petroleum IH in a range of $C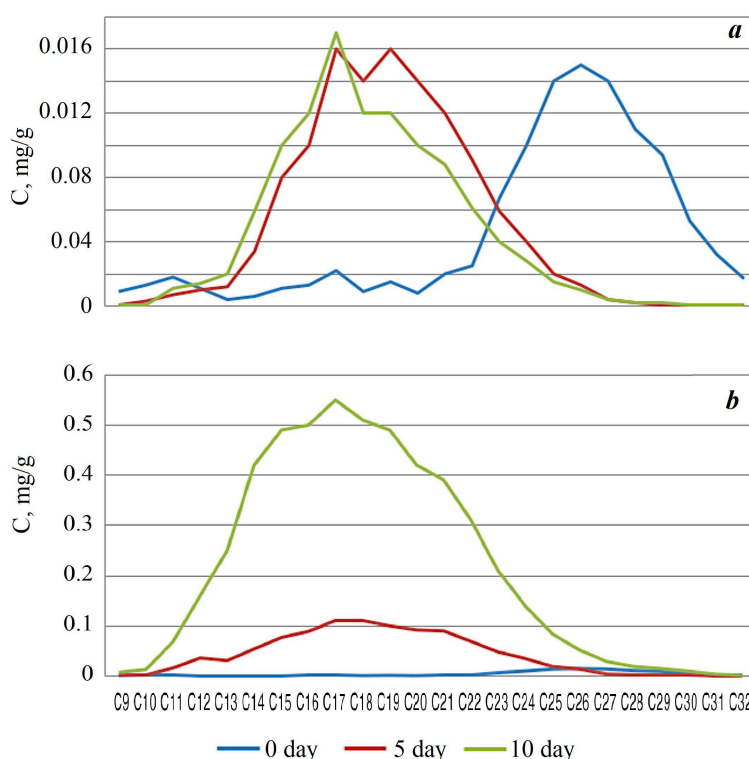_{23}$–$C_{30}$ (Fig. 2). It is important to note the absence of any expressed endogenous n-alkanes in ulva compared to algae living in polluted water areas [15, 16]. On the 5th day of the experiment without DF addition (control, day 5), gross IH content in ulva tissues decreased to 0.49 mg/g, on the 10th day – to 0.34 mg/g. The amount of n-alkanes in algal tissues also decreased fourfold, from 0.1 µg/g (day 0) to 0.026 mg/g (day 10). The value of the marker indicator ∑n-alkanes/∑PP also underwent a significant decrease from 0.19 (on the first day) to 0.08 (on days 5 and 10), indicating active IH transformation during the initial five days. The value of this indicator at the level of less than 0.1 is characteristic of algae growing in relatively clean water areas. The process of petroleum IH absorption by the surface of the algae is initiated upon the DF addition. In the experiment with the addition of DF at a concentration of 10 mg/L, the PP content in ulva tissues on the 5th and 10th days was recorded at 0.6 mg/g (Fig. 2, *a*). The marker ratio of ∑n-alkanes/∑PP was established at 0.2 during the course of the experiment. A slight decrease in this index to 0.18 on the 10th day signifies the onset of a transformation in the chemical structure of hydrocarbons. In the ulva sample where DF was added in the amount of 20 mg/L, this index on the 5th and 10th day was recorded at 0.25 and 0.28, respectively, indicating an active process of hydrocarbon absorption which was not yet completed on the 10th day. The maximum PP content in the algae was recorded on the 10th day of the experiment when 20 mg/L was added, and was found to be 18 mg/g (Fig. 2, *b*).

Table demonstrates generalised results of the experiment conducted with *Ulva lactuca*.

The processes of PP absorption and transformation are characteristic for ulva as well as for all previously studied macrophyte algal species [12, 14]. In comparison with another green alga, acrosiphonia [14], ulva exhibits a higher rate of IH absorption/transformation, which can be attributable to the disparity in thalli structure, with ulva exhibiting a lamellar configuration and acrosiphonia displaying a siphonal structure. It can be assumed that the thallus lamellar structure is more favourable for the location of epiphytic hydrocarbon-oxidising bacteria.

Gross content of petroleum hydrocarbons (PH) in water (mg/L) and in algae (mg/g) during the experiment with the addition of 20 mg/L (400 MPC) DF

Time, days	PH in water	PH in algae
0	20	0.54
5	2.8	4
10	4.2	18

Conclusion

The experiments demonstrated that the impact of summer DF at a concentration of 10 mg/L (200 MPC) for 10 days and at a concentration of 20 mg/L (400 MPC) for 5 days at a temperature of 8–10°C was not lethal for the littoral species of green algae *Ulva lactuca*. It has been demonstrated that, under natural conditions, long-term growth at PP concentrations of approximately 0.6 mg/L (12 MPC) enables ulva cells to develop adaptive reactions and withstand single PP discharges (leaks). It has also been demonstrated that *U. lactuca* incorporates itself rapidly into the process of bioremediation in instances where seawater has been contaminated with petroleum products. It can be assumed that a relatively wide range of tolerance to petroleum products is one of the factors that has enabled *U. lactuca* to occupy a certain ecological niche on the littoral zone of the Murmansk coast of the Barents Sea, which is currently characterised by a high degree of petroleum pollution. This hypothesis is supported by the experimental evidence and existing literature data.

REFERENCES

1. Semanova, E.V., Shlykova, D.S., Semenov, A.M., Ivanov, M.N., Shelyakov, O.V. and Netrusov, A.M., 2009. Bacteria-Epiphytes of Brown macro Alga in Utilization of Oil in Ecosystems of North Sea. *Vestnik Moskovskogo Universiteta. Seriya 16. Biologiya*, (3), pp. 18–22 (in Russian).

2. Pugovkin, D.V., Liaimer, A. and Jensen, J.B., 2016. Epiphytic Bacterial Communities of the Alga *Fucus vesiculosus* in Oil-Contaminated Water Areas of the Barents Sea. *Doklady Biological Sciences*, 471, pp. 269–271. https://doi.org/10.1134/S0012496616060053

3. Malavenda, S.V., Shoshina, E.V. and Kapkov, V.I., 2017. Species Diversity of Seaweeds in Different Areas of the Barents Sea. *Vestnik of MSTU*, 20(2), pp. 336–351. https://doi.org/10.21443/1560-9278-2017-20-2-336-351 (in Russian).

4. Wrabel, M.L. and Peckol, P., 2000. Effects of Bioremediation on Toxicity and Chemical Composition of No. 2 Fuel Oil: Growth Responses of the Brown Alga *Fucus vesiculos*us. *Marine Pollution Bulletin*, 40(2), pp. 135–139. https://doi.org/10.1016/S0025-326X(99)00181-2

5. Liu, Y.X., Liu, Y., Lou, Y.D. and Li, N., 2019. Toxic Effect of Oil Spill on the Growth of *Ulva pertusa* by Stable Isotope Analysis. In: IOP, 2019. *IOP Conference Series: Earth and Environmental Science. The 5th International Conference on Water Resource and Environment (WRE 2019), 16–19 July 2019, Macao, China*. IOP Publishing. Vol. 344, 012062. https://doi.org/10.1088/1755-1315/344/1/012062

6. Pilatti, F.K., Ramlov, F., Schmidt, E.C., Kreusch, M., Pereira, D.T., Costa, C., de Oliveira, E.R., Bauer, C.M. and Rocha, M., 2016. *In vitro* Exposure of *Ulva lactuca* Linnaeus (Chlorophyta) to Gasoline–Biochemical and Morphological Alterations. *Chemosphere*, 156, pp. 428–437. https://doi.org /10.1016/j.chemosphere.2016.04.126

7. El Maghraby, D. and Hassan, I., 2021. Photosynthetic and Biochemical Response of *Ulva lactuca* to Marine Pollution by Polyaromatic Hydrocarbons (PAHs) Collected from Different Regions in Alexandria City, Egypt. *Egyptian Journal of Botany*, 61(2), pp. 467–478. https://doi.org/10.21608/ejbo.2021.37571.1531

8. Salakhov, D.O., Voskoboinikov, G.M. and Ryzhik, I.V., 2020. The Influence of Diesel Fuel on the Growth of Plants of *Ulva lactuca* L. (Chlorophyta) of the Barents Sea. *Nauka Yuga Rossii = Science in the South of Russia*, 16(1), pp. 55–59. https://doi.org/10.7868/S25000640200107 (in Russian).

9. Salakhov, D. Pugovkin, D., Ryzhik, I. and Voskoboinikov, G., 2021. The Changes in the Morpho-Functional State of the Green Alga *Ulva intestinalis* L. in the Barents Sea under the Influence of Diesel Fuel. In: IOP, 2021. *IOP Conference Series: Earth and Environmental Science.* IOP Publishing. Vol. 937, iss. 2, 022059. https://doi.org/10.1088/1755-1315/937/2/022059

10. Malavenda, S., Makarov, M., Ryzhik, I., Mityaeva, M. and Malavenda, S., 2018. Occurrence of *Ulva lactuca* L. 1753 (Ulvaceae, Chlorophyta) at the Murman Coast of the Barents Sea. *Polar Research*, 37, 1503912. https://doi.org/10.1080/17518369.2018.1503912

11. Patin, S.A., 2008. *Oil Spils and Their Impact on the Marine Environment and Living Resources.* Moscow: Izd-vo VNIRO, 508 p. (in Russian).

12. Voskoboinikov, G.M., Ryzhik, I.V., Salakhov, D.O., Metelkova, L.O., Zhakovskaya, Z.A. and Lopushanskaya, E.M., 2020. Absorption and Conversion of Diesel Fuel by the Red Alga Palmaria palmata (Linnaeus) F. Weber et D. Mohr, 1805 (Rhodophyta): The Potential Role of Alga in Bioremediation of Sea Water. *Russian Journal of Marine Biology*, 46(2), pp. 135–141. https://doi.org/10.1134/S1063074020020108

13. Voskoboinikov, G.M. and Kamnev, A.N., 1991. [*Morphological and Functional Changes of Chloroplasts in the Algae Ontogenesis*]. Saint Petersburg: Nauka, 95 p. (in Russian).

14. Voskoboinikov, G.M., Metelkova, L.O., Pugovkin, D. and Salakhov, D., 2023. The Effect of Crude Oil on the Symbiotic Association of the Green Alga *Acrosiphonia arcta* (Dillwyn) Gain and Epiphytic Bacteria. *Marine Biological Journal*, 8(1), pp. 16–26.

15. Mironov, O.G., 1985. *Interaction Between Sea Organisms and Oil Hydrocarbons*. Leningrad: Gidrometeoizdat, 127 p. (in Russian).

16. Binark, N., Güven, K.C., Gezgin, T., Ünlü, S., 2000. Oil Pollution of Marine Algae. *Bulletin of Environmental Contamination and Toxicology*, 64, pp. 866–872. https://doi.org/10.1007/s001280000083

About the authors:

Grigory M. Voskoboinikov, Head of Laboratory , Murmansk Marine Biological Institute of RAS (17 Vladimirskaya Str., Murmansk, 183038, Russian Federation), DSc (Biol.), Professor, **ResearcherID: G-4094-2016, Scopus Author ID: 7004206680,** *grvosk@mail.ru*

Larisa O. Metelkova, Senior Research Associate, Murmansk Marine Biological Institute of RAS (17 Vladimirskaya Str., Murmansk, 183038, Russian Federation), PhD (Chem.), *Larissa.metelkova@list.ru*

Dmitry O. Salakhov, Junior Research Associate, Murmansk Marine Biological Institute of RAS (17 Vladimirskaya Str., Murmansk, 183038, Russian Federation), *Salahov04@yandex.ru*

Ekaterina O. Kudryavtsteva, Senior, Murmansk Marine Biological Institute of RAS (17 Vladimirskaya Str., Murmansk, 183038, Russian Federation), *ekato393@mail.ru*

Contribution of the authors:

Grigory M. Voskoboinikov – ideology and statement of the study problem, electron microscopic work, writing the article, editing the text

Larisa O. Metelkova – analytical studies of the content, transformation of diesel fuel in water and algae, analysis and discussion of the results, participation in the preparation of the article for publication

Dmitry O. Salakhov – selection of algae and water for the study, setting up the experiment, analysis of the literature on the study topic, analysis and discussion of the results, preparing the article for publication

Ekaterina O. Kudryavtsteva – participation in setting up and conducting the experiment, fixing and preparing material for light and electron microscopy, participation in preparing the article for publication

All the authors have read and approved the final manuscript.

Trophic State of the Limensky Bay Water Area (Southern Coast of Crimea, Black Sea)

K. A. Slepchuk *, T. V. Khmara

Marine Hydrophysical Institute of RAS, Sevastopol, Russia
* e-mail: skira@mhi-ras.ru

Abstract
Increase in the water area trophic state is one of the unfavourable consequences of anthropogenic impact on the ecological state of the marine environment. The cause of water body eutrophication is often an excessive input of nutrients and easily oxidisable organics, the main source being river runoff and sewage. The main aim of the work is to determine seasonal changes in the trophic state of the Limensky Bay water area based on numerical modelling data. The data required to calculate the trophic state index were derived using a one-dimensional version of the water quality model and its eutrophication block. The annual course of chlorophyll a concentration, nitrate and nitrite nitrogen, ammonium, phosphate phosphorus and oxygen was obtained for the Limensky Bay water area. The trophic state index was calculated from these biogeochemical indicators. The sea water in the study area was of good quality and its state was mesotrophic. Only in the cold period on the 1st–104th and 356th–365th model days, the index was below 4, which corresponds to an oligotrophic state. The maximum index value (4.39) was on the 247th model day and the minimum value (3.82) was on the 365th model day. The best correlation of the trophic state index was observed for the concentration of chlorophyll a (r = 0.84), mineral nitrogen (r = 0.80) and total phosphorus (r = 0.78). The calculated relative contribution of the components, included in the calculated formula of the E-TRIX index, showed that the main factor determining the eutrophication level of Limensky Bay waters was the concentration of mineral forms of nitrogen. This study can be used for monitoring the areas where *in situ* sampling is difficult.

Keywords: trophic state, E-TRIX, Limensky Bay, biogeochemical modelling, chlorophyll a, total phosphorus, mineral nitrogen

Уровень трофности акватории Лименского залива (Южный берег Крыма, Черное море)

К. А. Слепчук *, Т. В. Хмара

Морской гидрофизический институт РАН, Севастополь, Россия
* e-mail: skira@mhi-ras.ru

Аннотация

Повышение уровня трофности акватории является одним из неблагоприятных последствий антропогенного воздействия на экологическое состояние морской среды. Причиной эвтрофирования водоемов часто является избыточное поступление в них биогенных веществ и легкоокисляемой органики, главным источником которых являются речной сток и сточные воды. Основная цель работы – определить сезонные изменения трофического состояния вод в районе Лименского залива на основе данных, полученных с помощью численного моделирования. Необходимые для расчета индекса трофности данные вычислялись по одномерному варианту модели качества воды и ее блоку эвтрофикации. Получен годовой ход концентрации хлорофилла *a*, азота нитратов и нитритов, аммония, фосфора фосфатов, кислорода для акватории Лименского залива. На основе этих биогеохимических показателей рассчитан индекс трофности. Исследуемая акватория обладает хорошим качеством морских вод со средним уровнем трофности. Лишь в холодный период с 1-го по 104-й и с 356-го по 365-й расчетные дни индекс ниже 4, что соответствует низкому уровню трофности. Максимальное значение индекса (4.39) приходится на 247-й расчетный день, минимальное (3.82) – на 365-й. Наибольшая корреляция индекса трофности наблюдается с концентрацией хлорофилла *a* ($r = 0.84$), минерального азота ($r = 0.80$) и общего фосфора ($r = 0.78$). Расчет относительного вклада компонентов, входящих в расчетную формулу индекса *E-TRIX*, показал, что основным фактором, определяющим уровень эвтрофикации вод Лименского залива, является концентрация минеральных форм азота. Данное исследование может использоваться при мониторинге зон, в которых отбор проб на месте трудно осуществить.

Ключевые слова: трофность, *E-TRIX*, Лименский залив, биогеохимическое моделирование, хлорофилл a, общий фосфор, минеральный азот

Introduction

The Southern Coast of Crimea is a territory with a unique recreational potential. However, tourism activities influence the environmental situation in the region. In Crimea, especially on its southern coast, environmental risks once arose due to the haphazard planning of cities, which did not consider issues most important

for the ecological state of the territories, including optimisation of the drainage system, primarily storm water drainage, transport infrastructure [1]. The main source of marine waters pollution of the Southern Coast of Crimea is wastewater discharge from sewage treatment facilities and recreational complexes such as health resorts and recreation centers [2]. At the height of tourist seasons, the risk of the coast overpopulation increases, which inevitably results in pollution of the beach zone and adjacent sea areas.

Recreational resources of the coastal sea zone rely mainly on the natural environment quality. Thus, the water area of the Crimean southern coast is monitored to determine the state of ecosystems and trends in their variability and to develop recommendations for the rational use of natural resources [2, 3].

One of the adverse consequences of anthropogenic impact on the ecological state of the marine environment may be an increase in the trophic state of the water area. Eutrophication of water bodies is often caused by excessive input of nutrients and easily oxidised organic matter, the main source of which is river runoff and wastewater, whose influence is local in nature. It is impossible to find a general method to assess the trophic state of different marine areas. Each study chooses an approach driven by the choice of indicators and their number when calculating various ecological indices, taking into account a limited set of measured parameters and indicators of the marine environment. The E-TRIX ecosystem trophic state index is based on the concentration of the main nutrients (nitrogen and phosphorus), the degree of water oxygenation and chlorophyll a concentration. The advantage of E-TRIX is the use of standard monitoring characteristics, which allows for a comparative analysis of trophic state in different marine areas, while not only qualifying but also quantifying the water body state.

In various studies (e. g. [4]), the E-TRIX index is calculated from monitoring data. However, a sufficient number of observations at different points in space is not always available. Mathematical modelling makes it possible to fill data gaps and assess the ecosystem state, while considering the variability of its components. In addition, mathematical modelling allows predicting the evolution of an ecosystem under the influence of natural, climatic and anthropogenic factors.

As study object, we have chosen Limensky Bay near the settlement of Katsiveli. This water area is under the least anthropogenic impact and distant from large-scale industrial sewage.

Limensky (Goluboy) Bay is located on the Southern Coast of Crimea between Cape Kikineiz and Mount Koshka. In the southwestern part of the bay, there is a stationary oceanographic platform (Fig. 1). The main pollution sources in the bay are wastewater from Katsiveli and the discharge pipe of used water from the fun water park Goluboy Zaliv.

The hydrological structure of the Limensky Bay waters mainly depends on coastal currents and their variability. An analysis of *in situ* data shows that
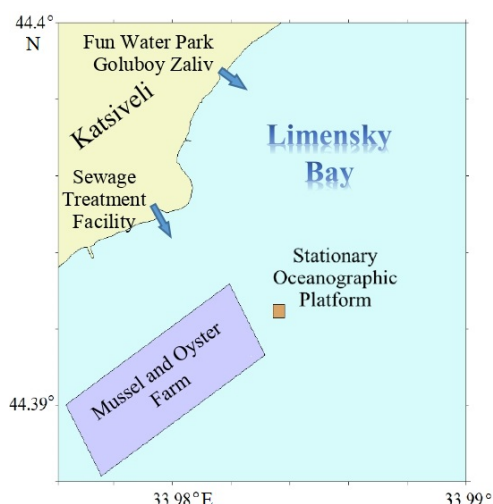
F i g . 1 . Study area

a quasi-stationary west-south-west current is observed along the coast near Cape Kikineiz. The average annual modulus of the current velocity vector was maximum in the near-surface layer and varied within 5.8–9.4 cm/s during the monitoring period [5].

Upwelling occurs in this area under longshore winds with a westerly component (southwesterly, westerly and northwesterly). Such a rise of cold nutrient-rich deep waters to the surface has the greatest impact on the content of hydrochemical components in spring and summer periods. As a result, partial pollution of the coastal zone is possible.

The chemical composition of Limensky Bay waters is unique. The content of dissolved oxygen directly depends on the temperature indicators, and its concentration increases sharply (up to 115%) when surging phenomena occur [6]. Hydrochemical studies showed the presence of two unfavourable areas with reduced dissolved oxygen content (97%) [7].

Coastal waters are generally characterised by moderate concentrations of nutrients. The absence of phosphate deficiency (~ 0.1 μM) is typical of this area even during the phytoplankton growth and development [8], which, in turn, indicates active dynamic processes contributing to phosphate input from the underlying sea layers. The concentration of nitrogen forms was relatively low (0.2 μM) according to the data of the studies carried out in the recreational areas of the Southern Coast of Crimea.

From March 2010 to March 2012, comprehensive ecological studies were performed in Limensky Bay near the mussel and oyster farm located on the traverse of Kikineiz Bay (Fig. 1). An analysis of the obtained data showed [9–11] that during the study period, the hydrochemical regime around the farm was characterised by good aeration of the water column, relatively low nutrient content and insignificant anthropogenic pressure. Extremely high water temperature (over 26 °C) in July–August 2010 determined low quantitative indicators of phytoplankton (20 mg/L).

No water bloom, typical of coastal waters and caused by the development of certain phytoplankton species, was observed during the study period. High content of ammonium nitrogen (up to 30.3 μg/L) in the warm period of the year, as compared to other mineral forms of nitrogen, was due to organic matter degradation.

The main objective of this work is to determine seasonal changes in the trophic state of waters in the Limensky Bay area using the E-TRIX index based on numerical modelling data.

Materials and methods

The trophic state of Limensky Bay was assessed using the E-TRIX index. It is a function containing the following parameters: dissolved oxygen, mineral nitrogen, total phosphorus and chlorophyll a. According to [12], the trophic state index is determined by the formula

$$E\text{-}TRIX = (\lg[Ch \cdot D\%O \cdot N \cdot P] + 1.5) / 1.2,$$

where Ch – concentration of chlorophyll a, µg/L; $D\%O$ – absolute deviation of oxygen saturation from 100%; N – concentration of dissolved form of mineral nitrogen, µg/L; P – concentration of total phosphorus, µg/L.

E-TRIX index values can range from 0 to 10. Depending on these values, there are four trophic states: oligotrophic (< 4), mesotrophic (4–5), eutrophic (5–6) and hypereutrophic (6–10).

If the trophic state index exceeds 6, the investigated water area contains high concentrations of nutrients and has low transparency, which can lead to hypoxia in the bottom layers of its waters. If the index does not exceed 4, there are insignificant concentrations of nutrients, good air exchange throughout the entire water column and high transparency [13].

The data on the concentration of chlorophyll a, dissolved oxygen, mineral nitrogen, and total phosphorus, necessary to calculate the E-TRIX index, were derived using a one-dimensional version of the water quality model and its eutrophication module [14]. Before calculating, the model was calibrated using data for 2010–2012 on phytoplankton biomass concentration from [9, 10] and concentrations of nutrients and oxygen from the oceanographic database of the Marine Hydrophysical Institute.

Meteorological data were used as model input parameters: wind speed and direction at 4 h intervals, air temperature at 3 h intervals, photosynthetic active radiation per day, humidity and cloud amount at 6 h intervals. We also used annual variations in transparency, values of seawater temperature, salinity and concentrations of phytoplankton, nutrients, oxygen, organic phosphorus and organic nitrogen. They were set starting from 1 January of the model year.

Results

During the model year, the E-TRIX index varied from 3.82 to 4.39 (average 4.09), which is a transitional trophic state of the study water area from the oligotrophic to mesotrophic one. It also indicates good water quality. The highest value on the 247th model day (5 September) coincided with the autumn peak of phytoplankton blooming, and the lowest value was recorded on the 365th day (31 December). From the 105th to 355th model day, the index exceeded 4, while on other days it was under that value. In terms of seasons, the average index was the highest in autumn (4.22) while in winter it was the lowest (3.96) (Table 1).

In paper [15], the trophic state index was calculated from *in situ* data in the Limensky Bay area using a modified formula. The authors used total nitrogen instead

T a b l e 1 . Change in E-TRIX index depending on the season

Season	Value range	Average
Winter	3.82…4.17	3.96
Spring	3.82…4.20	3.98
Summer	3.91…4.36	4.19
Autumn	4.07…4.39	4.22

of mineral nitrogen and added silicon concentration as a multiplier under the common logarithm sign. Total nitrogen was taken as recommended in paper [16]. Silicon concentration was included in the general formula by the authors of study [15] for a more accurate assessment of water quality, since silicon is an important nutrient. Therefore, the average E-TRIX value in the above work is slightly higher (4.42) than in our results. Due to the absence of silicon in the chemical-biological module of the water quality model we used, it is not possible to numerically verify the result obtained in paper [15] for Limensky Bay.

Fig. 2 shows the annual variability of the eutrophication indicator with chlorophyll a, total phosphorus, mineral nitrogen and absolute deviation of oxygen saturation from 100%. Of note, phosphates, organic phosphorus and ammonium did not have a pronounced seasonal variability. Nitrates had maximum concentrations in the cold period from December to March and minimum concentrations in the warm period of the year, which is shown in Fig. 2, *c*. A similar result was described by the authors of paper [9]. The winter nitrate input is caused by convective mixing of waters, while the summer one is due to upwelling. Nitrites have maximum values during the increased dynamic activity of waters from December to March. In the water area of Limensky Bay, the river runoff has no direct influence on the hydrochemical structure, which was noted in [10].

The relative contribution of the components included in the E-TRIX calculation formula was calculated. The highest relative percentage contribution to the calculation formula was made by mineral nitrogen (44.48...51.88%, average 48.17%), followed by the chlorophyll a module (−38.71...−24.02%, average −31.19%), total phosphorus (26.59...30.12%, average 28.32%). The smallest contribution was made by absolute deviation of oxygen saturation from 100% (19.44...28.49%, average 24.09%).
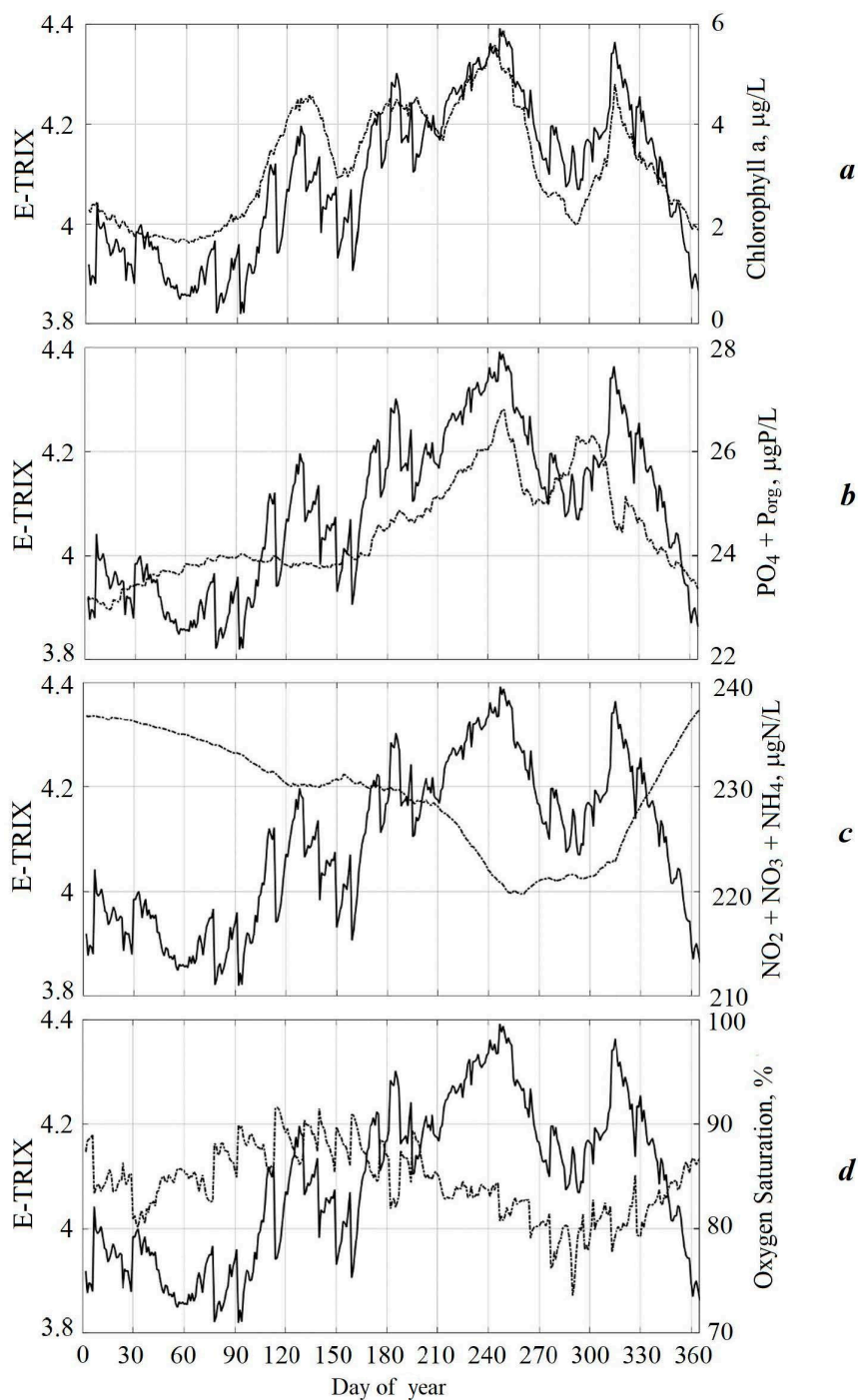
F i g . 2 . Annual variations of E-TRIX index (solid curve) and concentrations (dashed-dotted curve) of chlorophyll a (*a*), total phosphorus (*b*), mineral nitrogen (*c*), oxygen saturation (*d*) in the Limensky Bay waters

T a b l e 2 . Relative contribution (%) of the components to the E-TRIX calculation formula

E-TRIX	$D\%O$	Ch	N	P
Max	24.27	−24.66	44.63	27.18
Min	23.86	−38.36	51.88	29.86

Table 2 shows the relative contribution in percent of the components resulting from the formula at the minimum and maximum values of the eutrophication index. At the maximum value of the index, the relative contributions of mineral nitrogen and chlorophyll a modulus are minimal, and at the minimum value of E-TRIX, the contributions of these components are maximal. A similar fact was described in paper [17] for Sevastopol and Yuzhnaya Bays.

If a hydrochemical parameter in the original formula is replaced by 1 (i. e. excluded from the formula), the trophic state index can either increase (if chlorophyll a concentration is excluded) or decrease (if total phosphorus concentration, mineral nitrogen concentration, absolute deviation of oxygen saturation from 100% are excluded) (Fig. 3). The figure shows that the E-TRIX value decreases most of all (almost twice) when mineral nitrogen is excluded, which once again shows that its contribution to the calculation formula in this region is maximum.

F i g . 3 . Contribution of individual hydrochemical characteristics to E-TRIX quantity

We calculated correlation coefficients between E-TRIX index and absolute deviation of oxygen saturation from 100%, concentration of total phosphorus, 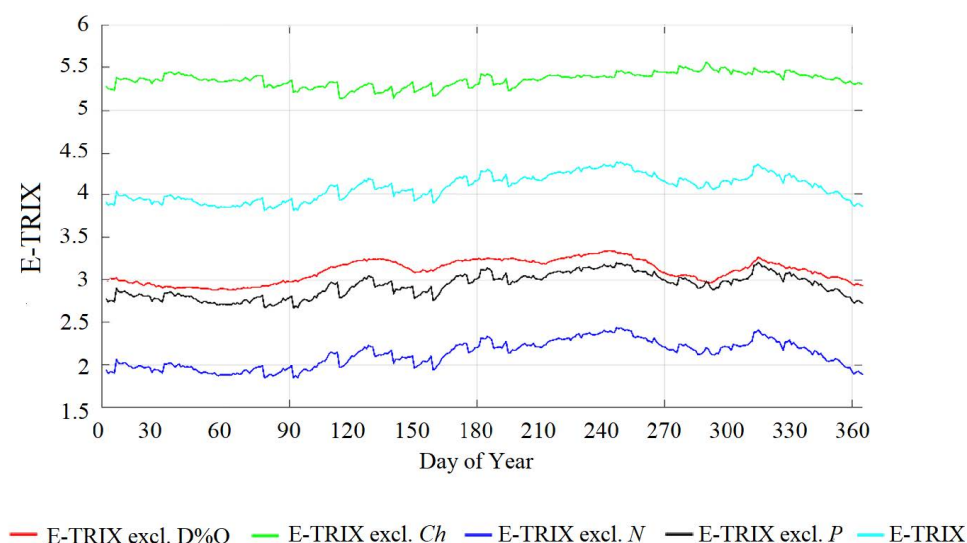mineral nitrogen and chlorophyll a. The highest values of the correlation coefficient were obtained with the concentration of chlorophyll a (r = 0.84), mineral nitrogen (r = 0.80) and total phosphorus (r = 0.78). The correlation with absolute deviation of oxygen saturation from 100% is weak (r = 0.47).

Conclusion

Modelling of biogeochemical indicators of Limensky Bay and further calculation of the trophic state index showed that the seawater quality of the water area is good with a transitional (from oligotrophic to mesotrophic) trophic state. During the cold period from the 1st to 104th and from 356th to 365th model days, E-TRIX was below 4, which corresponds to an oligotrophic trophic state, while on other model days it was higher. The maximum value of the index was on the 247th model day (4.39), and the minimum value was on the 365th day (3.82).

The highest correlation of the trophic state index is observed with the concentration of chlorophyll a (r = 0.84), mineral nitrogen (r = 0.80) and total phosphorus (r = 0.78). Calculation of the relative contribution of the components included in the E-TRIX calculation formula showed that the main factor determining the level of eutrophication of Limensky Bay waters is the concentration of mineral forms of nitrogen. Thus, ecosystem modelling and further calculation of E-TRIX may help to assess the ecological status of other water bodies, where *in situ* sampling is difficult.

REFERENCES

1. Vetrova, N.M., Ivanenko, T.A., Gaisarova, A.A. and Mannanov, E.E., 2019. The Problem of Ecological Risk Zones in the Coastal Areas of the Crimea. *Biospheric Compatibility: Human, Region, Technologies*, (2), pp. 59–73 https://doi.org/10.21869/23-11-1518-2019-26-2-59-73 (in Russian).

2. Gruzinov, V.M., Dyakov, N.N., Mezenceva, I.V., Malchenko, Y.A. and Zhohova N.V., 2018. Pollution of Coastal Waters Crimea Wastewater Discharge. In: I. M. Kabatchenko, ed., 2018. *Proceedings of N.N. Zubov State Oceanographic Institute*. Moscow. Vol. 219, pp. 124–151 (in Russian).

3. Dyakov, N.N., Malchenko, Yu.A., Lipchenko, A.E., Bobrova, S.A. and Timoshenko, T.Yu., 2020. Hydrological and Hydrochemical Characteristics of Crimean Coastal Waters and Necessary Measures to Reduce the Pollution Level of Recreation Zones. In: V. M. Gruzinov, ed., 2020. *Proceedings of N.N. Zubov State Oceanographic Institute*. Moscow. Vol. 221, pp. 163–194 (in Russian).

4. Skuratova, P.N., Khasanova, L.N. and Musina, S.A., 2024. Analysis of Trophic State of Waters of Ura Bay of Motovsky Bay, Lodeynaya Bay of Kola Bay and Kildinsky Strait of Murmansk Region Using E-TRIX Index. *Fisheries*, (2), pp. 26–34. https://doi.org/10.36038/0131-6184-2024-2-26-34 (in Russian).

5. Kuznetsov, A.S., 2022. Mean Long-Term Seasonal Variability of the Coastal Current at the Crimea Southern Coast in 2002–2020. *Physical Oceanography*, 29(2), pp. 139–151. doi:10.22449/1573-160X-2022-2-139-151

6. Yevstigneyeva, D.S., Kondratiyev, S.I. and Metic-Dijunova, V.V., 2012. Dynamics of Oxygen in the Surface Waters of the Coastal of the Blue Bay in Spring and Autumn. In: MHI, 2012. *Ekologicheskaya Bezopasnost' Pribrezhnoy i Shel'fovoy Zon i Kompleksnoe Ispol'zovanie Resursov Shel'fa* [Ecological Safety of Coastal and Shelf Zones and Comprehensive Use of Shelf Resources]. Sevastopol: ECOSI-Gidrofizika. Iss. 26, vol. 1, pp. 310–316 (in Russian).

7. Kondrat'ev, S.I., Lisichenok, A.D., Lyashenko, S.V. and Chepygenko, A.I., 2003. Hydrological and Chemical and Optical Parameters of the Goluboi Bay Water (Katcivali, September, 2002). In: MHI, 2003. *Ekologicheskaya Bezopasnost' Pribrezhnoy i Shel'fovoy Zon i Kompleksnoe Ispol'zovanie Resursov Shel'fa* [Ecological Safety of Coastal and Shelf Zones and Comprehensive Use of Shelf Resources]. Sevastopol: ECOSI-Gidrofizika. Iss. 8, pp. 119–131 (in Russian).

8. Kondratyev, S.I., Varenik, A.V., Vnukov, Yu.L., Gurov, K.I., Kozlovskaya, O.N., Kotelianets, E.A., Medvedev, E.V. and Orekhova, N.A., Svishchev, S.V., Khoruzhiy, D.S. and Konovalov, S.K., 2016. Blue Bay as a Sub-Satellite Ground for Evaluating Hydrochemical Characteristics in the Shelf Areas of the Crimea. *Physical Oceanography*, (1), pp. 49–61. https://doi.org/10.22449/1573-160X-2016-1-48-59

9. Pospelova, N.V., Troshchenko, O.A. and Subbotin, A.A., 2018. Variability of Food Reserve of Bivalves in the Two-Year Growing Cycle on the Mussel-Oyster Farm (Black Sea, Blue Gulf). *Scientific Notes of V.I. Vernadsky Crimean Federal University. Biology. Chemistry*, 4(5), pp. 148–164 (in Russian).

10. Troshchenko, O.A., Lisitskaya, E.V., Pospelova, N.V. and Subbotin, A.A., 2019. Structure of Phyto- And Meroplankton in the Marine Farm Area on the Background of Different Hydrological and Hydrochemical Conditions (the Black Sea, South Coast of Crimea, Blue Bay). *Problems of Fisheries*, 20(1), pp. 93–106 (in Russian).

11. Troshchenko, O.A., Kuftarkova, E.A., Lisitskaya, T.V., Pospelova, N.V., Rodionova, N.Yu., Subbotin, A.A. and Eremin, I.Yu., 2012. Results of Complex Ecological Research on the Mussel-Oyster Far, Waters of (the Blue Bay, Crimea, the Black Sea). In: MHI, 2012. *Ekologicheskaya Bezopasnost' Pribrezhnoy i Shel'fovoy Zon i Kompleksnoe Ispol'zovanie Resursov Shel'fa* [Ecological Safety of Coastal and Shelf Zones and Comprehensive Use of Shelf Resources]. Sevastopol: ECOSI-Gidrofizika. Iss. 26, vol. 1, pp. 291–309 (in Russian).

12. Vollenweider, R.A., Giovanardi, F., Montanari, G. and Rinaldi, A., 1998. Characterization of the Trophic Conditions of Marine Coastal Waters with Special Reference to the NW Adriatic Sea: Proposal for a Trophic Scale, Turbidity and Generalized Water Quality Index. *Environmetrics*, 9(3), pp. 329–357. https://doi.org/10.1002/(SICI)1099-095X(199805/06)9:3%3C329::AID-ENV308%3E3.0.CO;2-9

13. Moncheva, S. and Doncheva, V., 2000. Eutrophication Index ((E) TRIX) – an Operational Tool for the Black Sea Coastal Water Ecological Quality Assessment and Monitoring. In: SCSEIO, 2000. *International Symposium "The Black Sea ecological problems"*. Odessa: SCSEIO, pp. 178–185.

14. Ivanov, V.A. and Tuchkovenko, Yu.S., 2008. *Applied Mathematical Water-Quality Modeling of Shelf Marine Ecosystems*. Sevastopol: ECOSI-Gidrofizika, 311 p. (in Russian).

15. Gubanov, V.I. and Rodionova, N.Yu., 2013. Trophic Water Diagnosis in the Area of the Mussel-Oyster Farm Location (the Black Sea, Crimea, the Goluboy Bay). In: O. A. Petrenko, ed., 2013. *Current Fishery and Environmental Problems of the Azov and Black Seas Region: Materials of VIII International Conference. Kerch, 26–27 June 2013*. Kerch: YugNIRO Publishers', pp. 146–151 (in Russian).

16. Saroglia, M., Cecchini, S. and Saroglia-Terova, G., 2000. Review of Regulations and Monitoring of Italian Marine Aquaculture. *Journal of Applied Ichthyology,* 16, pp. 182–186. https://doi.org/10.1046/j.1439-0426.2000.00271.x

17. Slepchuk, K.A., Khmara, T.V. and Man'kovskaya, E.V., 2017. Comparative Assessment of the Trophic Level of the Sevastopol and Yuzhnaya Bays Using E-TRIX Index. *Physical Oceanography*, (5), pp. 60–70. https://doi.org/10.22449/1573-160X-2017-5-60-70

About the authors:

Kira A. Slepchuk, Junior Research Associate, Marine Hydrophysical Institute of RAS (2 Kapitanskaya St., Sevastopol, 299011, Russian Federation), **ORCID ID: 0000-0001-5437-4866, ResearcherID: H-9366-2017**, *skira@mhi-ras.ru*

Tatiyana V. Khmara, Research Associate, Marine Hydrophysical Institute of RAS (2 Kapitanskaya St., Sevastopol, 299011, Russian Federation), **Scopus Author ID: 6506060413, ResearcherID: C-2358-2016**, *xmara@mhi-ras.ru*

Contribution of the authors:

Kira A. Slepchuk – problem statement, numerical experiments, processing and interpretation of modelling results, preparation of text and graphic materials of the article

Tatiyana V. Khmara – analysis and description of the study results, preparation of the text

All the authors have read and approved the final manuscript.

Original paper

Application of the Raspberry Pi for *In Situ* Measurement Automation and Data Transfer and Storage

A. F. Rozvadovskiy

Marine Hydrophysical Institute of RAS, Sevastopol, Russia
e-mail: rozvadovsky@yandex.ru

Abstract

The paper considers issues of organization of remote workplaces for automation of *in situ* measurements of the marine environment. The workplace allows collection of data from a sensor system that measures characteristics of the marine environment in natural conditions; to transfer data to a remote data center via the Internet; to store and backup data. The paper presents algorithms for workplace organization based on modern technologies for data collection and transmission. The implementation of the workplace is detailed on the example of remote control of the weather station Davis Vantage Pro 2. This weather station was installed on the stationary oceanographic platform in Katsiveli to continuously measure parameters of the atmospheric surface layer. The remote control was organized on the basis of the hardware and software platform of a single-board personal computer Raspberry Pi. Two-year tests of the system allow concluding about its reliability and high efficiency. The proposed principles and algorithms can be applied to organization of remote workplaces for performing oceanological measurements in coastal areas with Internet access.

Keywords: automation, *in situ* measurements, marine environment, remote workplace, hardware and software platform, *Raspberry Pi*, weather station, *Davis Vantage Pro 2*, cloud storage, oceanographic platform, Katsiveli

Применение платформы *Raspberry Pi* для автоматизации натурных измерений морской среды, передачи и хранения полученных данных

А. Ф. Розвадовский

Морской гидрофизический институт РАН, Севастополь, Россия
e-mail: rozvadovsky@yandex.ru

Аннотация

Описана технология реализации рабочего места на основе аппаратно-программной платформы *Raspbery Pi* в качестве управляющего персонального компьютера метео-станции *Davis Vantage Pro* 2 и представлен пример ее использования для контроля и мониторинга морской среды. Рабочее место позволяет собирать данные системы датчиков, измеряющих характеристики морской среды в натурных условиях, и пере-давать их в удаленный центр сбора данных через Интернет, хранить и выполнять резервное копирование. Рабочее место обеспечивает пользователям доступ к данным и может быть использовано как средство удаленного управления работой датчиков. Представлены алгоритмы организации рабочего места, опирающиеся на современные технологии сбора и передачи данных. Детально описана реализация рабочего места на примере удаленного контроля метеостанции *Davis Vantage Pro* 2, установленной на стационарной океанографической платформе ФГБУН ФИЦ МГИ в пгт Кацивели для непрерывных измерений параметров приводного слоя атмосферы. Удаленный кон-троль организован на базе аппаратно-программной платформы одноплатного персо-нального компьютера *Raspberry Pi*. Двухлетние испытания системы позволяют сделать вывод о ее надежности и высокой эффективности. Предлагаемые принципы и алгорит-мы могут быть использованы при организации удаленных рабочих мест для выполне-ния океанологических измерений в прибрежных зонах с доступом к Интернету.

Ключевые слова: автоматизация, натурные измерения, морская среда, удаленное рабочее место, аппаратно-программная платформа, *Raspberry Pi*, метеостанция, *Davis Vantage Pro 2*, облачные хранилища, океанографическая платформа, Кацивели

Introduction

Monitoring of the marine environment is imperative to ensure the ecological safety of coastal zones, to control their resources and to study their current state and trends. Monitoring tasks entail continuous measurements and the obtained measurement data should be available at any time for further processing and analy-sis. To organise this observation process, it is necessary to create automated remote

workplaces providing reliable connection to the measuring equipment for control and data reading without the participation of an operator. This is of particular importance given that it facilitates the modernisation of existing hardware and software complexes (HSC) for measurement, data recording and storage (e.g. portable weather stations, wave-graphs, etc.), which assume long-term autonomous operation, but lack their own built-in remote control, monitoring and configuration capabilities.

Methods of sea surface monitoring are discussed in detail in the literature [1–4], but the issues of organising remote workplaces for data recording, processing and subsequent storage are given much less attention [5]. Work [6] provides an overview of the development of system solutions for weather stations since the mid-1990s. It shows that the development of means for measuring environmental parameters coincided with the trend of development of telecommunication and computer technologies. These technologies of meteorological measurements are based on software and hardware complexes that register data from sensors and transmit them to a remote terminal via radio channel. The paper [6] shows variants of realisations of software and hardware meteorological complexes including solutions [1)-4)], but not enough attention has been paid to the issue of the creation of automated workplaces itself. In fact, this direction (automation of workplaces) is diffused in the hardware and software complex of weather stations.

A more detailed and scrupulous approach to the issue of workplace automation is used in the development of software systems for the collection, visualisation, archiving, processing and transmission of hydrometeorological measurement data from automatic hydrometeorological complexes, in particular for sea surface monitoring. A notable example of such software is the ALMETA software package [5)], a special software operating on a personal computer with Windows operating system (OS), providing collection and processing of hydrometeorological information.

[1)] Wilhelm, R. and Haupt, F.S., 2011. Patent no. USRE42057E1, Int. Cl. G01W 1/00 (2006.01)," G01P"13/00 (2006.01). N 11/485,648. *Weather Station*. Filed 13 July 2006; Date of Reissued" Patent"25"January 2011. 7 p.

[2)] Strebkov, D.S., Dorzhiev, S.S. and Bazarova, E.G., 2013. Patent 2472186C2 Russian Federation. МПК G01W 1/00 (2006.01). [*Network of Autonomous Environmental Monitoring Stations*]: 2011110187/28. Applied 18.03.11, published 10.01.13. Bulletin no. 1. 7 p. (in Russian).

[3)] Fisher, G.A., 2009. Patent no. WO2009015370A1, Int. Pat. Cl. G0IW 1/10 (2006.01), G04B 47/06 (2006.01), G0IW 1/04 (2006.01) N PCT/US2008/071259. *Pocket Weather Station*. Filed 25 July 2008, published 29 January 2009. 25 p.

[4)] Runge, T.H., 2016. Patent no. US9301460B2, Int.Cl. G05D 11/00 (2006.01), AO1G 25/16 (2006.01) *Irrigation Controller with Weather Station*: N 13/406,410. Filed 27 February 2012, published 5 April 2016. 25 p.

[5)] [*Software Complex for Automated Hydrometeorological Complexes ALMETA. User Manual*]. 2018, 47 p.

However, its flexibility and functionality are excessive for specific tasks, such as *in situ* measurements of the marine environment. This is particularly problematic given its significant demand on the computing resources of a personal computer.

Technical solutions based on Arduino and Raspberry Pi hardware and software platforms require fewer resources. In [7–11], examples of Arduino-based weather station realisations are presented, and in [12–20] – Raspberry Pi-based. But these are hardware and software implementations of weather stations that record and process measurement results. The issues of automation and organisation of remote workplaces are hardly considered in these works.

In the Russian Federation, the Recommendations on the Operation of Automated Meteorological Complexes in Observation Units (R 52.04.818-2014) have been established, which set out the requirements for the installation, maintenance and operation of automated meteorological complexes (AMC), describe the standard procedure for meteorological observations in observation units (OU) equipped with AMC as well as the actions of OU personnel in the event of AMC failure. However, these recommendations do not permit to formulate technical requirements to the HSC, which are responsible for the automation of measurements and operation of the HSC in the autonomous mode. The purpose of the development is to create a remote automated workplace for continuous monitoring of the sea surface and environmental parameters using single-board computers. The paper describes a new technology of workplace implementation based on the hardware and software platform Raspbery Pi, used as a controlling personal computer (PC) of the weather station Davis Vantage Pro 2, and presents an example of its use for control and monitoring of the marine environment.

Equipment

The weather station Davis Vantage Pro 2 was chosen due to its measurement accuracy, functionality, number of settings [21] as well as presence of remote measurement sensors that provide radio transmission up to 300 m in the open space [6], which is relevant within the context of the MHI stationary oceanographic platform in Katsiveli. It is imperative to acknowledge that, in the absence of personnel on the platform at all times, the responsibility of remote access to control and retrieve data from the weather station Davis Vantage Pro 2 is of significant importance, as previously highlighted. This weather station allows connection to a PC using both in-house commercial WeatherLink software by Davis Instruments [7] and free WeeWX software [8].

The advantage of WeeWX software is that its source code is open (available for review, study and modification), which ensures its flexibility and adaptability

---

[6] Davis Instruments, 2021. *User Manual for Vantage Pro2 ™ and Vantage Pro2 Plus ™ Weather Stations*, 58 p.

[7] Davis Instruments, 1999. *Davis Weatherlink Software User's Manual*, 78 p.

[8] Keffer, N. *User's Guide to WeeWX.* 2024. [online] Available at: https://weewx.com/docs/4.10/usersguide.htm [Accessed: 10 December 2024].

to specific tasks. This software works in various GNU/Linux systems, in particular Debian, Ubuntu, Mint, Raspbian and others. Raspbian support allows the Raspberry Pi to be used as a control PC for the weather station Davis Vantage Pro 2.

As mentioned earlier, the Raspberry Pi is most often used as a stand-alone solution for building weather stations, when the Raspberry Pi board itself is used as a central processor to which external sensors are connected [22]. These solutions are inferior to the weather station Davis Vantage Pro 2 both in measurement accuracy and in the flexibility of software settings.

It is rare for Raspberry Pi-based solutions to be used as a controlling HSC, with ordinary PCs most often being used for remote access and control. However, in conditions of limited access to the platform in Katsiveli and a lack of permanent staff, not only the performance of PCs, but also their reliability and energy efficiency to ensure stable autonomous operation, become critical. In this context, Raspberry Pi has been shown to exhibit superiority over ordinary PCs, with its power consumption typically not exceeding 15 W.

The following is an example of realisation of remote access and control of the weather station Davis Vantage Pro 2 using Raspberry Pi HSC as well as the results of its pilot operation on the platform in Katsiveli.

Results and discussion

At the initial stage of the remote access organisation, a Raspberry Pi B+ was used as a control PC to collect and transmit data from the weather station Davis Vantage Pro 2.

The choice of this model is due to its computing resources, the performance of which ensures stable operation of WeeWX software when receiving, processing and transmitting data to a remote server. The 700 MHz processor core clock and 512 MB of RAM of this HSC provide support for any version of Raspbian OS, in which the WeeWX software runs. Connection to the Internet is provided through the built-in Ethernet port. Wireless connection to the Internet can be made via a USB-modem – in our case TP-Link TL-WN727N. Four USB ports make it possible to connect the weather station Davis Vantage Pro 2 as well as a mouse and a keyboard (Fig. 1).

As previously stated, the WeeWX software incorporates built-in support for the weather station Davis Vantage Pro 2, facilitating the aggregation of data on a local PC, specifically a Raspberry Pi B+.

The data are presented graphically in Fig. 2 and stored in the data file weewx.sdb. It is possible to present measurement results in a similar manner on a remote server. However, additional settings are required for monitoring via the Internet.

One of the limitations of the WeeWX software when running in Raspbian is the use of FTP (File Transfer Protocol) for data transfer. Thus, it is important

F i g . 1 . The appearance of the workplace for automated measurements, transmission and storage of the weather station Davis Vantage Pro 2 data using a Raspberry Pi B+
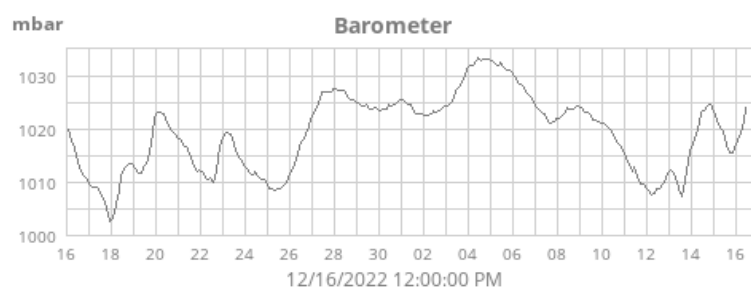
a
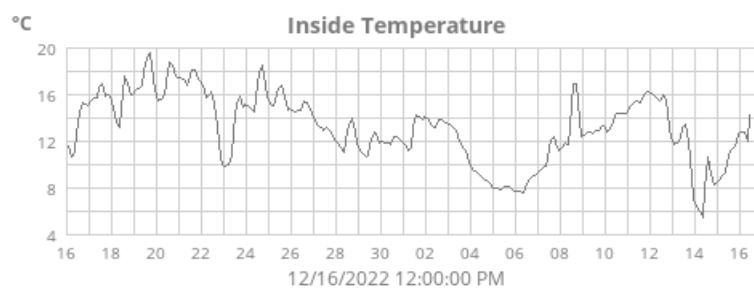
b

F i g . 2 . Example of view of data on pressure (*a*) and inside temperature (*b*) on the platform in Katsiveli from 16 November 2022 to 16 December 2022

to choose a server that supports this protocol. FreeHostingEU (available at: https://www.freehostingeu.com) was chosen as such a server (hosting). On this server, an account with ID: 4089596 was registered, for which a third-level domain was created – vantagepro2.eu5.net, providing data display.

The FTP server settings are made in the WeeWX software configuration file, weewx.conf, and are as follows:

```
[[FTP]]
#FTP'ing the results to a webserver is treated as just another report,
# albeit one with an unusual report generator!
skin = Ftp
#If you wish to use FTP, set @enable@ to @true@, then
# fill out the next four lines.
# Use quotes around passwords to guard against parsing errors.
enable = true
user = 4089596
passwort -= ************
server = vantagepro2.eu5.net
path = / vantagepro2.eu5.net/
#Set to True for an FTP over TLS (FTPS) connection. Not all servers
# support this.
secure_ftp = False
# To upload files from something other than what HTML_ROOT is set
# to above, specify a different HTML_ROOT here.
# HTML_ROOT = /var/www/html/weewx
# Most FTP serverts use port 21
port = 21
# Set to 1 to use passive mode, zero for active mode
Passive = 1
```

It should be noted that when organising automatic data backup using Raspberry Pi there were some difficulties, which were not considered by the technical support of the FreeHostingEU FTP server and were solved experimentally – by selecting the settings of the HSC. The path for saving data from the weather station Davis Vantage Pro 2 in the configuration file weewx.conf differs from the default path recommended on the FreeHostingEU technical support site – /home/www. In the settings of the weewx.conf configuration file, the path is specified as /vantagepro2.eu5.net/. If you leave it as it is written by default, the data will not be sent to the FTP server and will not be displayed on the page www.vantagepro2.eu5.net.

As a result of the above settings, data from the built-in sensors of the weather station Davis Vantage Pro 2 were obtained (Fig. 2). Measurement results of the Davis Vantage Pro 2 weather station during operation are continuously recorded by the WeeWX software into the weewx.sdb data file, which is stored on the local disc of the Raspberry Pi in the /var/lib/weewx/weewx.sdb folder. To process and analyse the results of measurements as well as their backup, it is advisable to copy this file from Raspberry Pi to another PC or network data storage. Fig. 3 shows the block diagram of the algorithm for connecting and saving data in the network storage.
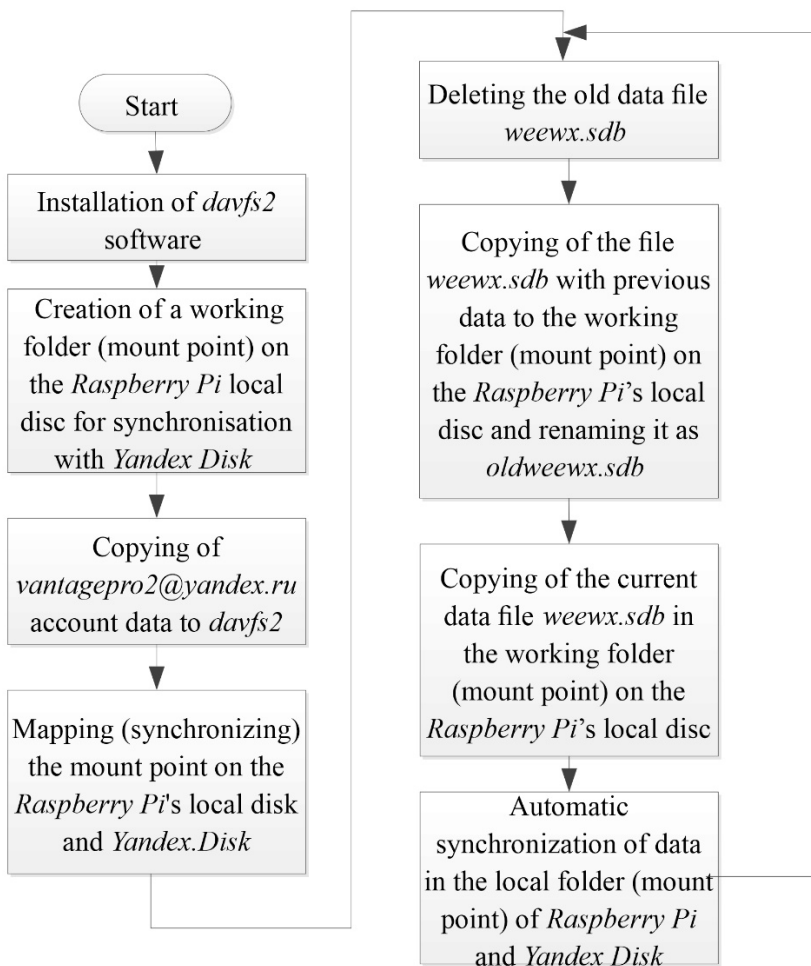
F i g . 3 . Block diagram of the algorithm for backing up a file with weewx.sdb data on Yandex Disk

In view of the above, it was decided to copy the weewx.sdb data file on a scheduled basis to Yandex Disk, a cloud service of the Yandex company that allows storing data on servers in the cloud and transferring them to other users on the Internet. Access to this service is possible through WebDAV (Web Distributed Authoring and Versioning), a set of extensions and additions to the HTTP (HyperText Transfer Protocol) which supports collaborative work of users on file editing and file management on remote web servers. For this purpose, davfs2 software was installed on Raspberry Pi, which makes it possible for Raspbian OS to connect to WebDAV storages (in our case – Yandex Disk) as if they were local discs. A folder (mount point) /mnt/yandex.disk/ has been created on the local disc of Raspberry Pi where weewx.sdb data file is copied with specified periodicity. This folder is

further synchronised with the folders of Yandex Disk network storage and thus the data are transferred to the cloud.

To work with Yandex Disk, a new account was created – vantage-pro2@yandex.ru, with its parameters (login and password) specified in the corresponding file of the davfs2 software – /etc/davfs2/secrets. It should be noted that Yandex Disk makes it possible to set a password different from the account password (in our case vantagepro2@yandex.ru). Raspberry Pi configuration work has shown that it is advisable to do this. In this case, connection to the NAS (authorisation on it) is more stable and access failures are excluded.

Synchronisation of the contents of the Raspberry Pi local folder and Yandex Disk is provided using the built-in configuration file of Raspbian OS – fstab. This file contains information about different file systems and storage devices used by Raspberry Pi. It also specifies how the created mount point /mnt/yandex.disk/ will be used.

It is necessary to note an important point that arose when configuring the remote workplace. For Raspberry Pi, when configuring the fstab file for the /mnt/yandex.disk/ folder, it is important to specify the _netdev parameter. In this case, connection of Raspbian OS to Yandex Disk is performed only after connection to Wi-Fi or Ethernet network. If this parameter is not specified, Raspbian OS will try to connect to the remote network storage before connecting to the Internet. The attempt will be unsuccessful and it will be necessary to try to connect again manually after Wi-Fi or Ethernet connection is established.

The above settings are made once and stored in the Raspberry Pi settings.

Data copying – weewx.sdb file – was performed cyclically, twice a day in order to avoid data loss. The built-in Cron task scheduler utilised in Raspbian [9] was employed for this purpose. For automatic copying of data, an executable file (script) ya_sdb_update.sh was prepared, the contents of which are given below:

> #!/usr/bin/env bash //A service line indicating the start of the script
> sudo rm /mnt/yandex.disk/olweex.sdb //Deleting a file with outdated information
> sudo mv /mnt/yandex.disk/weewx.sdb /mnt/yandex.disk/oldweex.sdb //Copying with renaming the file with data for the previous period
> sudo cp /var/lib/weewx/weewx.sdb /mnt/yandex.disk/ //Copying the file with up-to-date data

This file implements the data backup algorithm (Fig. 3).

During initial setup, two data files were saved on Yandex Disk:
- *oldweewx.sdb* – for the previous period;
- *weewx.sdb* – for the current period.

---

[9] Hentzen, W., 2004. *Cron Explained*. Hentzenwerke Publishing, Inc., 12 p.

In the course of executing the ya_sdb_update.sh executable file, the file oldweewx.sdb stored on Yandex Disk is identified as outdated resulting in its deletion. The weewx.sdb file contains the data preceding the measurement data, which is the data available at the moment of command file launch. In order to facilitate the restoration of the data, the weewx.sdb file is renamed to oldweewx.sdb. The actual data itself is written to the file weewx.sdb.

As mentioned earlier, data transfer was carried out in Wi-Fi network via TP-Link TL-WN727N USB modem. Connection to open Wi-Fi networks is performed through the graphical interface by selecting the network and entering the password. Connection to hidden networks requires additional settings in Raspbian configuration file – wpa_supplicant.conf. For each newly connected network the following entry is made in it:

Network = {ssid = "Network name"
scan_ssid = 1
psk = "Password"
key_mgmt = WPA-PSK //Type of encryption }

In the process of establishing a connection to the concealed Wi-Fi network on the oceanographic platform in Katsiveli, it is imperative to consider the scan_ssid parameter. This parameter is crucial as it instructs the system to establish a connection to the wireless network even in the absence of a name transmission from the network. In the absence of this parameter, the connection process is unsuccessful, and consequently, data transmission is not facilitated. It is imperative to note that the scan_ssid value has been set to one.

The experimental operation of Raspberry Pi B+ exposed a significant disadvantage inherent to this HSC: the absence of software and hardware mechanisms for remote control and configuration of the HSC.

The configuration of the wireless network in Katsiveli does not assume the use of static IP addresses for PCs connected to it. Therefore, it is difficult to use the system of remote access to the Raspberry Pi desktop using the RFB (Remote FrameBuffer) protocol. Whenever the HSC is restarted (e.g. in case of a power failure), its IP address will change randomly. To regain access to it, the new IP address must be learnt, which is difficult and, in some cases, can only be done by connecting locally to the HSC directly on the oceanographic platform itself.

In such cases, the optimal solution is the utilisation of specialised software for the remote control and configuration of HSC, in particular AnyDesk. The merits of this software are manifold, including its ease of installation and configuration, wide range of supported operating systems, autoloading functionality and ability to activate the HSC remotely over the local network (e.g. following a reboot or power failure) via the Wake-on-LAN function. However, it should be noted that this software is only compatible with Raspberry Pi 2 and subsequent models of this HSC. This was the reason for abandoning the Raspberry Pi B+ and switching to the Raspberry Pi 2.

The installation of AnyDesk on the Raspberry Pi 2B necessitated the implementation of additional preliminary settings. It should be noted that the AnyDesk

software package utilises the EGL graphical interface [23], which necessitated the configuration of the Raspberry Pi HSC. This entailed the installation of the additional software packages Libegl1-mesa and libminizip1, which were initially absent by default. It was only subsequent to the completion of these steps that the AnyDesk package on Raspberry Pi 2B commenced functioning correctly.

The WeeWX software and database backup settings for the Raspberry Pi 2B were configured in the same way as for the Raspberry Pi B+.

In the pilot operation on the oceanographic platform in Katsiveli together with the Davis Vantage Pro 2 weather station from August to December 2022, a PC in the following configuration was used:
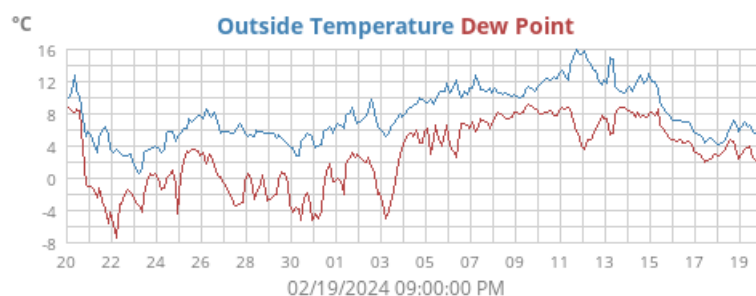
- model – Raspberry Pi 2B;
- remote access software – AnyDesk;
- FTP server for data output – FreeHostingEU;
- server to store the data file – Yandex Disk;
- task scheduler (scheduled data file uploads) – Cron.

In December 2022, the MHI own FTP server – Asustor AS5304T – was put into operation. Additional backup of available data was organised on it. Taking into account the fact that there is no pre-installed HTTP-server and, accordingly, there is no possibility to display data in the form shown in Fig. 2, the contents of the data folder on Raspberry Pi B – /var/www/html/weewx/ – are copied to the specified folder of the FTP-server Asustor AS5304T. The Cron task scheduler is used to automate the process. Copying the contents of the /var/www/html/weewx/ folder was organised with the help of the cURL program pre-installed in Raspbian, which sequentially transfers all files from Raspberry Pi 2B to the /Home/www/html/weewx/ folder of the FTP storage. A new executable file (script) asustor_ftp.sh was prepared with the following contents:
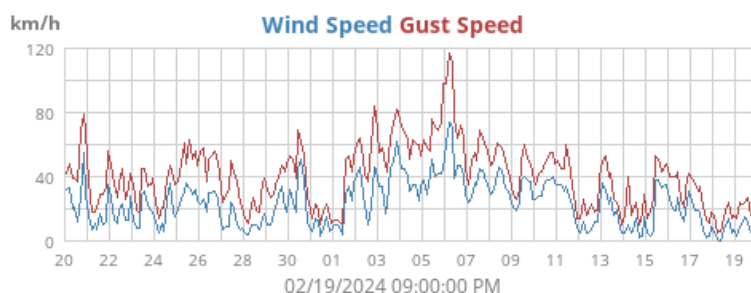
```
#!/usr/bin/env bash //A service line indicating the script start
cd /var/www/html/weewx/ //Switching to the data folder
find -type f -exec curl -u username:password –ftp-create-dirs T {} ftp://ip_ftp-server:port/Home/www/weewx/ \; //Copying the data folder to an FTP server.
```

In order to facilitate the subsequent checking and processing of the measurement results obtained, it is necessary to copy the folder to a local PC and open it in an Internet browser in a form that is similar to that shown in Fig. 2.

In September 2023, a further workplace modernisation was undertaken. External sensors measuring temperature, humidity, wind direction and speed were connected to the weather station Davis Vantage Pro 2. The Wi-Fi wireless connection was replaced with a wired LAN connection in order to enhance the reliability of remote access. Disabling the Wi-Fi modem also led to a reduction in the power consumption of the Raspberry Pi 2B PC. This modification enabled the utilisation of an external power supply with a voltage of 5 V and a current of less than 2 A, which also had a favourable effect on the stability of operation. This configuration has been in operation at the workplace since October 2023. Fig. 4 presents an example of the measurement results obtained from the weather station Davis Vantage Pro 2 in January and February 2024.

°C

Outside Temperature **Dew Point**

02/19/2024 09:00:00 PM

a

km/h

Wind Speed **Gust Speed**

02/19/2024 09:00:00 PM

b

F i g . 4 . Data on outside temperature (*a*) and wind speed (*b*) on the platform in Katsiveli from 20 January 2024 to 19 February 2024

The graphs demonstrate the stability of a Raspberry Pi 2B PC-based remote workplace in terms of its capability to record and store the Davis Vantage Pro 2 weather station data.

Conclusion

An example of implementing a remote automated workplace to access and control the weather station Davis Vantage Pro 2 using Raspberry Pi HSC is described. This workplace allows continuous automatic data storage locally, directly on the Raspberry Pi 2B, as well as backup to external FTP servers and network storage.

The ability to access, control and modify the parameters of the Raspberry Pi 2B HSC remotely eliminates the need for constant technical specialists to be present on the oceanographic platform in Katsiveli.

The results of the Raspberry Pi 2B HSC operation on the oceanographic platform in Katsiveli have shown that the possibility of creating automatically executable files (scripts) inside Raspbian OS and providing stable remote access to this HSC increase the reliability of recording, storage and backup of data received by the weather station Davis Vantage Pro 2.

REFERENCES

1. Bondur, V.G., Ivanov, V.A., Vorobiev, V.E., Dulov, V.A., Dolotov, V.V., Zamshin, V.V., Kondratiev, S.I., Lee, M.E. and Malinovsky, V.V., 2020. Ground-to-Space Monitoring of Anthropogenic Impacts on the Coastal Zone of the Crimean Peninsula. *Physical Oceanography*, 27(1), pp. 95–107. https://doi.org/10.22449/1573-160X-2020-1-95-107

2. Lavrova, O.Yu., Kostianoy, A.G., Lebedev, S.A., Mityagina, V. I., Ginzburg, A.I. and Sheremet, N.A., 2011. *Complex Satellite Monitoring of the Russian Seas*. Moscow: IKI RAN, 480 p. (in Russian).

3. Smirnov, G.V., Eremeev, V.N., Ageev, M.D., Korotaev, G.K., Yastrebov, V.S. and Motyzhev, S.V., 2005. [Modern Means and Methods of Oceanological Research]. In: IO RAS, 2005. [*Proceedings of IX International Scientific and Technical Conference Modern Methods and Means of Oceanological Research. Moscow*]. Moscow: Izd-vo Instituta Okeanologii RAN. Part 1, 146 p. (in Russian).

4. Veremyev, V.I., Kutuzov, V.M., Plotnitskaya, K.S., Kovalenko, V.V. and Telegin V.A., 2019. High-Frequency Radar for Coastal Areas Monitoring. *Journal of the Russian Universities. Radioelectronics*, 22(2), pp. 31–43. https://doi.org/10.32603/1993-8985-2019-22-2-31-43 (in Russian).

5. Smolov, V.E. and Rozvadovskiy, A.F., 2020. Application of the Arduino Platform for Recording Wind Waves. *Physical Oceanography*, 27(4), pp. 430–441. https://doi.org/10.22449/1573-160X-2020-4-430-441

6. Golovinov, E.E., Aminev, D.A., Kulakov, V.A., Bakirov, Sh.M. and Grigoriev, P.V., 2018. Analysis of System Solutions for Portable Weather Stations. *Nanoindustry*, (9), pp. 144–149. https://doi.org/10.22184/1993-8578.2018.82.144.149 (in Russian).

7. Kusriyanto, M. and Putra, A.A., 2018. Weather Station Design Using IoT Platform Based on Arduino Mega. In: IEEE, 2018. *International Symposium on Electronics and Smart Devices (ISESD), Bandung, Indonesia, 2018*. IEEE, pp. 1–4. https://doi.org/10.1109/ISESD.2018.8605456

8. Saini, H., Thakur, A., Ahuja, S., Sabharwal, N. and Kumar, N., 2016. Arduino Based Automatic Wireless Weather Station with Remote Graphical Application and Alerts. In: IEEE, 2016. *3rd International Conference on Signal Processing and Integrated Networks (SPIN), 11–12 February 2016, Noida, India*. IEEE, pp. 605–609. https://doi.org/10.1109/SPIN.2016.7566768

9. Singh, J., Mohammed, R., Kankaria, M., Panchal, R., Singh, S. and Sharma, R., 2018. Arduino-Based Weather Monitoring System. *International Journal of Advanced in Management, Technology and Engineering Sciences*, 8(3), pp. 1076–1079. Available at: https://www.ijamtes.org/gallery/29.%20mar%20ijamtes%20-%20317.pdf [Accessed: 28 November 2024].

10. Gao, J., Ma, H. ... Liu, H., 2016. The Intelligent Weather Station System Based on Ar-duino. In: J. Kao and W.-P. Sung, eds., 2016. *Proceedings of the 2016 International Conference on Engineering and Advanced Technology. Hong Kong, 22–23 December 2016*. ICEAT. Vol. 82, pp. 300–308. https://doi.org/10.2991/iceat-16.2017.61

11. Katyal, A., Yadav, R. and Pandey, M., 2016. Wireless Arduino Based Weather Station. *International Journal of Advanced Research in Computer and Communication Engineering*, 5(4), pp. 274–276. https://doi.org/10.17148/IJARCCE.2016.5470

12. Kishorebabu, V. and Sravanthi, R., 2020. Real Time Monitoring of Environmental Parameters Using IOT. *Wireless Personal Communications*, 112(2), pp. 785–808. https://doi.org/10.1007/s11277-020-07074-y

13. Rasal, M.V. and Rana, J.G., 2016. Raspberry Pi Based Weather Monitoring System. *International Journal of Advanced Research in Computer and Communication Engineering*, 5(10), pp. 119–122. Available at: https://ijarcce.com/wp-content/uploads/2016/10/IJARCCE-24.pdf [Accessed: 28 November 2024].

14. Muck, P.Y. and Homam, M.J., 2018. IoT Based Weather Station Using Raspberry Pi 3. *International Journal of Engineering and Technology*, 7(4.30), pp. 145–148. https://doi.org/10.14419/ijet.v7i4.30.22085

15. Vatsal, S. and Bhavin, M., 2017. Using Raspberry Pi to Sense Temperature and Relative Humidity. *International Research Journal of Engineering and Technology*, 4(2), pp. 380–385. Available at: https://www.irjet.net/archives/V4/i2/IRJET-V4I276.pdf [Accessed: 28 November 2024].

16. Baste, P. and Dighe, D.D., 2017. Low Cost Weather Monitoring Station Using Raspberry Pi. *International Research Journal of Engineering and Technology*, 4(5). https://doi.org/10.5281/zenodo.2599637

17. Vilayatkar, S.R., Wankhade, V.R., Wangekar, P.G. and Mundane, N.S., 2019. IoT Based Weather Monitoring System Using Raspberry Pi. *International Research Journal of Engineering and Technology*, 6(1), pp. 1187–1190. Available at: https://www.irjet.net/archives/V6/i1/IRJET-V6I1220.pdf [Accessed: 28 November 2024].

18. Gheorghe, A.C. and Chiran, M.S., 2018. Raspberry Pi Based Weather Station. *The Scientific Bulletin of Electrical Engineering Faculty*, 18(2), pp. 63–66. https://doi.org/10.1515/sbeef-2017-0037

19. Mathur, V., Saini, Y., Giri, V., Choudhary, V. Bharadwaj, U. and Kumar, V., 2021. Weather Station Using Raspberry Pi. In: IEEE, 2021. *2021 Sixth International Conference on Image Information Processing (ICIIP), India, Shimla, 26–28 November 2021*. IEEE, pp. 279–283. https://doi.org/10.1109/ICIIP53038.2021.9702687

20. Savić, T. and Radonjić, M., 2015. One Approach to Weather Station Design Based on Raspberry Pi Platform. In: IEEE, 2015. *2015 23rd Telecommunications Forum Telfor (TELFOR), Serbia, Belgrade, 24–26 November 2015*. IEEE, pp. 623–626. https://doi.org/10.1109/TELFOR.2015.7377544

21. Jenkins, G., 2014. A Comparison Between Two Types of Widely Used Weather Stations. *Weather*, 69(4), pp. 105–110. https://doi.org/10.1002/wea.2158

22. Bharadwaj, A., Sudhir, A., Shekhar, H., Khandelwal, N. and Kishor, I., 2021. Raspberry Pi Based Weather Monitoring System. *International Journal of Research in Engineering, Science and Management*, 4(8), pp. 114–117. https://doi.org/10.13140/RG.2.2.23682.45763

23. Tatarchuk, I.A., Mamrosenko, K.A. and Giatsintov, A.M., 2024. Graphical GLX-applications functioning ensuring on industrial equipment using the EGL API. *Radioelectronics. Nanosystems. Information Technologies*, 16(3), pp. 407–418. https://doi.org/10.17725/rensit.2024.16.407 (in Russian)

About the authors:

Andrey F. Rozvadovskiy, Junior Research Associate, Marine Hydrophysical Institute of RAS (2 Kaptanskaya St., Sevastopol, 299011, Russian Federation), Ph. D. (Engin.), *rozvadovsky@yandex.ru*

Author has read and approved the final manuscript.

Original article

Software PhotoCoasts of Crimea

M. P. Vetsalo *, E. A. Godin, E. A. Isaeva, L. K. Galkovskaya

Marine Hydrophysical Institute of RAS, Sevastopol, Russia
* e-mail: mvetsalo@mhi-ras.ru

Abstract

The article describes the information retrieval system PhotoCoasts of Crimea developed by the staff of the Oceanographic Data Bank group based on the concept of the software PhotoCoasts to systematize and catalogue the collection of digital images of the Crimean Peninsula coasts. The system also ensures effective work with this collection while conducting scientific research. The software system is written in the Python programming language. The application interface is developed using the tkinter package. The system core is a catalogue of meta-information on photosurvey objects. The catalogue is based on faceted classification and includes descriptive facets "Date and Time", "Type of Photosurvey" and specialised facets "Geographic Region", "Coast Genetic Type". The method of extended Boolean retrieval was applied to form the query results in the software system. New images are uploaded and metadata of existing catalogue elements are edited in the metadata editor. Work with the geoinformation part of the metadata base is performed in the geodata editor. The developed software has a significant potential for further evolution and after appropriate adjustment can be used for work with coast images of other regions. It also allows systematisation and classification of image collections in various fields.

Keywords: coasts, images, visualisation, systematisation, cataloguing, faceted classification, information retrieval system

For citation: Vetsalo, M.P., Godin, E.A., Isaeva, E.A. and Galkovskaya, L.K., 2024. Software PhotoCoasts of Crimea. *Ecological Safety of Coastal and Shelf Zones of Sea*, (4), pp. 131–140.

Программный продукт «ФотоБерега Крыма»

М. П. Вецало *, Е. А. Годин, Е. А. Исаева, Л. К. Галковская

Морской гидрофизический институт РАН, Севастополь, Россия
* e-mail: mvetsalo@mhi-ras.ru

Аннотация

Описывается информационно-поисковая система «ФотоБерега Крыма», разработанная сотрудниками группы «Банк океанографических данных» на основе концепции программного продукта «ФотоБерега» для систематизации и каталогизации коллекции цифровых изображений берегов Крымского полуострова, а также обеспечения эффективной работы с этой коллекцией при проведении научных исследований. Программная система написана на языке программирования *Python*. Интерфейс приложения разработан с использованием пакета *tkinter*. Центральной частью системы является каталог метаинформации объектов съемки, который построен на основе фасетной классификации и включает описательные фасеты «Дата и время», «Вид съемки» и специализированные фасеты «Географический регион», «Генетический тип побережья». Для формирования поисковой выдачи в программной системе применен метод расширенного булева поиска. Загрузка новых изображений и редактирование метаданных существующих элементов каталога выполняется в редакторе метаданных. Работа с геоинформационной частью базы метаинформации осуществляется в редакторе геоданных. Созданный программный продукт имеет значительный потенциал для дальнейшего развития и после соответствующей настройки может быть использован для работы с изображениями берегов других регионов, а также для систематизации и классификации коллекций изображений в самых различных областях.

Ключевые слова: берега, изображения, визуализация, систематизация, каталогизация, фасетная классификация, информационно-поисковая система

Introduction

The transition from drawing to photography and film shooting with high resolution has rendered images the most durable medium for capturing the state of natural objects. When image acquisition is undertaken with sufficient accuracy in terms of place and time, a comparison of images facilitates analysis of changes in the state of objects under the influence of natural and anthropogenic factors. However, a significant proportion of images has not yet been digitised. These images are often stored in various collections and lack proper systematisation and cataloguing, which can result in their loss and limited accessibility to researchers. This situation is particularly problematic for images of seashores,

including the Crimean coast. It can be remedied by organising the digitisation of images and creating special software to work with them.

Currently, it is evident that there is a substantial number of software available for the creation of digital image catalogues. However, these products often prove to be inadequate in terms of their efficiency for the purpose of scientific research. Analysis of open source information [1), 2), 3)] and personal user experience have demonstrated that the catalogue in most existing software products was typically constructed on the basis of the user computer file system hierarchy (Adobe Bridge, ACDSee Photo Studio, etc.) or its own hierarchical structure (folders in Adobe Lightroom and Corel AfterShot Pro, collections in darktable, digiKam albums, etc.). This approach is inherently disadvantageous due to the limitations of such classifications. The rigid structure of the hierarchy is a particular problem as it makes it difficult to include new levels of division. The classification process becomes excessively cumbersome and challenging to utilise when the number of levels is substantial, yet it lacks sufficient informative value when the number of levels is minimal. Moreover, such products are primarily oriented towards the management of image metadata (i.e. image parameters, geolocation, etc.), yet their capabilities in determining the characteristics of the photosurveyed object are not sufficiently developed to enable the execution of research tasks. It is also note-worthy that a considerable proportion of existing software is commercial, with closed sources precluding modification to align with user needs. A further impediment to the procurement and utilisation of prevailing commercial digital image cataloguing software pertains to the sanctions policy of multiple states against the Russian Federation.

Taking into account the disadvantages of the existing software described above, the staff of the Shelf Hydrophysics Department and the Oceanographic Data Bank group of Marine Hydrophysical Institute of RAS developed the software PhotoCoasts concept including following general approaches to the creation of software for visualisation, systematisation and cataloguing of digital images for scientific research:

– provision of maximum independence from external factors, use of freely distributed open source components only;

– work with the catalogue (including its extensibility) taking into account the specifics of using images in solving scientific problems;

– geoinformation base support;

– support for working with digital image metadata (time of photosurvey, geopositioning);

– mass import of images.

[1)] Sazhko, D., 2018. [10 Apps to Organize a Photocollection]. *Lifehacker*. [online] Available at: https://lifehacker.ru/kak-organizovat-kollekciyu-fotografij/ [Accessed: 25 November 2021] (in Russian).

[2)] @dnowicki, 2014. [Overview of Windows Applications for Keeping Photo Archives in Order]. *Habr*. [online] Available at: https://habr.com/ru/post/226123/ [Accessed: 25 November 2021] (in Russian).

[3)] Shlyakhtina, S., 2004. [Cataloguing and Storage of Digital Images]. *ComputerPress*. [online] Available at: https://compress.ru/article.aspx?id=12397 [Accessed: 25 November 2021] (in Russian).

The article presents the findings of research conducted on the implementation of this concept in the development of the specialised information retrieval system PhotoCoasts of Crimea. This system has been optimised for solving a practical problem, namely the systematisation and classification of the collection of digital images of the Crimean Peninsula shores. These images have been collected by the MHI Shelf Hydrophysics Department for a period exceeding a century and a half, and the article discusses the effective work that has been carried out with them.

Approaches and methods

The system core is constituted by a catalogue of meta-information on photo-survey objects. The catalogue is based on faceted classification, a method that has been demonstrated to possess greater semantic power than hierarchical classification [3, 4]. At the inception of catalogue formation, a set of concepts (terms) is defined, which are required to describe the catalogue element (image). Then the terms are subjected to semantic or other grouping into so-called facets. The classification of catalogue elements, in turn, is not predetermined, but is constructed by selecting elements from facets and forming a linear chain of them, called a facet formula. The position of each facet in the facet formula is strictly fixed. In this context, the task of information retrieval within the catalogue can be addressed by determining the sequence of transformation of user information needs into a facet formula (retrieval query) and by considering the classification obtained from this formula as a retrieval output.

The method of extended Boolean retrieval was applied to form the query results in the software system [5], when the result is determined by a logical expression formed on the basis of a user request. The retrieval query (facet formula) is converted into a logical expression, which is applied to the metadata of each catalogue element. In order to increase the speed of retrieval formation, reverse indexing of the image metadata database [5, 6] by individual facets is applied. Acceleration of application work when using the index is achieved by reducing significantly (in general) the number of catalogue elements involved in operations and switching to the use of operations on sets instead of performing logical operations (Boolean retrieval) for all images from the program database.

Implementation

To implement the software system, the Python programming language was selected, as it has both a well-developed standard library and sufficient number of freely accessible third-party open source libraries.

The catalogue of the system PhotoCoasts of Crimea includes descriptive facets "Date and Time" (D), "Type of Photosurvey" (T) and specialised ones "Geographic Region" (R), "Coast Genetic Type" (G). The facet "Date and Time", in turn, is divided into three sub-facets: "Date of Period Beginning" (D_B), "Date of Period End" (D_E) and "Seasonality of Photosurvey" (S). The resulting facet formula for the applied classification is as follows:

$$\langle D_B : D_E : S : R : T : G \rangle.$$

A part of facets contains a finite set of concepts defined during the application development, determined by the semantics of the corresponding feature or the specifics of the system under development. For example, the generally accepted division of the annual cycle into calendar seasons {'winter', 'spring', 'summer', 'autumn'} is used as descriptions for photosurvey seasonality (sub-facet "Seasonality of Photosurvey"), and the content of the facet "Coast Genetic Type" is determined by the geomorphology of the Crimean Peninsula and corresponds to monograph [7].

The content of the facet "Geographic region" and sub-facets "Date of Period Beginning" and "Date of Period End" is not fixed in the application code and can be modified by the user. In particular, the system provides possibility to work with data on photosurvey region, which are the ground for geoinformation base.

To store the catalogue and data of the geoinformation part of the software, the embedded SQL-oriented freely distributed open source DBMS SQLite3 [4] was used. The table Picture contains the basic metadata of a photograph and the identifiers of its relationships to catalogue facet elements. When displaying the catalogue structure, a separate table has been allocated for each facet and sub-facet "Seasonality of Photosurvey" (Fig. 1). Data of sub-facets "Date of Period Beginning" and "Date of Period End" do not exist without a corresponding picture and are implemented as picture attributes in the table Picture. In general, in order to obtain a normalised database, the relationship between a particular photograph and catalogue facets is constructed in one of the following ways:

– for facets with a cardinality of 1 : 1 or 1 : N, the link is organised by including the corresponding identifier in the table Picture;

– for facets with a cardinality of M : N, an additional table is created.

The mapping of the hierarchical facet "Geographic Region" to the relational structure of the database is performed using the list of adjacency from the table GeoRegion [8, 9].
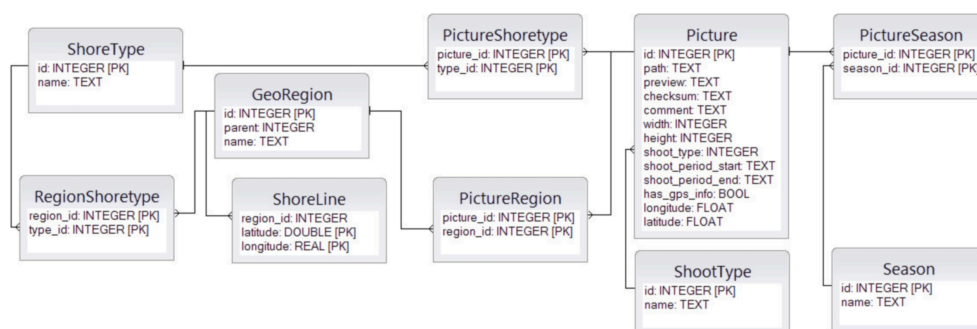

F i g . 1. The scheme of the database for the software system PhotoCoasts of Crimea

The software system uses a hierarchy in the hard disc file system to store the original data. Each photograph corresponds to a separate directory containing the original digital image and a thumbnail.

The application interface is developed using the tkinter package [5] and consists of main window, metadata editor and geodata editor (Fig. 2).

The user defines the required set of image characteristics by forming a query with the use of the retrieval panel located on the left side of the main application window. The retrieval panel contains a separate section for each facet of the catalogue and makes it possible to compose a query in an intuitive way without using specialised query languages. The retrieval result is displayed in the working area of the main window and visualised in two main modes. Library mode provides an estimate of the retrieval and an overview of the retrieval results. In its turn, view mode provides an opportunity to examine each image and its associated meta-information in detail. Since digital images obtained using modern photosurvey equipment can have high resolution, which significantly exceeds the resolution of a computer monitor, the view mode has a function of image scaling including automatic scaling to fit the application window size.

The uploading of new images and the editing of the metadata of existing catalogue items are performed in the metadata editor (Fig. 3). It can be used to change the coordinates of the photosurvey location, its geographical region, date, season, photosurvey method, coast genetic type as well as to make adjustments to the photograph
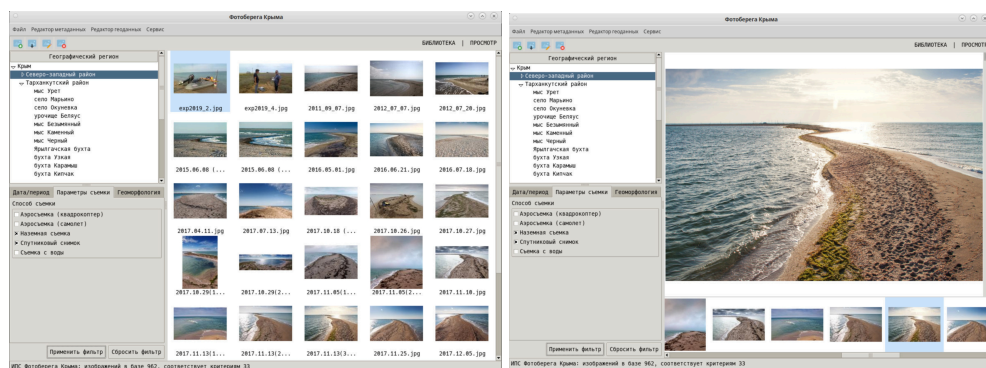
a   *b*

F i g . 2 . The user interface of the application main window: LIBRARY mode (*a*) and VIEW mode (*b*)

[5] Python Software Foundation: Graphical User Interfaces with Tk. *Python*. 2001. [online] Available at: https://docs.python.org/3/library/tk.html [Accessed: 2 December 2024].
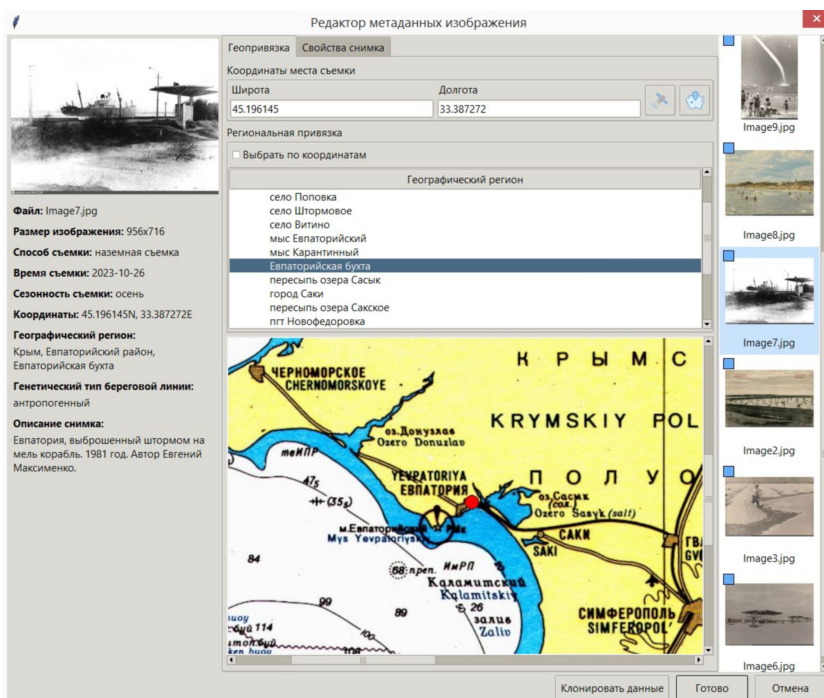
F i g . 3 . The Image metadata editor window

description. The mass upload mode provides the user with the ability to quickly add images with similar metadata to the database, such as the results of an expedition photosurvey at a particular location.

When entering the image metadata, the software system under development implemented the ability to read data from the Exif headers of uploaded files (including the coordinates of the photosurvey location according to GPS data and the date of the photosurvey) and introduced functionality that makes it possible to determine the region and genetic type of the coast by the coordinates of the photosurvey location. The closest region known to the application is chosen as a photosurvey one. Thus, the database of the IRS PhotoCoasts of Crimea contains the information about 140 coastal regions from monograph [7]. To find the region closest to the photosurvey point, the software uses coastline geodata indexing on a uniform grid in the polar coordinate system [10] centred at 45.5° N, 34.0° E.

Work with the geoinformation part of the meta-information base is carried out in the geodata editor (Fig. 4), which can be used to create, delete and correct information about photosurvey regions including coordinates, name and genetic type of the coast.
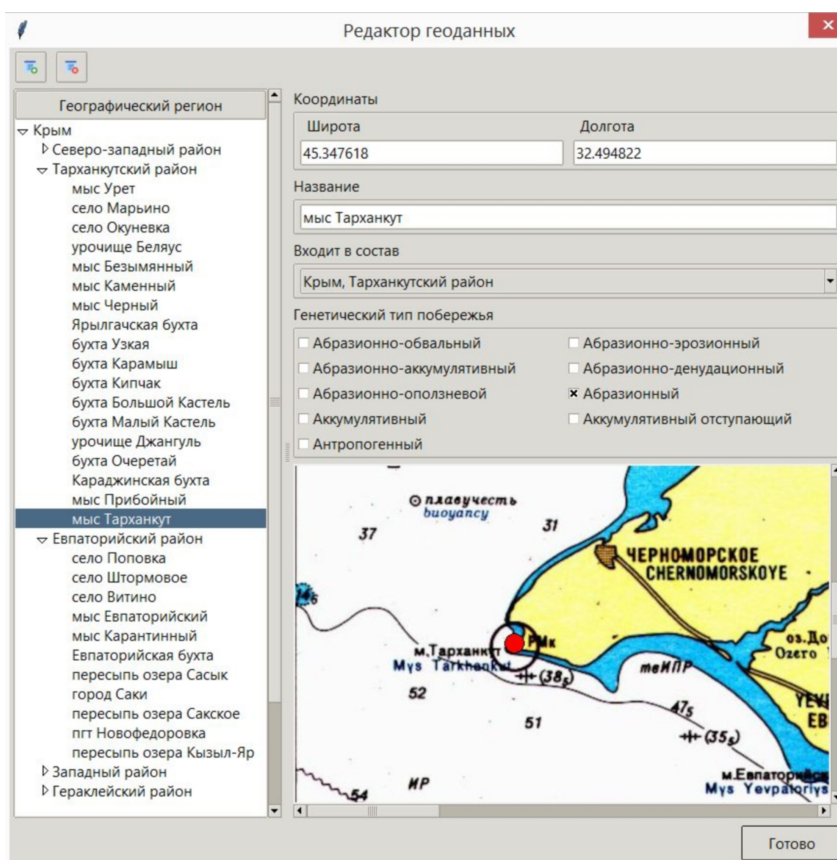
F i g . 4 . The Geodata editor window

Conclusion

The information retrieval system PhotoCoasts of Crimea was developed based on the concept of the software PhotoCoasts. It was optimised for solving the practical task of systematisation, classification and work with the collection of digital images of the Crimean Peninsula coasts in the course of scientific research. The article describes the structure of the image catalogue and the method of storing metadata of the photosurvey subject. The order of work with the system when searching for information and loading new images is described. The key feature of the developed software is the module of formation of the geoinformation base about the Crimean coast. The use of geoinformation together with the ability of reading digital image metadata and mass loading of images significantly facilitates entering information into the system catalogue.

The developed information retrieval system PhotoCoasts of Crimea has a significant potential for further evolution. Its functionality can be extended and adapted

to work with images from other regions. Following appropriate adjustment, this versatile software will allow systematisation, classification and work with digital image collections in a wide variety of scientific fields.

REFERENCES

1. Godin, E.A., Vetsalo, M.P., Galkovskaya, L.K., Goryachkin, Yu.N., Zhuk, E.V., Ingerov, A.V., Isaeva, E.A., Kasyanenko, T.E. and Plastun, T.V., 2022. Information Support of Research in the Black Sea and the Sea of Azov Coastal Zones. In: B. V. Chubarenko, ed., 2022. *All-Russian Conference with International Participation "XXIX Coastal Conference: Field – Based and Theoretical Research in Shore Use Practice".* Kaliningrad: Publishing House of IKBFU, pp. 330–333 (in Russian).

2. Vetsalo, M.P. and Godin, E.A., 2022. Development of a Software System for the Data-base of Photographic Images of the Crimean Coasts. In: MHI, 2022. *The Seas of Rus-sia: Challenges of the National Science. Proceedings of the All-Russian Scientific Con-ference. Sevastopol, 26 – 30 September 2022.* Sevastopol: MHI, pp. 287–289 (in Rus-sian).

3. Cherny, A.I., 1975. [*Introduction to Information Retrieval Theory*]. Moscow: Nauka, 238 p. (in Russian).

4. Ranganathan, S.R., 1987. *Colon Classification*. Bangalore: Sarada Ranganathan En-dowment for Library Science.

5. Manning, C.D., Raghavan, P. and Schütze, H., 2008. *Introduction to Information Retrieval.* Cambridge: Cambridge University Press. 2008, 506 p.

6. Witten, I.H., Moffat, A. and Bell, T.C., 1999. *Managing Gigabytes: Compressing and Indexing Documents and Images*. Morgan Kaufmann, 519 p.

7. Goryachkin, Yu.N. and Dolotov, V.V., 2019. *Sea Coasts of Crimea*. Sevastopol: Colorit, 256 p. (in Russian).

8. Bogdanov, D., 2009. Optimal Store and Processing Method for Tree-Structures in Relative Databases. *Software and Systems*, (1), pp. 140–142 (in Russian).

9. Tarassov, S.V. and Burakov, V.V., 2013. Methods of Relational Modeling of Hierarchical Structures of Data. *Information and Control Systems*, (6), pp. 58–66 (in Russian).

10. Bentley, J.L. and Friedman, J.H., 1979. Data Structures for Range Searching. *ACM Computing Surveys*, 11(4), pp. 397–409. https://doi.org/10.1145/356789.356797

About the authors:

Maksim P. Vetsalo, Leading Software Engineer, Marine Hydrophysical Institute of RAS (2 Kapitanskaya St., Sevastopol, 299011, Russian Federation), **ORCID ID: 0000-0002-3543-2124**, **Scopus Author ID: 57222028338**, *mvetsalo@mhi-ras.ru*

Evgeny A. Godin, Research Associate, Marine Hydrophysical Institute of RAS (2 Kapitanskaya St., Sevastopol, 299011, Russian Federation), **ORCID ID: 0000-0002-6469-1379, Scopus Author ID: 56950615200, Researcher ID: AEP-0342-2022,** *godin_ea@mhi-ras.ru*

Elena A. Isaeva, Leading Software Engineer, Marine Hydrophysical Institute of RAS (2 Kapitanskaya St., Sevastopol, 299011, Russian Federation), **ORCID ID: 0000-0002-1860-0026, Scopus Author ID: 57191413519**, *isaeva-ea@mhi-ras.ru*

Lyudmila K. Galkovskaya, Leading Software Engineer, Marine Hydrophysical Institute of RAS (2 Kapitanskaya St., Sevastopol, 299011, Russian Federation), *galkovskaya@gmail.com*